DOT/FAA/TC-16/52
Federal Aviation Administration
William J. Hughes Technical Center
Aviation Research Division
Atlantic City International Airport
New Jersey 08405

Flight Test Results of Direct-Measure and Derived Angle-of-Attack Systems for General Aviation Airplanes

November 2017

Final Report

U.S. Department of Transportation
Federal Aviation Administration

NOTICE

Technical Report Documentation Page

1. Report No.	2. Government Accession No.	3. Recipient's Catalog No.
DOT/FAA/TC-16/52		

4. Title and Subtitle	5. Report Date
FLIGHT TEST RESULTS OF DIRECT-MEASURE AND DERIVED ANGLE-OF-ATTACK SYSTEMS FOR GENERAL AVIATION AIRPLANES	November 2017
	6. Performing Organization Code 541330

7. Author(s)	8. Performing Organization Report No.
E. Bruce Jackson and Keith D. Hoffler	

9. Performing Organization Name and Address	10. Work Unit No. (TRAIS)
Adaptive Aerospace Group, Inc. 100 Exploration Way, Suite 330 Hampton, VA 23666	
	11. Contract or Grant No. DTFACT-15-C-00005

12. Sponsoring Agency Name and Address	13. Type of Report and Period Covered
U.S. Department of Transportation Federal Aviation Administration FAA Central Regional Office 901 Locust St Kansas City, MO 64106	Final Report March 2015–February 2016
	14. Sponsoring Agency Code AIR-714

15. Supplementary Notes

The FAA William J. Hughes Technical Center Aviation Research Division COR was Robert J. McGuire.

16. Abstract

Two commercial off-the-shelf angle of attack (AoA) systems were evaluated in flight against a calibrated AoA probe in an instrumented Cessna R182. One of the systems used a direct-measuring sensor that was mounted in the flow field. This is referred to as "sensed AoA." The other system consisted of an algorithm to derive AoA from a commercial attitude and heading reference unit (hence the term "derived AoA"). In addition, a novel derived AoA estimation algorithm was developed and tested in both ground simulation and in post-processing of actual flight test data for a variety of stalls.

Some effort was required to obtain satisfactory results from the sensed AoA commercial system, including relocation of the sensor. Following relocation, the sensed AoA system worked well, as did the derived AoA system using a commercially developed algorithm and Attitude and Heading Reference System unit.

The novel derived AoA algorithm used parameters available from a certified electronic flight information system. It also relied on estimates of key aerodynamic parameters, such as the lift slope coefficient, obtained through in-flight calibrations at different flap and landing-gear configurations. It also required readily available aircraft information (e.g., weight, surface area, and sensor location). This approach shows promise, but additional work is required to make it commercially feasible, including reducing the number of input signals required and simplification of the calibration procedure. A study of the sensitivity of the algorithm indicated which inputs are important for good AoA estimation and suggests other inputs that could be approximated.

Testing of the novel algorithm showed good comparisons with calibrated AoA to near-stall conditions, where output signal limiting of the calibrated AoA probe led to poor comparisons with flaps extended, but tests with flaps retracted showed excellent estimation up to a stalled flight condition.

17. Key Words	18. Distribution Statement
Angle of attack, Flight test, Derived AoA, Sensed AoA, Direct-measurement AoA, Stall margin, Stall protection, Simulation	This document is available to the U.S. public through the National Technical Information Service (NTIS), Springfield, Virginia 22161. This document is also available from the Federal Aviation Administration William J. Hughes Technical Center at actlibrary.tc.faa.gov.

19. Security Classif. (of this report)	20. Security Classif. (of this page)	21. No. of Pages	22. Price
Unclassified	Unclassified	107	

ACKNOWLEDGEMENTS

Adaptive Aerospace Group, Inc. would like to thank Aspen Avionics, Inc., Aeroprobe Corporation, and Garmin Ltd. for their assistance in this research, and members of the FAA Small Airplane Directorate for their support.

TABLE OF CONTENTS

LIST OF FIGURES

LIST OF TABLES

LIST OF SYMBOLS AND ACRONYMS

$\Delta\alpha_{avg}$	Average difference between true and derived AoA
$\Delta\alpha_{max}$	Maximum difference between true and derived AoA
σ	Standard Deviation
a_Z	Body frame vertical axis acceleration, ft/s^2 (+down)
C_N	Coefficient of normal force
$C_{N\alpha}$	Slope of the coefficient of normal force with AoA
g	Acceleration due to gravity, 32.174 ft/s^2
N_Z	Body frame vertical axis acceleration, *g* units (+up)
X	Body frame longitudinal axis (+forward)
Z	Body frame vertical axis (+down)
AAG	Adaptive Aerospace Group, Inc.
ADAGE	AAG Digital AoA G-based Estimator
ADAHRS	Air Data Attitude Heading Reference Systems
AEA	Aircraft Electronics Association
AoA	Angle of attack
AWOS	Automated weather-observing system
CG	Center of gravity (actually center of mass)
COTS	Commercial off-the-shelf
FAF	Final approach fix
GA	General aviation
IAF	Initial approach fix
ILS	Instrument landing system
KCAS	Knots calibrated airspeed
KIAS	Knot indicated airspeed
KPVG	Hampton Roads (Chesapeake, Virginia) Executive Airport
KTAS	Knots true airspeed
MSL	Mean sea level
OAT	Outside air temperature
PFD	Primary Flight Display
POH	Pilot’s Operating Handbook

EXECUTIVE SUMMARY

Two commercial off-the-shelf angle of attack (AoA) systems were evaluated in flight against a calibrated AoA probe in an instrumented Cessna R182. One of the systems used a direct-measuring sensor that was mounted in the flow field. This is referred to as “sensed AoA.” The other system consisted of an algorithm to derive AoA from a commercial attitude and heading reference unit (hence the term “derived AoA”). In addition, a novel derived AoA estimation algorithm was developed and tested in both ground simulation and in post-processing of actual flight test data for a variety of stalls.

Some effort was required to obtain satisfactory results from the sensed AoA commercial system, including relocation of the sensor. Following relocation, the sensed AoA system worked well, as did the derived AoA system using a commercially developed algorithm and Attitude and Heading Reference System unit.

The novel derived AoA algorithm used parameters available from a certified electronic flight information system. It also relied on estimates of key aerodynamic parameters, such as the lift slope coefficient, obtained through in-flight calibrations at different flap and landing-gear configurations. It also required readily available aircraft information (e.g., weight, surface area, and sensor location). This approach shows promise, but additional work is required to make it commercially feasible, including reducing the number of input signals required and simplification of the calibration procedure. A study of the sensitivity of the algorithm indicated which inputs are important for good AoA estimation and suggests other inputs that could be approximated.

Testing of the novel algorithm showed good comparisons with calibrated AoA to near-stall conditions, where output signal limiting of the calibrated AoA probe led to poor comparisons with flaps extended, but tests with flaps retracted showed excellent estimation up to a stalled flight condition.

1. INTRODUCTION

The relative angle between the oncoming relative wind and the chord line of the wing of an aircraft, known as the angle of attack (AoA), is of great significance to the performance of the aircraft. Conventional fixed-wing aircraft can only operate safely within a limited range of AoA. Best rate of climb, best angle of climb, and best power-out glide (best lift-to-drag) are achieved (in still air) at nearly fixed values of AoA. More importantly, from a safety point of view, is the existence of a critical AoA beyond which lift rapidly decreases and drag increases as the wing stalls. This critical AoA can be reached well above conventional stall speed (e.g., during maneuvering or steep turns). An AoA indicator serves as a lift-reserve indicator in all speed regimes [1, 2].

1.1 PURPOSE

This study was performed to assist the FAA in evaluating four means of estimating AoA of a typical general aviation (GA) aircraft in normal and slow-speed flight. Two methods used a direct-measurement technique involving multi-hole probes in the flow field beneath the wing, and two methods used onboard instrumentation plus pitot-static measurements to estimate the AoA in pseudo real time. A third derived AoA estimate purely from inertial sensors was briefly examined as well.

The purpose was to gain insight into the usefulness and accuracy of these systems and methods with an eye to recommending certification requirements.

This research is part of a larger FAA plan to look into the efficacy of using AoA (sensed and derived) in simple stall-prevention systems, autopilots, and augmented flight-path control systems. The FAA believes this core capability will be an essential building block to achieving low-cost implementation of integrated flight-path control systems, which is in turn an essential part of achieving future automation goals to enable safer GA transportation systems and on-demand mobility concepts.

1.2 OUTLINE

This paper will describe two commercial off-the-shelf (COTS) AoA indication systems that were tested in flight and a third AoA measurement system that served as a calibrated truth source. A novel means of estimating AoA from onboard sensor measurements, performed after the flight tests, is also described, including the sensitivity and robustness of this method to measurement errors based on tests conducted in a simulation tool. Results of flight-testing of each AoA system are given and discussed, including the sensitivity of each system to installation, calibration, and configuration differences. Finally, some implications on certification of these systems is discussed.

1.3 DIRECT-MEASURE SENSORS

Two multi-hole airflow probes were used in this study: a Garmin® AoA indicator system test article, and an Aeroprobe Corporation Air Data Probe (truth source).

The Garmin sensor probe was mounted below the wing of the test aircraft on a reinforced inspection hole cover, following the manufacturer's instructions. The Garmin system drove a dedicated indexer display that was mounted above the glareshield on the pilot's side that provided

a 10-segment, colorized display of relative AoA from low AoA (green) to on-speed (green "doughnut") to higher AoA (yellow) and near-stall AoA (red) (see figure 1).

Figure 1. Garmin GI 260 indicator on left side of glareshield in test aircraft

The Garmin AoA probe installation instructions included a calibration procedure. Digital data from the Garmin AoA system were not available in this experiment, so the characterization data came from direct observation of the Garmin indexer display.

The Aeroprobe Air Data Probe was affixed to the right wing strut using a modified camera mount that allowed some freedom in the orientation of the probe, but ensured repeatability when removed and reapplied. This system provided raw, local-flow AoA and angle-of-sideslip measurements as well as static and total pressure to the Adaptive Aerospace Group, Inc. (AAG) data-recording system. Therefore, it had to be calibrated using an AAG-developed procedure to estimate free-stream AoA (sideslip angle measurements were not calibrated or used).

1.4 DERIVED AOA ALGORITHMS

Two derived AoA algorithms were used in this study: a recent software upgrade to the Aspen Avionics EFD-1000 Evolution Pro® 1000 Electronic Flight Information System that provided two estimates of AoA (flaps-up and full-flaps-down configurations) and an AAG in-house derived AoA estimate using system identification techniques from data obtained from onboard GPS and Air Data Attitude Heading Reference Systems (ADAHRS). The Aspen software upgrade included

a supplement to the Pilot's Operating Handbook (POH) that gave a calibration procedure; the AAG algorithm was calibrated using a custom calibration procedure to estimate free-stream AoA.

2. DIRECT-MEASUREMENT SYSTEMS

Calibration and characterization of the two multi-hole probes, mounted in the airflow under the wing of the test aircraft, are described in this section.

2.1 GARMIN MULTI-HOLE PROBE (TEST ARTICLE)

The Garmin AoA system consisted of a Garmin GAP 26 multi-hole probe mounted under the left wing of the aircraft (see figures 2 and 3), a Garmin GSU 25 data-processing unit located behind the instrument panel, and a multi-segment Garmin GI 260 AoA indicator mounted on the upper-left corner of the glareshield inside the test aircraft (see figure 1).

Figure 2. Initial location of Garmin multi-hole GAP 26 probe sensor in test aircraft

Figure 3. Relocated Garmin GAP 26 probe on test aircraft

The manufacturer-provided installation instructions included calibration procedures that involved flying the aircraft configured for landing in two different flight conditions (desired approach and at initial stall indication) in reasonably calm air. The unit then depicted, via illumination of ten different LED segments in the indicator, the relative proximity to stall AoA and gave a qualitative indication of AoA. No quantitative AoA estimate was provided.

The initial testing with the Garmin probe semi-permanently mounted on the wing at approximately 49% of chord length as specified in the manual (see figure 2) gave repeatable results, as shown in figures 4 and 5, but the results were strongly dependent on flap position. An accurate indication of both “on-speed” and “stall speed” were provided only for the single calibrated flap deflection.

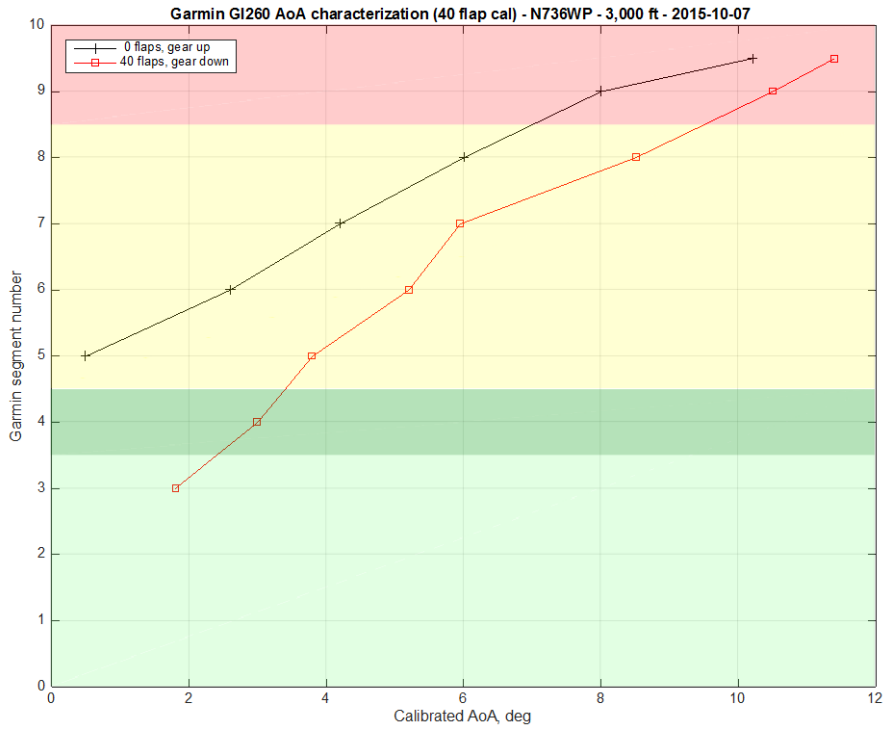

Figure 4. Characterization of Garmin AoA indicator vs. calibrated AoA for two flap positions (original sensor location)

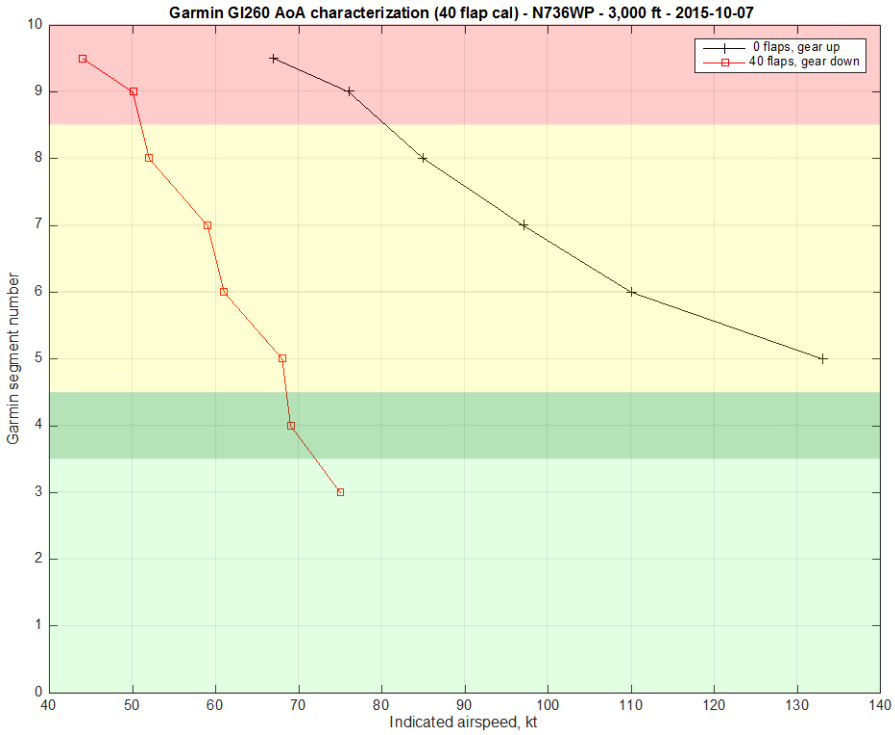

Figure 5. Characterization of Garmin AoA indicator vs. indicated airspeed for two flap positions (original sensor location)

In both figures, each data point represents the calibrated AoA or indicated airspeed at which the numbered segment came on with a steady indication.

The probe was subsequently relocated closer to the leading edge of the wing (at approximately 17% of chord length; see figure 3), which necessitated a new inspection hole to be cut and a mounting plate to be fabricated, and was recalibrated. As shown in figure 3, both the original and the new locations were well outside the slipstream of the propeller and outboard of the left wing flap. After relocation, the Garmin AoA system worked satisfactorily, giving repeatable results that were much less dependent on flap setting, as shown in figures 6 and 7. In these figures, the data points plotted between ordinal segment numbers indicate where the next-higher segment began to flash, so the data points shown for segment 2.5 represent the calibrated AoA at which segment 2 was steadily illuminated and segment 3 first began to flash.

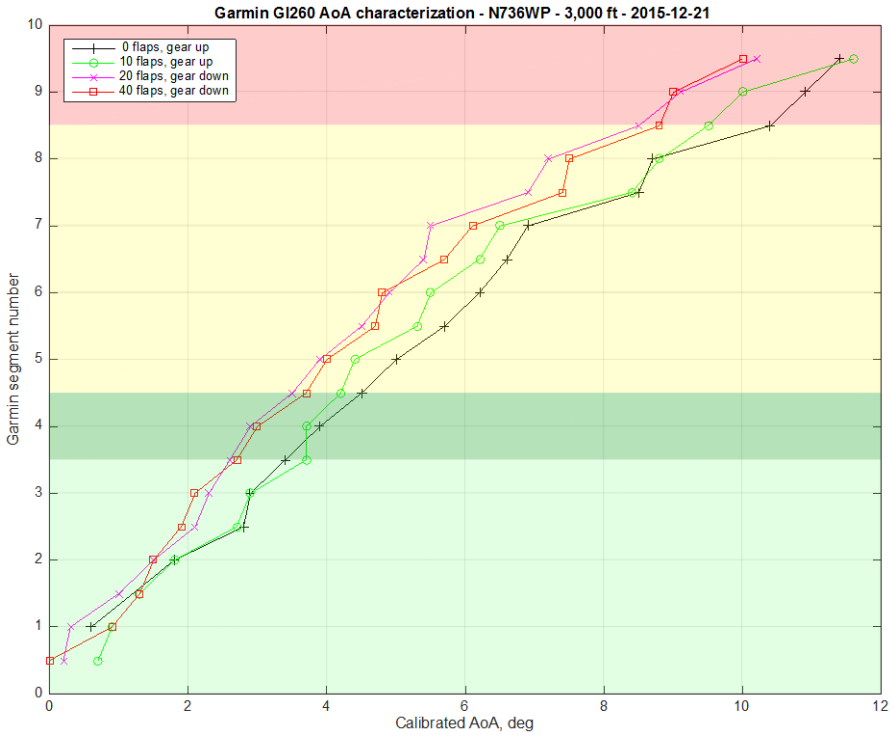

Figure 6. Characterization of Garmin AoA indicator vs. calibrated AoA for four flap positions (relocated sensor location)

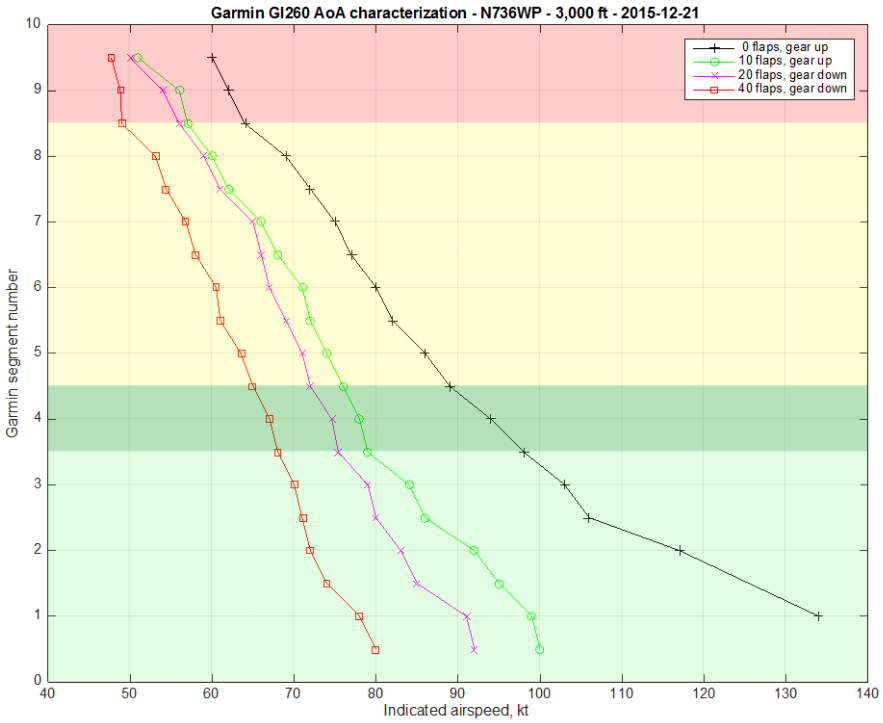

Figure 7. Characterization of Garmin AoA indicator vs. indicated airspeed for four flap positions (relocated sensor location)

Results of this experience and subsequent in-flight characterization of the probe were provided to the manufacturer and contributed to an update of their installation manual.

2.2 AEROPROBE MULTI-HOLE AIR DATA PROBE (TRUTH DATA SOURCE)

Another direct-measure AoA sensor was installed to provide flight-test-quality AoA measurement. This consisted of a multi-hole probe developed by Aeroprobe Corporation. This probe was intended for use in wind-tunnel and flight-test applications versus GA use. It was installed on the right wing strut with a removable mount (see figure 8) and connected to an Aeroprobe data-processing unit. This system provided quantitative measurements of AoAs, sideslip, static pressure, total pressure, and pressure altitude via a digital interface. The location was well outside the propeller slipstream but upwind of the right wing flap.

Figure 8. Location of Aeroprobe sensor

Because this system was removable, it was deemed prudent to recalibrate after each reinstallation. The system was in a flow-field strongly influenced by flap setting, and, therefore, each aircraft configuration was calibrated using an AAG-developed calibration procedure, which is outlined in appendix C. Depending on aircraft configuration, the system occasionally reached a maximum AoA measurement limit during stall maneuvers. It served as the primary source of calibrated AoA when not limited. The Aeroprobe data from four flights (a pre-test calibration flight and the three test flights for data) were combined for a single calibration for data reduction and the AoA comparisons found in this report. The probe was not removed/reinstalled between these four flights.

3. DERIVED AoA ALGORITHMS

In contrast to AoA indication systems that involve a probe in the flow field of the aircraft, AoA can be derived based on kinematics of the aircraft itself as measured by onboard instruments.

3.1 ASPEN EFD-1000 DERIVED AoA ESTIMATION

The test aircraft included an Aspen Avionics EFD-1000 Evolution Pro® 1000 Primary Flight Display (PFD) unit. During the course of this investigation, a derived AoA estimation capability was being developed for the Aspen PFD, providing qualitative indications of proximity to stall AoA. AAG was able to obtain a pre-release version of this capability and compare its performance to the calibrated AoA information provided by the Aeroprobe sensor. By the final flight test of this

effort, the production version of the Aspen derived AoA algorithm was installed and was characterized in parallel with tests of the other systems (AAG was not privy to any details of the Aspen algorithm).

The production version of the Aspen AoA estimator provides a graphical depiction of remaining stall margin and stall margin trend, simultaneously for no flaps and full (40°) flaps/gear down, on the PFD display. The ability to show the AoA full-time or only during slower flight was selectable in pilot preference options. When properly configured, the PFD showed the words “AOA AUTO” when flown at lower AoA (higher speeds), as shown in figure 9(a). When AoA increased as the vehicle decelerated, however, the text was replaced with a vertical display bar with two indicator triangles that moved vertically along the bar, depicting “clean” (0° flaps/gear up) and “dirty” (40° flaps/gear down) configuration AoA in a qualitative sense, with higher movement along the bar indicating higher AoA (see figure 9(b)).

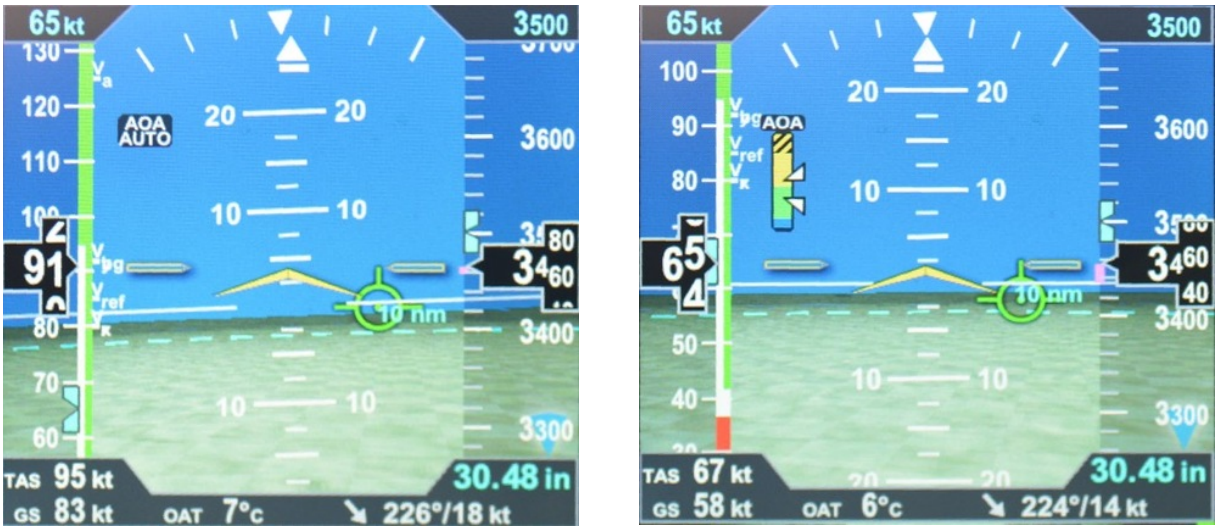

(a) Low AoA conditions (e.g., cruise)

(b) AoA indication scale with “clean” (upper) and “dirty” (lower) indicators

Figure 9. Aspen PFD AoA display formats

Figure 10 compares the qualitative AoA indication of the Aspen for six different combinations of flap settings and gear positions obtained during the flight test for this study. The background colors in the plot correspond with the colors of the Aspen AoA scale, except the reddish area on the plot represents the yellow and black hatched area on the Aspen AoA scale. The dashed lines, associated with the two clean configurations (0° flaps in coordinated and uncoordinated flight), depict the approximate position of the upper triangular index on the Aspen AoA scale, and the solid lines, associated with flap-down configurations, refer to the approximate location of the lower triangular index on the Aspen AoA scale. Note that the relative position of the two AoA indicators reflect the observation by the test pilot rather than a quantitative measurement. In a similar fashion, figure 11 compares the same approximate AoA indications relative to aircraft indicated airspeed. These characterizations were made during the first data flight.

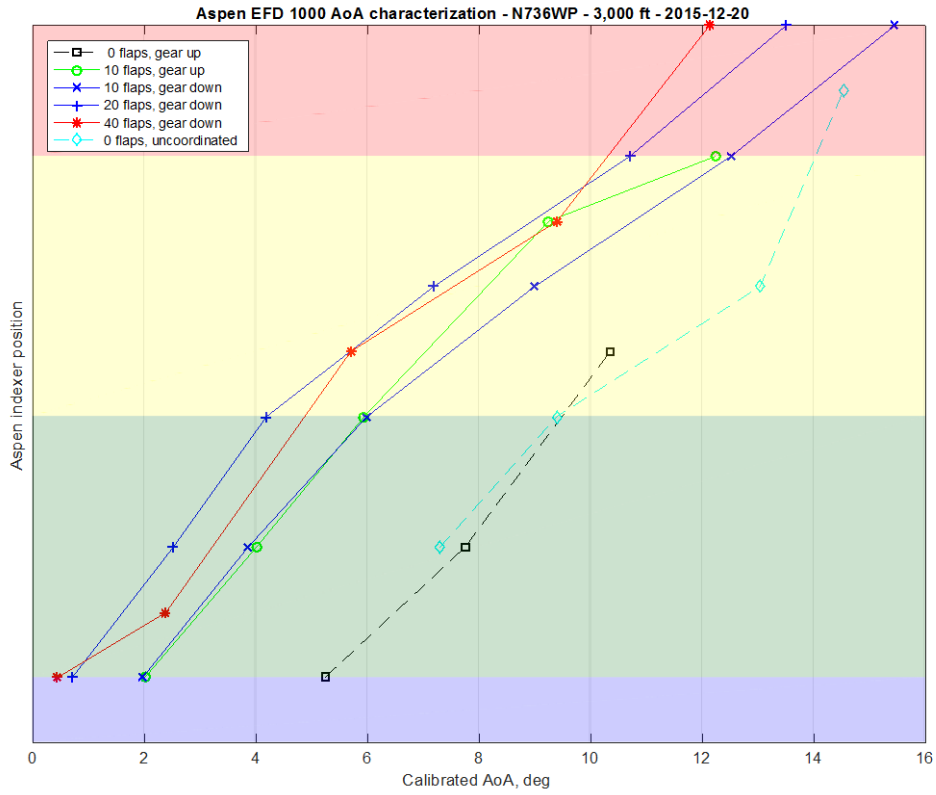

Figure 10. Characterization of Aspen AoA indicators vs. calibrated AoA for six different combinations of flap and gear positions (dashed lines refer to location of the upper indicator)

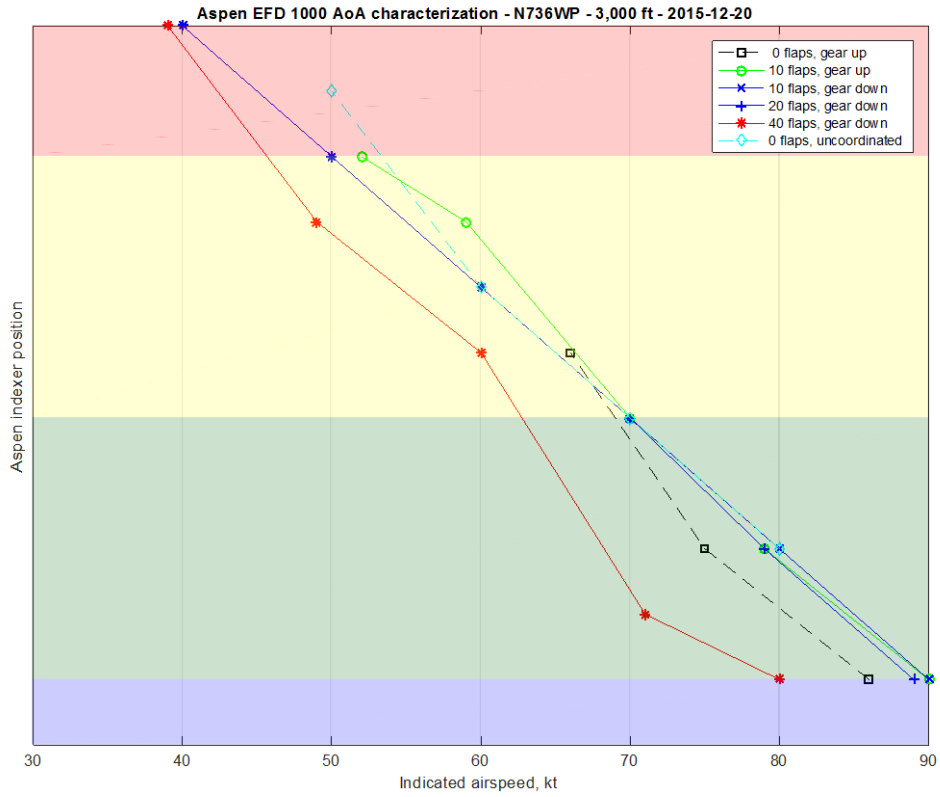

Figure 11. Characterization of Aspen AoA indicators vs. indicated airspeed for six different combinations of flap and gear positions (dashed lines refer to location of the upper indicator)

As shown in figures 10 and 11, the Aspen AoA estimate was repeatable across vehicle configurations.

Aspen provided the interface documentation to allow AAG to obtain several internally calculated parameters from the EFD-1000 via a digital bus, and, therefore, access to the "clean" configuration (i.e., flaps and gear up) numerical estimate for AoA for comparison purposes. However, no "dirty" configuration (i.e., flaps/gear extended) derived AoA estimate was available for comparison.

AAG had no knowledge of the theory or implementation behind this Aspen derived AoA algorithm.

3.2 AAG IN-HOUSE DERIVED AOA ALGORITHM

As part of this study, AAG developed an independent derived AoA estimation algorithm using system-identification techniques and first principles of flight mechanics, and implemented it using in-flight calibration of the vehicle and its sensors. The AAG Digital AoA G-based Estimator (ADAGE) algorithm relies on measurements of normal acceleration (N_Z), indicated airspeed, vehicle weight, outside air temperature, inertial (ground-relative) velocity from GPS, pitch and bank angle, and sensor offset from the center of gravity, plus vehicle latitude. The algorithm relies on a priori identification of the normal force coefficient (C_N) as a function of vehicle configuration

(flap and gear positions) and AoA; in operation, N_Z and true airspeed are used to estimate C_N. The previously identified C_N vs. AoA relationship is used to estimate AoA for the current vehicle configuration.

3.2.1 Assumptions

The following assumptions were made in the initial development of the ADAGE algorithm:

1. Input data had to be available or derivable from any ADAHRS-/GPS-equipped GA aircraft.
2. Lift and drag due to elevator deflection would be correlated with trimmed AoA (true in straight-and-level flight).
3. Engine thrust would act parallel to the body X-axis.
4. Estimates would be obtained in quasi-steady flight with very small angular accelerations.
5. Roll rates would be close to zero.
6. Pitch rate would have little effect on normal force.

As discussed in the results section, some further simplifications appear possible that reduce the parameters needed by the estimate.

3.2.2 Derivation

Theory behind the development of ADAGE is given in appendix A.

3.2.3 Advantages

Because this method does not rely on integration of inertial acceleration, it is unaffected by steady vertical atmospheric motion. It also appears relatively insensitive to location, orientation, or atmospheric variations from standard (e.g., static temperature and pressure).

3.2.4 Limitations

A drawback of this algorithm is the need for knowledge of current vehicle configuration to choose the proper C_N vs. AoA calibration coefficients. A workaround is apparent in the
Aspen derived AoA implementation in that only two configurations are “identified” during calibration: clean and landing configurations. When activated, the Aspen display shows two indicators for derived AoA corresponding to the two configurations, and the pilot must refer to the correct one for the current configuration.

Another limitation is that the estimate of C_N vs. AoA is linear and does not capture the flattening of the lift curve near stall. The trimmed calibration points used to identify C_N vs. AoA are necessarily obtained at AoA below stall, whereas a typical C_N vs. AoA “lift curve” becomes fairly non-linear near stall AoA while remaining relatively linear at lower AoA. The assumption of a linear C_N vs. AoA relationship means this characteristic of the flight envelope is not captured in the model and will likely lead to an overestimate of AoA near stall AoA. However, this is not a significant limitation if the purpose of the algorithm is to warn of approaching stall conditions because the overestimation is actually conservative (overestimates AoA) in this case.

Finally, the flight test showed power effects on the elevator that imply the assumption about elevator effects being correlated only with AoA was incorrect, because power effects are evident in the derived AoA test results. Some type of correction for power would be beneficial in an improved algorithm because changes to the slipstream (due to throttle changes) over the elevator changed its effectiveness.

3.2.5 Implementation

The ADAGE algorithm prototype was realized using The Mathworks, Inc. MATLAB®/Simulink® block diagram modeling system. The algorithm was executed using data recorded during flight and was not operated in real time onboard the test aircraft. However, this in-flight execution is entirely feasible because no significant processing is required to operate the algorithm.

The algorithm is shown in figure 12 in block diagram form. A more complete set of diagrams can be found in appendix B.

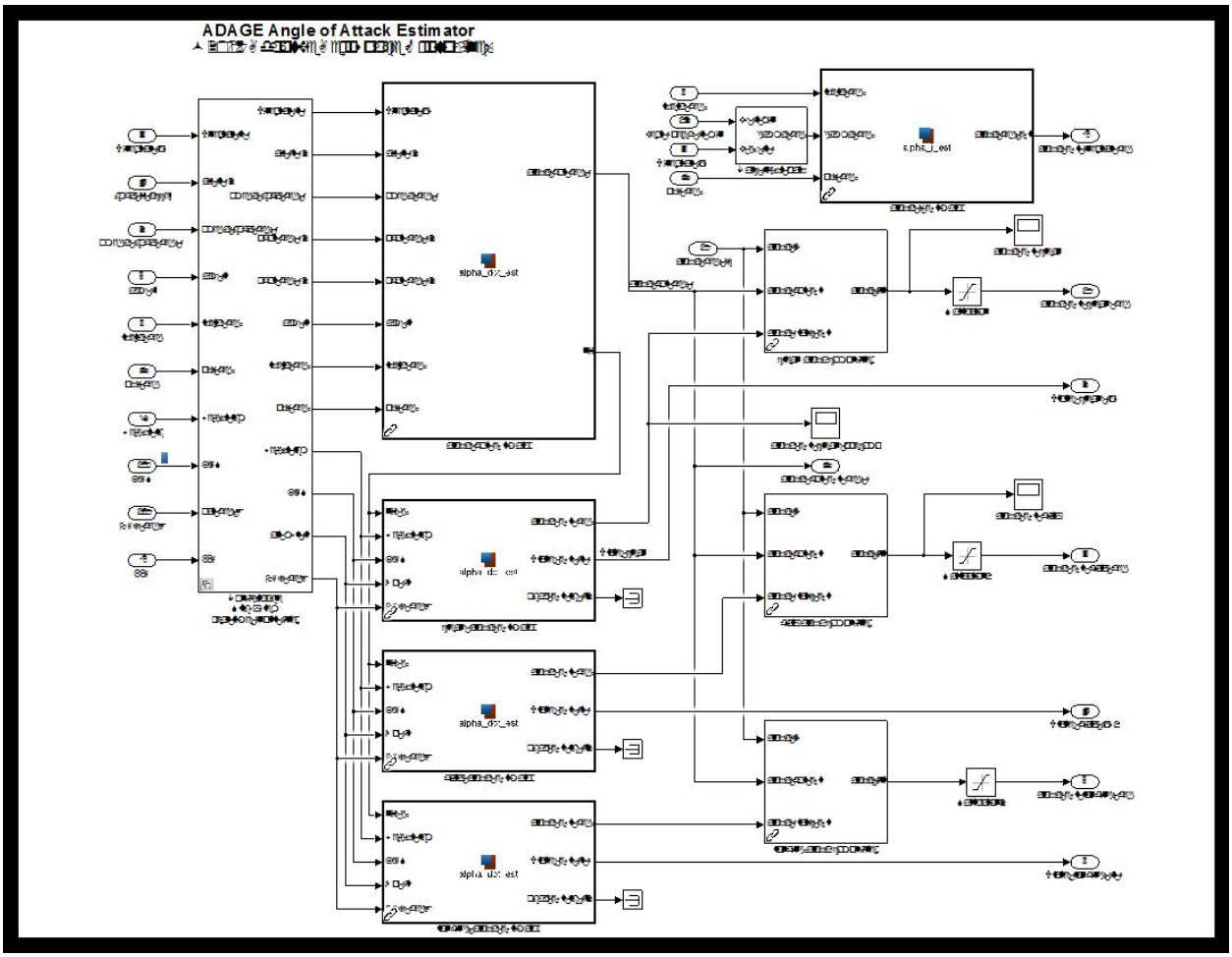

Figure 12. Block diagram of the ADAGE algorithm

3.2.6 Calibration

The ADAGE algorithm relies on calibration of several ADAHRS sensors and estimation of the characteristics of the relationship between trimmed C_N and true AoA. This calibration was obtained by flying the test aircraft in trimmed, level flight in still air at a given flap deflection and landing gear position for several seconds while data were recorded. A calibration algorithm (see appendix C) then determined true AoA, true airspeed, dynamic pressure, and C_N. From these values, a line was fitted through all the C_N vs. AoA points for the given configuration. Figure 13 shows the line fits obtained during the ADAGE calibration flight subsequently used for all data reduction for this report.

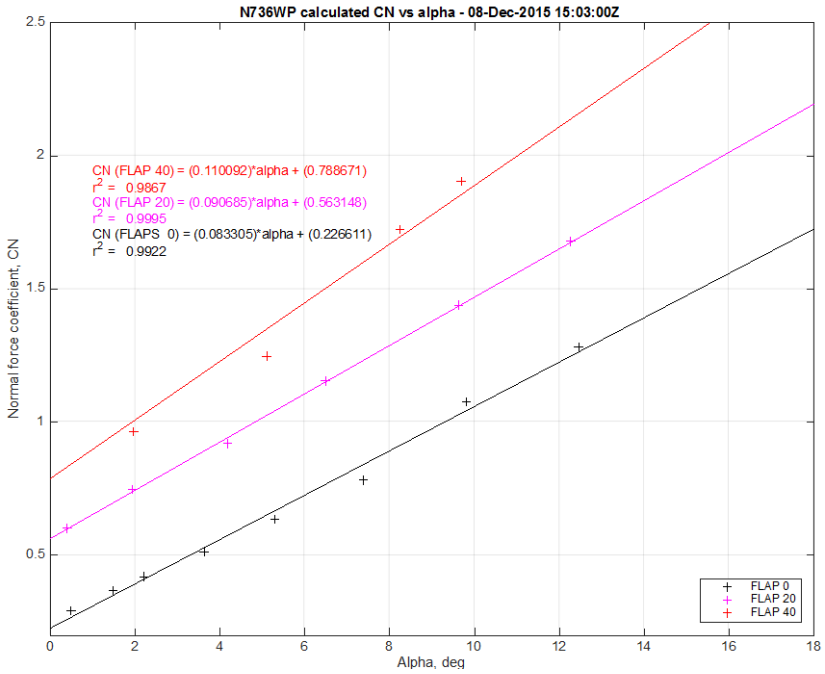

Figure 13. C_N vs. AoA line fits used for all data flights

Note that in figure 13 the slope of the line fit varies with flap deflection. A minimum of two calibration points for each configuration are required to obtain a linear calibration for an aircraft such as the Cessna R182 test aircraft with Fowler flaps that increase the wing area.

During the same calibration flight, biases associated with rate sensors and accelerometers were determined from averages of measurements of these sensors for all flight conditions with near-zero bank angle, and a line was fit through the normal acceleration (a_Z) measurements, as shown in figure 14.

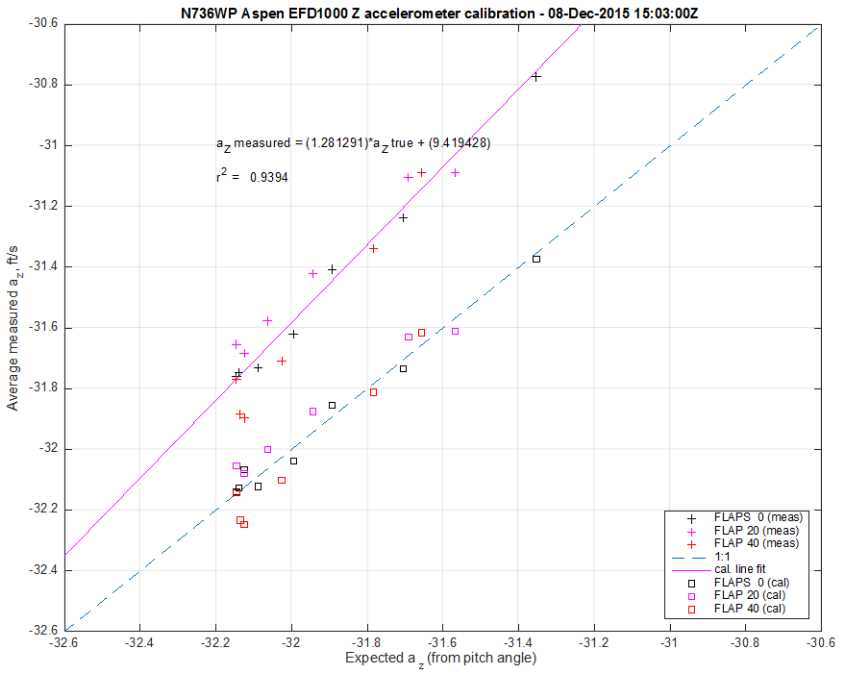

Figure 14. Normal (Z-axis) accelerometer calibration curves used for all data flights

3.3 AoA DERIVED FROM INERTIAL MEASUREMENTS

A third method of estimating AoA was briefly investigated. This consisted of determining the angular separation between aircraft body X-axis pointing angle and flight-path angle, resolved into the aircraft's plane of symmetry (in level flight, the difference between pitch attitude and vertical flight-path angle). This estimate is shown on some of the AoA comparison plots but compared poorly to the sensed, derived, and calibrated AoA, primarily due to not having a good estimate of vertical flight-path angle.

4. SIMULATION TESTING

A simulation of a Cessna 172 was developed to assist in debugging the ADAGE algorithm and to determine the sensitivity of the algorithm to sensor errors, biases, sensor and thrust misalignment, weight differences, altitude differences, turbulence, gusts, wind shear, and other sources of error. This simulation was developed using a combination of C code and The Mathworks Simulink block diagram modeling tool.

4.1 SIMULATION MODEL

A top-level view of the Cessna 172 simulation is shown in figure 15. This model included a "bare" vehicle model, a sensor model, and a block containing the ADAGE algorithm. An outer-loop maneuvering autopilot (scenario generator) was also developed to simulate flight of the aircraft through an approximately 6-minute flight involving a steep turn, vertical and horizontal gusts, and interception and tracking of an instrument landing system (ILS)-like landing with a level deceleration (ending prior to touchdown).

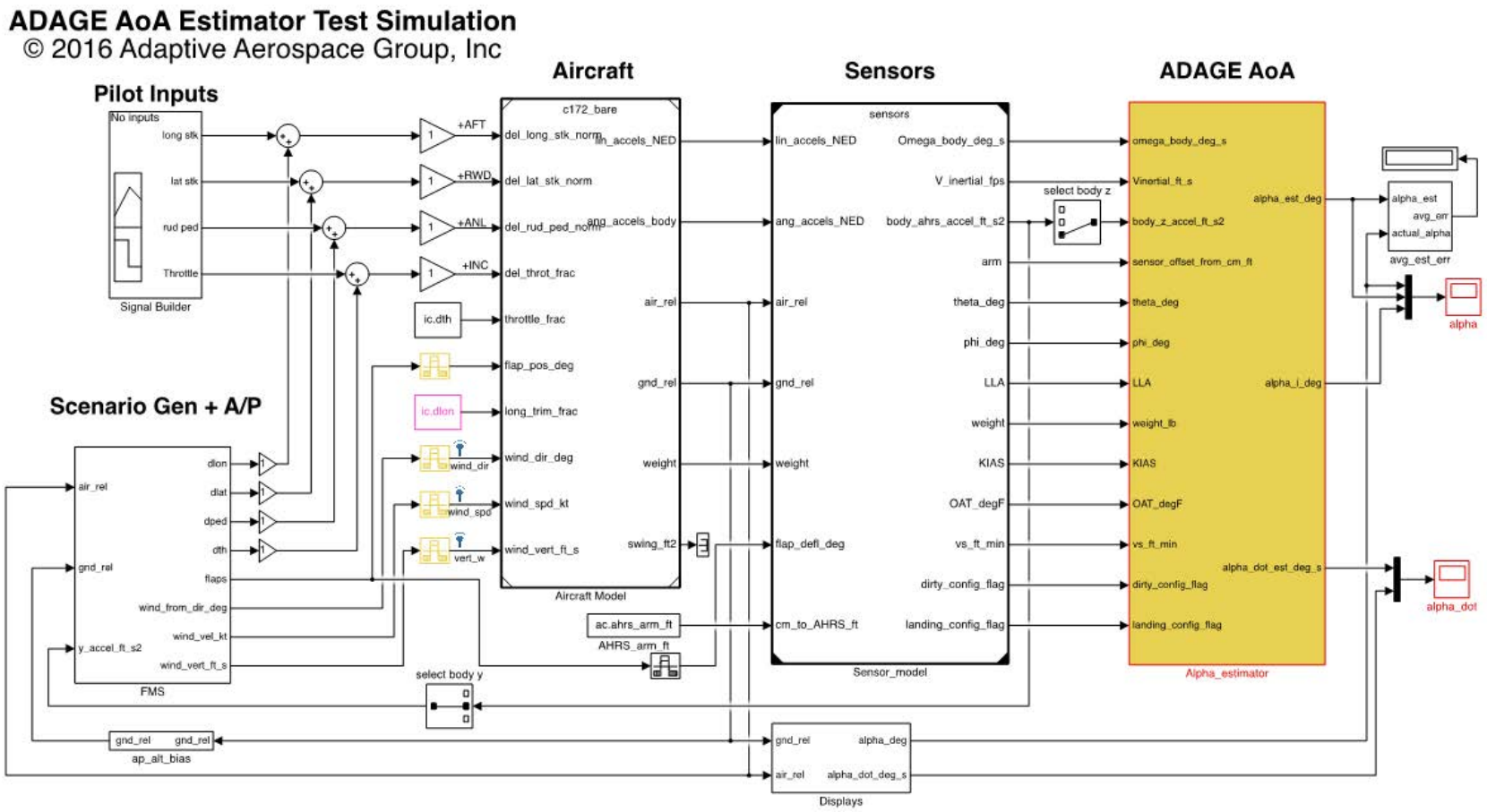

Figure 15. Cessna 172 Simulink simulation model structure overview

The vehicle model included a non-linear approximation of aerodynamics of an aircraft similar to a Cessna 172. It assumed fixed inertias and a simple engine model that simply scaled the throttle input to generate pure thrust along a specified direction relative to the body of the vehicle. No landing gear was modeled except for the drag associated with fixed landing gear. Two flap settings were modeled (0° and 20°) in the aerodynamics model, which was obtained from the FlightGear open-source simulation project's Cessna 172 source code [3].

A set of scripts was developed to trim the vehicle in the longitudinal plane using throttle, elevator, and pitch angle for a specified indicated airspeed.

A Dryden gust model was also included that allowed selection of pseudo-random turbulence at various levels: zero, light (σ = 5 ft/s), moderate (σ = 10 ft/s), and severe (σ = 22 ft/s), in accordance with the definitions in MIL-STD-1797 [4].

4.2 SENSITIVITY/ROBUSTNESS

Prior to performing the sensitivity study, the C_N vs. AoA of the simulated aircraft was generated at the test altitude for two flap settings in a manner similar to in-flight calibration described previously: the simulated aircraft was trimmed at a series of decreasing indicated airspeeds, and the necessary C_N for level flight was calculated and recorded along with the AoA. A line was fit through the resulting points. Figure 16 shows the resulting line fit versus the trim points along with the actual values of C_N vs. AoA from the C code-based aerodynamics model for no flaps. Figure 17 shows the same for flaps extended to 20° as in the landing approach and flare portions of the test maneuver. Both exhibit a very good match until near stall.

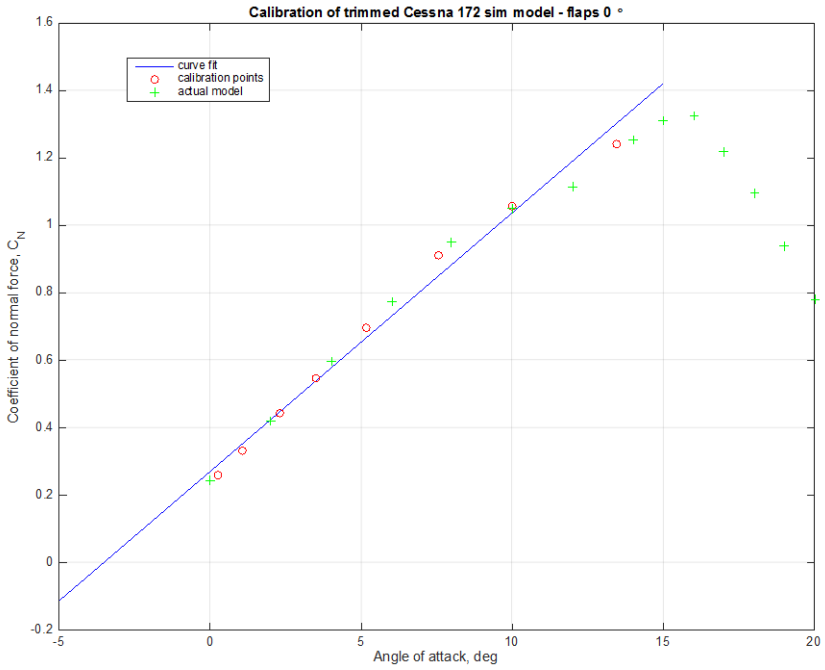

Figure 16. Plot of trimmed, actual, and calibrated C_N vs. AoA for simulated Cessna 172 with no flaps

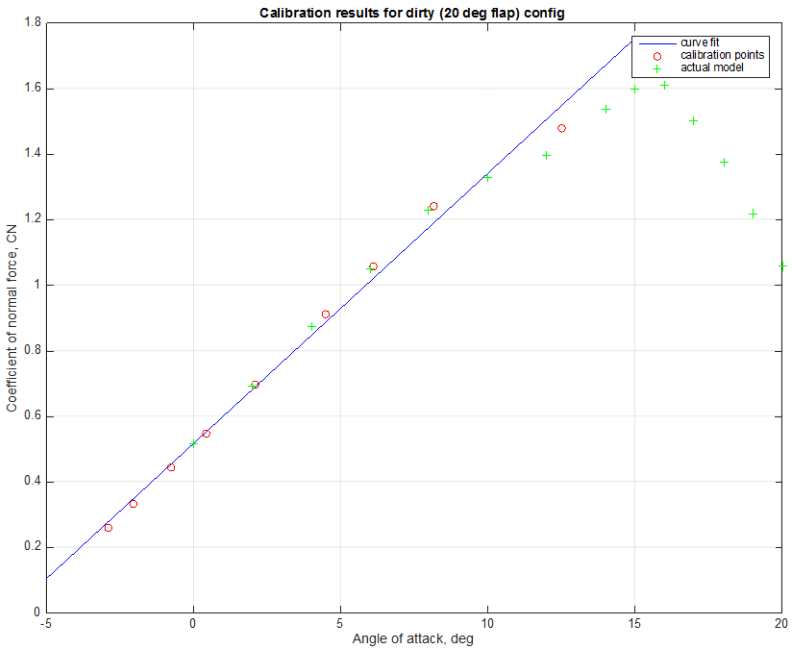

Figure 17. Plot of trimmed, actual, and calibrated C_N vs. AoA for simulated Cessna 172 with 20° flaps

The simulation was used to generate a nominal maneuvering trajectory, as shown in figure 18. The vehicle was trimmed at a specified initial altitude (nominally 2000 ft mean sea level [MSL]) and airspeed (nominally 130 kt true airspeed, thanks to a sufficiently powerful engine model) and then "flown" along the specified trajectory. During this simulated flight:

1. The vehicle flew straight-and-level for 5 seconds (autopilot in altitude hold/bank hold/airspeed hold mode).
2. At 5 seconds, the vehicle was commanded to make a steep 360° (60° bank) left turn.
3. When heading within 58.5° of north, a rollout to wings-level was commanded, and the lateral autopilot's heading mode was selected.
4. Forty seconds after rollout was commanded, a vertical 10-knot gust was encountered. The gust was smoothly introduced over 1 second with a 1-cos function and similarly smoothly ramped back down to 0 amplitude 10 seconds later.
5. Sixty seconds after rollout was commanded, a lateral 2-knot gust from the right was encountered. This smooth-edged gust lasted 4 seconds, including both a 1-second 1-cos function introduction and removal.
6. Eighty seconds after rollout was commanded, lateral navigation mode was selected on the autopilot and commanded to turn toward an initial approach fix (IAF) located approximately along the current path, 25,000 ft north of the starting point, for a somewhat shortened ILS approach to a runway.
7. At 3500 ft from the IAF, the vehicle was commanded to turn toward a final approach fix (FAF) located 10,000 ft due east of the IAF, descend to 1000 ft MSL, and slow to 90 kt true airspeed.

8. At 300 ft from the FAF, the flaps were extended to 20° (at 2° per second), and vertical navigation was commanded to follow the glideslope to a runway at 0 ft MSL and aligned due east.
9. At 100 ft above the runway, the aircraft was commanded to hold altitude and the commanded airspeed was gradually lowered from 90 knots true airspeed (KTAS) at 0.5 kt/sec. This caused the aircraft to flare as if landing with increasing AoA.
10. When commanded, airspeed was reduced to 57.5 KTAS. The deceleration ended.
11. The simulation was normally ended a few seconds later.

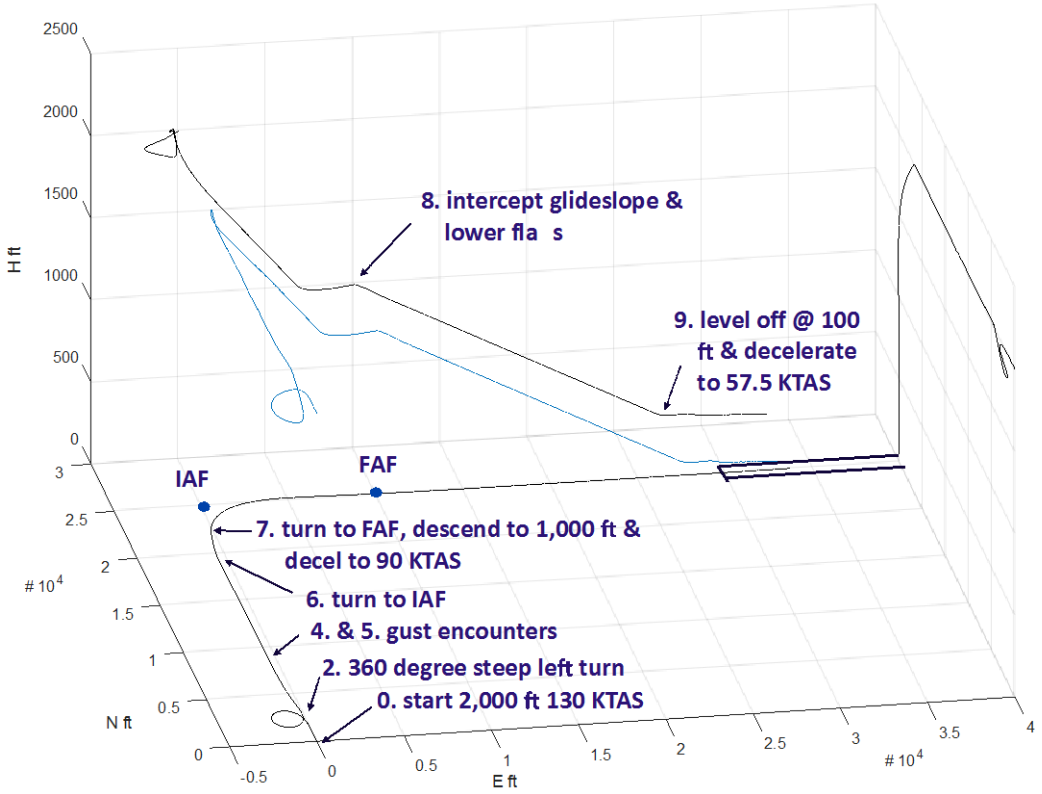

Figure 18. Nominal 3-D trajectory of simulated C-172 during maneuvering, approach, and landing flare (shown in north, east, and altitude axes; numbered maneuvers refer to previous text)

The ADAGE algorithm was executing during the simulation run, providing an estimate of AoA. This value was compared with true AoA; the absolute value of the difference was integrated with time and then divided by elapsed time (with protection against divide by zero at start). This value, $\Delta\alpha_{avg}$, was recorded for the nominal flight and then compared with the same value for flights with errors, biases, or environmental changes included to judge the sensitivity of the estimator to these changes.

Similarly, the maximum difference between true and derived AoA ($\Delta\alpha_{max}$) was calculated for nominal and off-nominal runs to determine the effect of each parameter on the worst match.

4.3 SIMULATION RESULTS

In an attempt to quantify the sensitivity of the ADAGE-derived AoA algorithm to various system parameters, simulation runs were made in which selected parameters were varied. Listed in the tables 1-6 below are the parameters varied, the amount of variance, the change in average and maximum AoA estimator error, and the sensitivity of the ADAGE algorithm per unit variation, based on executing the same maneuver in the Simulink simulation. Note that in some cases, the effect of recalibrating the sensors in the presence of the variation was determined.

An example of this comparison is shown in figure 19. The time histories of several simulation parameters are shown, including Euler angles, AoA and sideslip angle, true airspeed, the two values of the error between derived and actual AoA (aoa_err), and the running average (avg_err) calculated by integrating aoa_err and dividing by elapsed time. The final value of this average is given in tables 1-6 as $\Delta\alpha_{avg}$; the maximum value of aoa_err is given as $\Delta\alpha_{max}$.

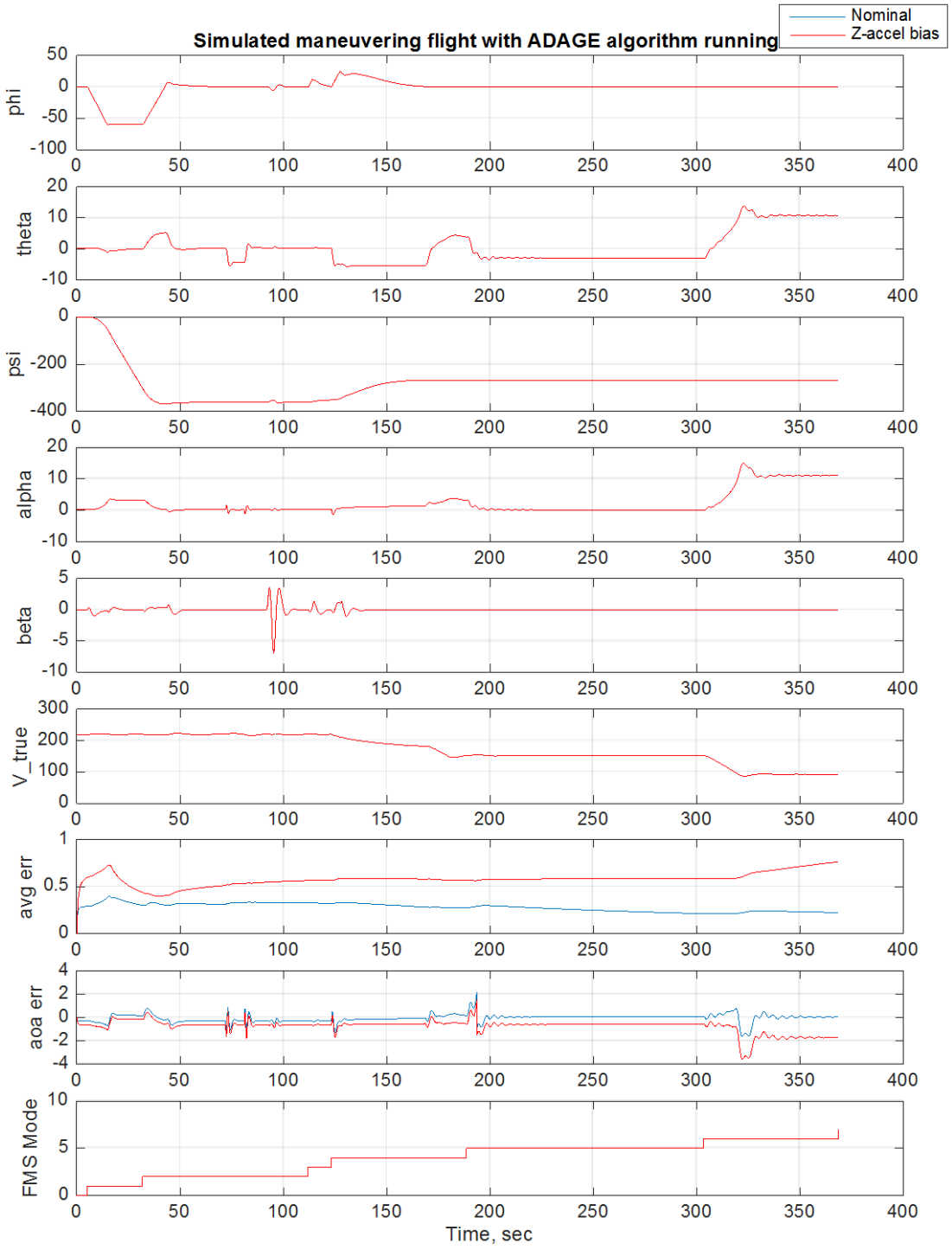

Figure 19. Example parameter time history of effect of inserting bias in Z-accelerometer (red) overplotted with a nominal maneuver trajectory (blue)

Table 1 shows the effect of performing the entire maneuver at an altitude 500 ft higher than the altitude at which the calibration was performed (by adding a bias to the autopilot). The derived AoA algorithm knows the correct altitude, however, so the only effects are because of changes in

aircraft performance and dynamic pressure due to changes in atmospheric density. The estimator seems to have only a small average sensitivity (0.0022 deg/100 ft) to operating at a different altitude than calibrated.

Table 1 shows the effect of reducing vehicle mass by 10% (250 lbm for the Cessna 172 model used). Only a small sensitivity to this reduction is apparent and is likely due to slight differences in mass-based dynamics and a different trim point (products- and moments-of-inertia values were not changed).

Table 1. Effect of operating in out-of-calibrated conditions on average and maximum AoA estimate from the ADAGE algorithm

	$\Delta\alpha_{avg}$, deg	$\Delta\alpha_{max}$, deg	Change in $\Delta\alpha_{avg}$, deg	Change in $\Delta\alpha_{max}$, deg	Sensitivity		
					$\Delta\alpha_{avg}$	$\Delta\alpha_{max}$	Units
Nominal (before bias)	0.2243	2.1702					
500 ft higher altitude	0.2352	2.1952	0.0108	0.0250	0.0022	0.0050	deg/ 100 ft
10% reduction in vehicle mass	0.2963	2.2093	0.0720	0.0391	-0.0072	-0.0039	deg/%

Table 2 shows the effect of shifting the location of the sensor package from the nominal position (at the simulated center of mass) without correcting the algorithm's moment arm for the change. Despite inserting a significant offset, the sensitivity is fairly low again. This is likely due to the lack of aggressive maneuvering that would affect the vertical accelerometer. Few nominal GA maneuvers are aggressive.

Table 2. Effect of variation of uncorrected sensor location offsets on average and maximum AoA estimate from the ADAGE algorithm

	$\Delta\alpha_{avg}$, deg	$\Delta\alpha_{max}$, deg	Change in $\Delta\alpha_{avg}$, deg	Change in $\Delta\alpha_{max}$, deg	Sens., deg/ft	
					$\Delta\alpha_{avg}$	$\Delta\alpha_{max}$
Nominal (before offset)	0.2243	2.1702				
10 ft X (toward nose)	0.2275	2.1933	0.0031	0.0232	0.0003	0.0023
10 ft Y (toward right wing)	0.2242	2.1704	-0.0001	0.0002	0.0000	0.0000
10 ft Z (downward)	0.2225	2.1702	-0.0018	0.0000	-0.0002	0.0000
1 ft X, 0.5 ft Y, -3 Z (3-D displacement)	0.2245	2.1626	0.0002	-0.0076	0.0000	-0.0008

Table 3 shows the effect of adding an angular alignment error to the sensor package, resulting in rate and acceleration cross-talk between axes for each type of sensor. Although 10° was chosen for convenience, it is a fairly small angle, and the estimator shows only a small sensitivity to this amount of alignment. There is certain to be a non-linear effect with larger alignment errors, but 10° appears tolerable.

Table 3. Effect of variation of uncorrected 10° sensor alignment error on average and maximum AoA estimate from the ADAGE algorithm

	$\Delta\alpha_{avg}$, deg	$\Delta\alpha_{max}$, deg	Change in $\Delta\alpha_{avg}$, deg	Change in $\Delta\alpha_{max}$, deg	Sens., deg/deg	
					$\Delta\alpha_{avg}$	$\Delta\alpha_{max}$
Nominal (no error)	0.2243	2.1702				
Roll alignment error	0.2500	2.2602	0.0257	0.0900	0.0026	0.0090
Pitch alignment error	0.2270	2.1621	0.0026	-0.0081	0.0003	-0.0008
Yaw alignment error	0.2244	2.1587	0.0000	-0.0115	0.0000	-0.0011

The effect of tilting the thrust angle of the simulated engine in the aircraft upwards by 5° on derived AoA is shown in table 4. This is also a small effect. Note that no change to the aerodynamic interactions of thrust on the horizontal tail was made.

Table 4. Effect of variation of 5° thrust-line pitch angle increase on average and maximum AoA estimate from the ADAGE algorithm

	$\Delta\alpha_{avg}$, deg	$\Delta\alpha_{max}$, deg	Change in $\Delta\alpha_{avg}$, deg	Change in $\Delta\alpha_{max}$, deg	Sens., deg/deg	
					$\Delta\alpha_{avg}$	$\Delta\alpha_{max}$
Nominal (before bias)	0.2243	2.1702				
With thrust pitch tilt 5°	0.2420	2.1144	0.0176	-0.0558	0.0035	-0.0112

Table 5 shows the effect of inserting biases in the significant inputs of the ADAGE algorithm. Some larger sensitivity values are apparent in this table, including the pitch-rate sensor, airspeed errors, and the Z-body axis accelerometer. Clearly, these three inputs are the most important to have properly calibrated to avoid large errors in derived AoA.

Table 5. Effect of biases applied to various ADAGE input sensors on average and maximum AoA estimate from the ADAGE algorithm

	$\Delta\alpha_{avg}$, deg	$\Delta\alpha_{max}$, deg	Change in $\Delta\alpha_{avg}$, deg	Change in $\Delta\alpha_{max}$, deg	Sensitivity		
					$\Delta\alpha_{avg}$	$\Delta\alpha_{max}$	Units
Nominal (0 bias)	0.2243	2.1702					
Roll rate sensor	0.2243	2.1702	0.0000	0.0000	0.0000	0.0000	deg/ (deg/s)
Pitch rate sensor	0.2396	2.2702	0.0152	0.1000	0.0152	0.1000	deg/ (deg/s)
Yaw rate sensor	0.2243	2.1702	0.0000	0.0000	0.0000	0.0000	deg/ (deg/s)
Inertial velocity bias of +20 ft/s	0.2280	2.1702	0.0037	0.0000	0.0295	0.1013	deg/ (ft/s)
Indic. airspeed bias of +5 kt	0.8143	4.1959	0.5899	2.0257	0.0699	0.2399	deg/ (ft/s)
Vertical speed bias of 100 ft/s	0.2243	2.1702	0.0000	0.0000	0.0000	0.0000	deg/ (ft/s)
Z-accelerometer bias of 3.2 ft/s^2	0.7636	3.5526	0.5393	1.3824	0.1685	0.4320	deg/ (ft/s^2)
Air temperature bias of 20°F	0.2243	2.1702	0.0000	0.0000	0.0000	0.0000	deg/°F
Latitude bias of -20 deg	0.2217	2.1572	-0.0027	-0.0130	0.0001	0.0006	deg/ deg

Also of note is the insensitivity of the ADAGE algorithm to aircraft latitude (used to correct for local gravitation) and air temperature inputs (used to calculate Mach number) because these had no measurable effect on derived AoA (e.g., local gravitation changes by 0.33% between Florida and Alaska). This study shows a fixed value for gravity and a standard atmospheric temperature can be assumed, and these inputs can be removed from the algorithm. The insensitivity to biases on roll and yaw rate measurement biases was not unexpected because yaw rate is not used in the algorithm, and roll rate is used only to estimate roll acceleration for off-axis sensor locations. Vertical speed (which is needed to calculate inertial AoA) is not used in the primary implementation studied here.

The effect of pure transport delays in inputs to the AoA sensor, inserted to mimic digital avionics communication delays, is shown in table 6. Only delays in obtaining attitude (Euler angles) had a significant effect on the difference between derived and actual AoA using the ADAGE algorithm. Delays on some sensors had no effect on the error: with the sensor at the center of mass, only pitch rate is used by the algorithm to correct for steady-state turn rate in estimating AoA rate (alpha-dot). The portion of flight involving steady turns is very small, and changes slowly, so a 1/4-second delay had no measureable effect. Vertical speed is not used in the current implementation and, therefore, delays in obtaining a current value had no effect on errors in derived AoA.

Table 6. Effect of delays applied to various ADAGE input sensors on average and maximum AoA estimate from the ADAGE algorithm, deg/s

	Delay, sec	$\Delta\alpha_{avg}$, deg	$\Delta\alpha_{max}$, deg	Change in $\Delta\alpha_{avg}$, deg	Change in $\Delta\alpha_{max}$, deg	Sensitivity	
						$\Delta\alpha_{avg}$	$\Delta\alpha_{max}$
Nominal	0	0.2243	2.1702				
Attitude sensors	0.25	0.2410	2.0900	0.0167	-0.0802	0.0666	-0.3206
GPS position	1.0	0.2229	2.1701	-0.0014	-0.0001	-0.0014	-0.0001
Rate sensors	0.25	0.2243	2.1702	0.0000	0.0000	0.0000	0.0000
Inertial velocity	0.25	0.2280	2.1797	0.0036	0.0095	0.0145	0.0381
Indic. airspeed	0.25	0.2244	2.1702	0.0000	0.0000	2.4E-5	4.0E-5
Vertical speed	0.25	0.2243	2.1702	0.0000	0.0000	0.0000	0.0000
Z-accelerometer	0.25	0.2243	2.1702	-4.0E-6	0.0000	-1.6E-5	0.0000
Air temperature	10	0.2179	2.1683	-0.0064	-0.0019	-0.0006	-0.0002

It is interesting that the algorithm was not sensitive to a delay in the two input signals on which a bias had a significant effect (indicated airspeed and the Z-axis accelerometer). This may be due to indicated airspeed changing relatively slowly and the Z-axis input being used for low-frequency changes in derived AoA. Pitch and roll attitudes, however, are used to estimate AoA rate and therefore affect the higher-frequency value of derived AoA.

4.4 SENSITIVITY SUMMARY

Based on the simulation results, it is apparent that accurate pitch rate, indicated airspeed, and Z-axis acceleration are essential for a good derived AoA estimate. Of lesser importance is minimizing delay in attitude sensing.

The algorithm appears to be insensitive to errors in moment arm, vehicle mass, sensor alignment, roll and yaw rate measurements, vertical speed, outside air temperature, local gravity (latitude), and transport delays in most other inputs.

5. FLIGHT TESTING

The testing of the two COTS AoA estimation systems along with a separately calibrated AoA measurement system in a high-wing single-engine Cessna is described in this section.

5.1 TEST AIRCRAFT

The in-flight portion of sensor testing was conducted in a 1979 Cessna R182, N736WP. The aircraft was based at Hampton Roads Executive Airport (KPVG) in Chesapeake, Virginia. The vehicle included a digital data collection system, described in section 5.1.1.

5.1.1 Instrumentation

Figure 20 shows a schematic of the AAG-developed data-collection system involved in this study, which included data collected from the Aeroprobe direct-measure sensor, a Garmin 430W navigator, the Aspen PFD display, and a Garmin GLO GPS receiver.

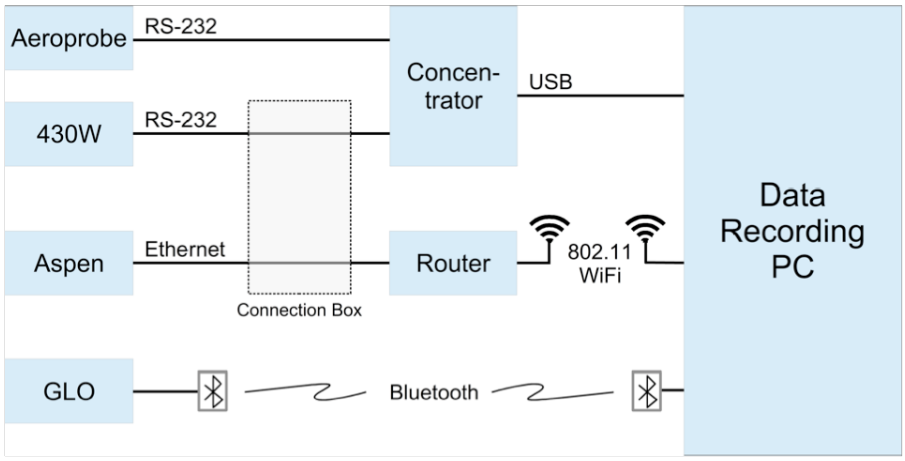

Figure 20. Schematic of onboard sensors and data-recording system data paths

5.2 CALIBRATION PROCEDURE

As described in appendix C, the following system calibrations and aerodynamic parameter identifications were performed:

1. The aircraft's pitot- and static-pressure-based airspeed system was calibrated to obtain calibrated vs. indicated airspeed.
2. The Aeroprobe Air Data Probe was calibrated to match the best-estimated free-stream AoA for different aircraft configurations and uncoordinated flight, using a second-order polynomial fit.
3. X and Z accelerometer bias and scale factors were identified.
4. Angular rate sensor biases were identified.
5. A linear approximation of C_N vs. AoA was obtained for each flap setting.

These calibrations were performed on each data flight and required wind triangles to be flown to obtain horizontal atmospheric motion at the start and end of each flight. An example of a pair of wind triangles obtained in a data flight is shown in figure 21.

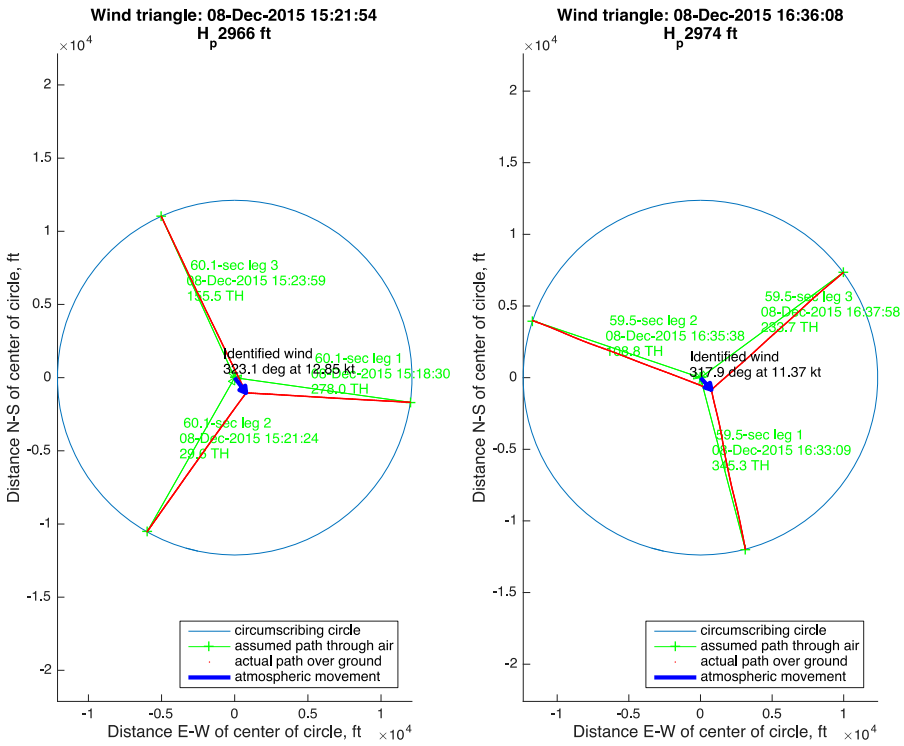

Figure 21. Example wind triangle pair from start and end of data flight

A best-estimated value of free-stream AoA at each trim point was determined as described in appendix C. These values were used to fit a second-order polynomial to the measured Aeroprobe AoA to provide calibration curves for each vehicle configuration tested.

Airspeed calibration was also performed at each trim point using GPS-derived groundspeed corrected with time-interpolated wind speed to obtain true airspeed. Mach number was then determined from outside air temperature and true airspeed; calibrated airspeed was then determined using Mach number. Because indicated airspeed was recorded digitally, the values of calibrated airspeed vs. indicated airspeed for a given vehicle configuration could then be plotted, as shown in figure 22. The airspeed calibration agreed well with the aircraft POH [3].

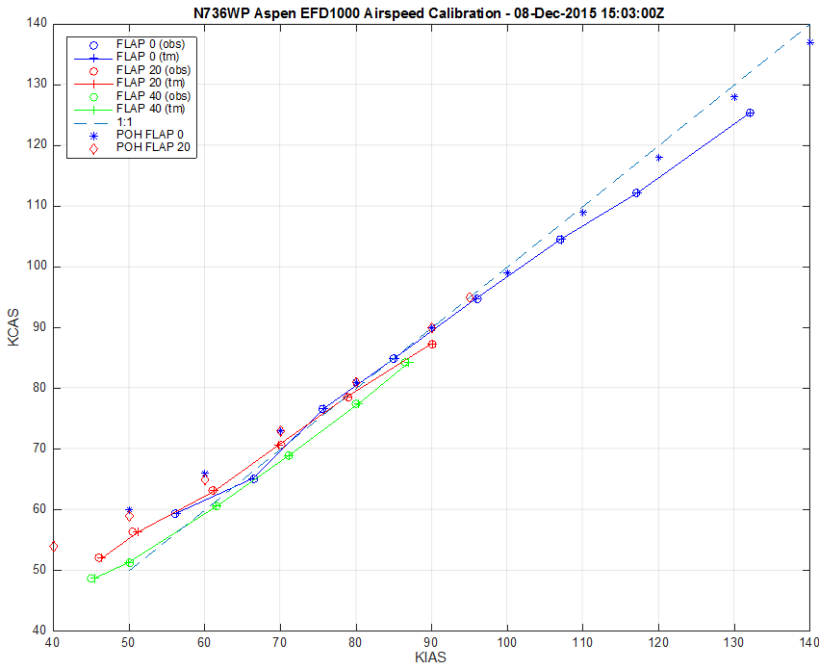

Figure 22. Example of airspeed calibration curves vs. values from the POH from a data flight [5]

In the flight-testing results that follow, while wind data and Aeroprobe calibrations were taken to support data reduction on every flight, the ADAGE algorithm derived AoA values were generated using calibration data taken on a previous flight 12 days prior.

5.3 FLIGHT TEST PROCEDURE

A flight test plan with specific maneuvers was developed and approved by the customer (see appendix D). It called for performing a series of trim points at decreasing airspeeds, followed by an incipient stall and power-off stall, for several aircraft configurations: 0° flaps, 10° flaps/gear up, 10° flaps/gear down, 20° flaps/gear down, and 40° flaps/gear down in coordinated flight, as well as 0° flaps uncoordinated flight. In addition, an accelerated stall at a 45° bank angle was performed. This series was conducted at 3000 ft MSL and again at 9000 ft MSL; selected maneuvers were repeated at 3000 ft MSL with a different fuel margin to see the effect of weight on the sensors.

The Aspen AoA values were based on a single calibration performed after installation of the production software several weeks prior to the test flights. The ADAGE derived AoA values are based on calibration data obtained just a few days prior to the test flights. The Aeroprobe values, treated as the best-calibrated AoA, are based on a per-flight calibration for best comparisons with the other measures.

Figure 13 shows the C_N vs. AoA calibration that was used during these data flights. The Z-axis accelerometer calibration is shown in figure 14. Figures 23(a)–(c) show the calibration of the Aeroprobe for each of the three data flights. To improve accuracy of this important measurement, the best-estimate AoA and Aeroprobe measured AoA for each trim point of both the pre-test

calibration flight and the three flights-for-data were combined at each vehicle configuration, as shown in figure 23(d). Note that the “uncoordinated” test maneuvers were treated as a separate vehicle configuration.

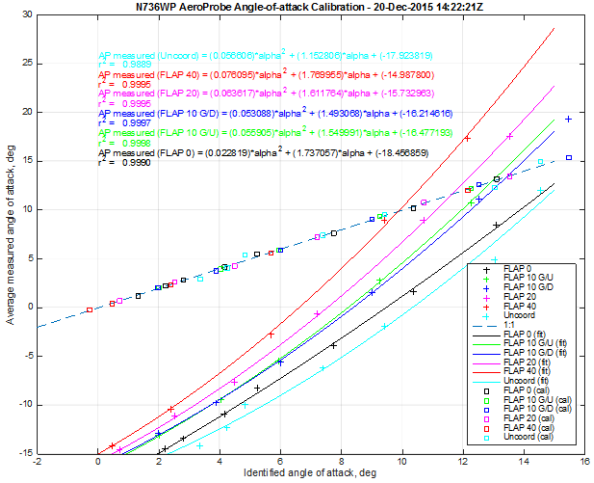

(a) 3000 ft

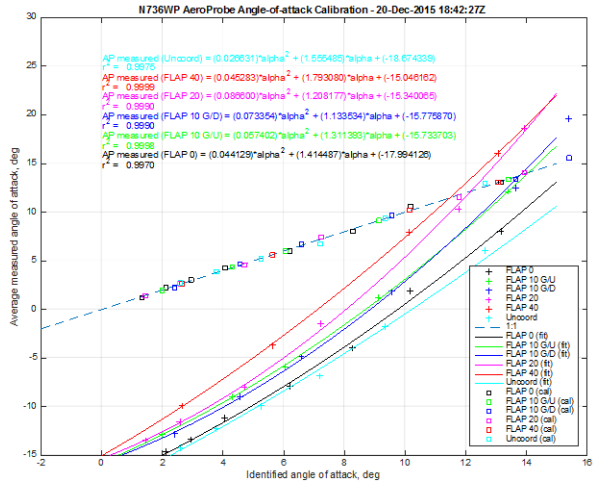

(b) 9000 ft

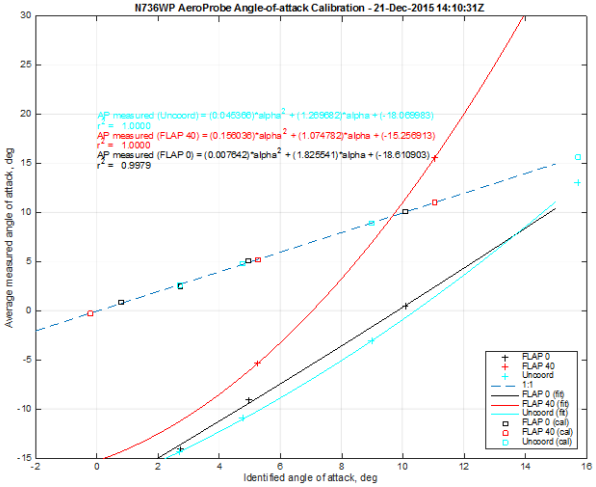

(c) 3000 ft (selected repeats)

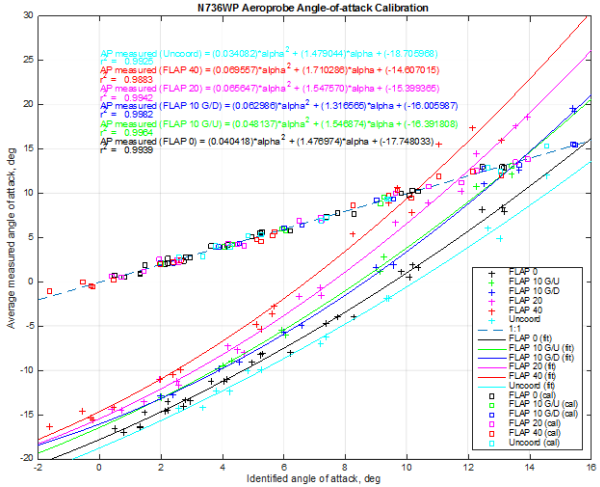

(d) Combined calibration curves used for all data reduction

Figure 23. Per-flight and combined calibrations of the Aeroprobe Air Data Probe AoA measurement

5.4 FLIGHT TEST RESULTS

Comparison plots of various AoA measures and estimates at different aircraft configurations and flight conditions are shown in this section. The calibration series of trimmed points ("trim shots") are depicted first and show the values of AoA obtained from the Aspen PFD's derived AoA, the ADAGE algorithm, the calibrated Aeroprobe sensed measurement, and a derived AoA based on attitude and inertial (navigated) velocities. These calibration plots are followed by data recordings made during various stall maneuvers that compare the calibrated Aeroprobe AoA with the ADAGE derived AoA. In these stall time history plots, the maneuver is marked by a pair of vertical dashed lines indicating that event record; the stall occurs just prior to the ending dashed line. Some data appear before the dashed line that may contain a portion of the previous maneuver.

The stalls included power-off stalls, partial power stalls, and accelerated stalls (clean configuration only). It should be noted that a true aerodynamic stall was not obtained in the test airplane with power at idle because of reduced elevator effectiveness without some thrust being produced. The attempt usually resulted in a pitch oscillation often characterized as "porpoising." The partial-power stalls were usually performed with the power level required for trimmed level flight at the slowest speed calibration point flown just prior to the stall series; it did not represent a full-power-on stall, which was not performed.

5.4.1 AoA Estimation Comparisons (Clean Configuration)

Figure 24 compares four quantitative estimates of AoA compared to calibrated AoA at each of the trim points during the deceleration with the clean (flaps and gear up) configuration for three test flights: the low-altitude, high-altitude, and low-altitude repeat flights. Shown in figure 24 are the Aeroprobe AoA measurement (based on a curve-fitted calibration for each flight), the ADAGE algorithm value, the Aspen "clean" configuration derived AoA value, and an inertial AoA post-flight estimate calculated by AAG based on reconstructed flight-path angle and pitch angle. These are plotted with the "best estimate" of AoA at each of the trim points, based on the calibration method given in appendix C, depicted as the short black line segment connecting a triangle at the start and end of each trimmed segment.

The next set of plots (see figure 25) shows calibrated AoA measured by the Aeroprobe versus the derived AoA values given by the ADAGE algorithm and the Aspen algorithm for the three separate attempts at a trimmed-power stall. Here the throttle was held at approximately the same power setting as the final (low-speed) trim point shown in the previous figures. As shown in these plots, maximum AoA appears to be approximately 18° with partial engine thrust allowing sufficient elevator power for a good stall break. A fairly good comparison between calibrated (as measured by the Aeroprobe instrument) and derived AoA (given by the ADAGE algorithm) is also seen. The Aspen derived AoA appears to be conservative (overestimates AoA) for these stalls.

Figure 26 shows calibrated vs. two derived values of AoA for power-off stalls. In this case, the lack of engine thrust yields reduced elevator authority insufficient to achieve a good stall break, and a series of mushing, porpoising pitch excursions are apparent below 18°. Also in this case, the ADAGE algorithm underestimated the calibrated AoA by as much as 3°. This is attributed to the calibration data being obtained with partial (trimmed) thrust. The effect of thrust on the elevator

included both normal and axial forces that are not included in the ADAGE algorithm. The derived Aspen AoA compares well with calibrated AoA for this configuration.

Finally, calibrated vs. two estimates of AoA is shown in figure 27 for a set of accelerated stalls performed on each flight. In these stalls, the vehicle was banked approximately 45° in a level turn, then a smooth but firm pitch-up command was introduced to raise the nose while maintaining bank angle until stall occurred. The maximum calibrated AoA was close to 18° in all cases, but the derived AoA values tended to be a few degrees higher. This is likely due to the same effects of thrust on the elevator forces and moments not accounted for in the ADAGE algorithm. The Aspen algorithm tended to be more conservative (overestimating AoA) than the ADAGE algorithm.

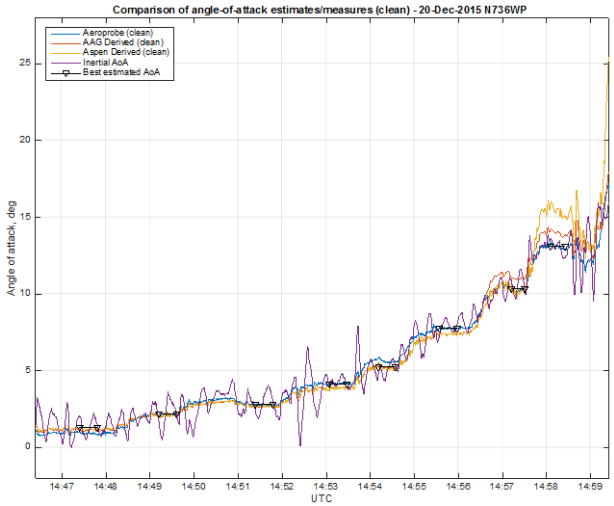

(a) 3000 ft

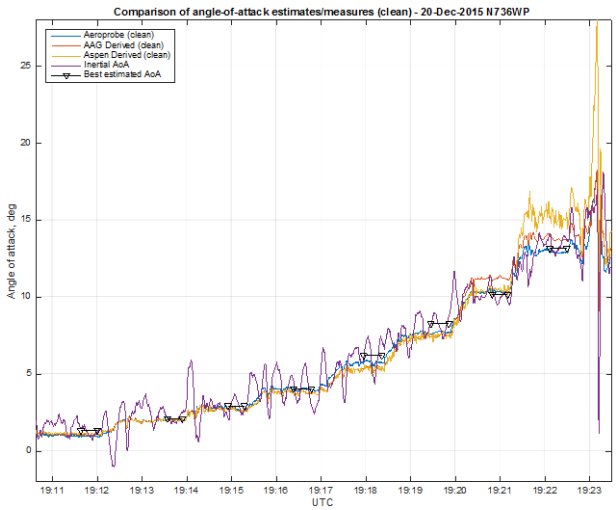

(b) 9000 ft

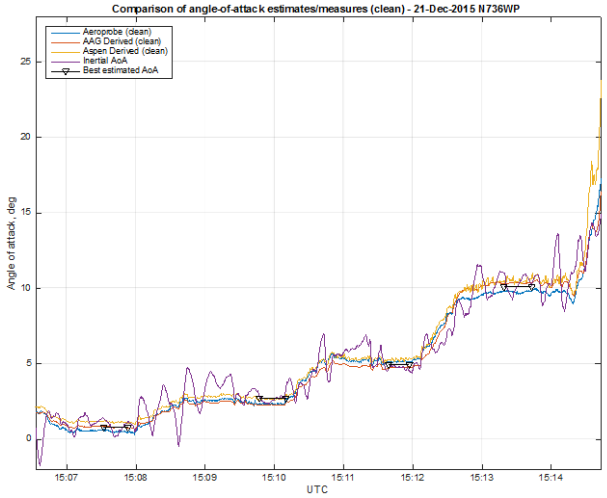

(c) 3000 ft (selected repeats)

Figure 24. Comparison of sensed and derived AoA values during trimmed flight (clean configuration)

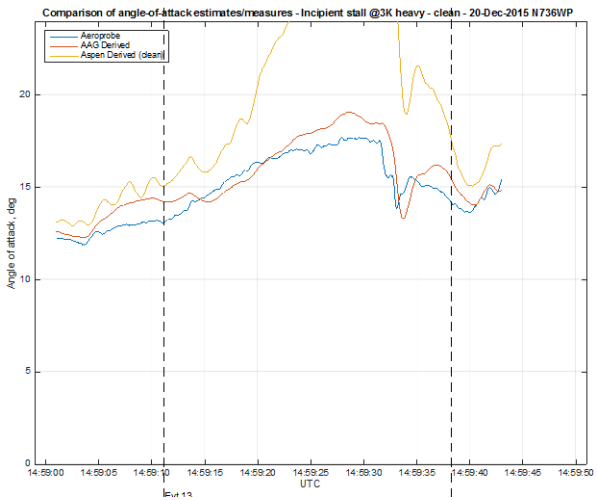

(a) 3000 ft

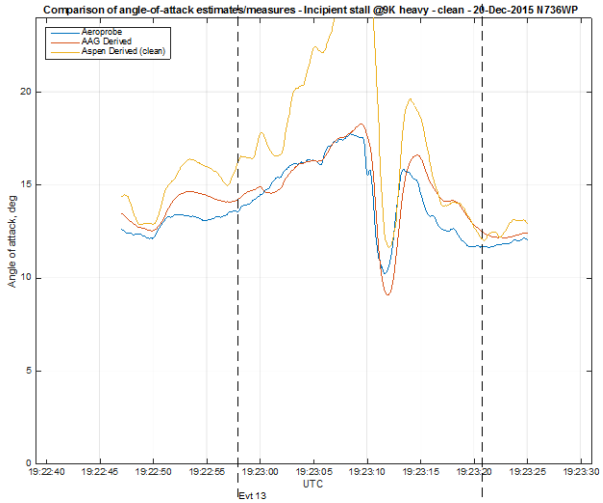

(b) 9000 ft

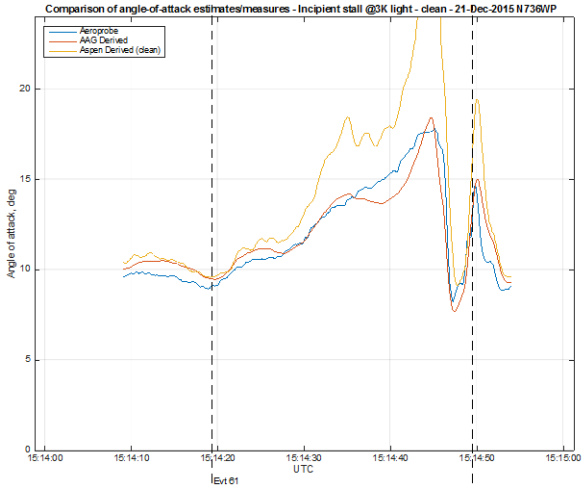

(c) 3000 ft (repeat)

Figure 25. Comparison of calibrated and two derived values of AoA during partial power stalls (clean configuration)

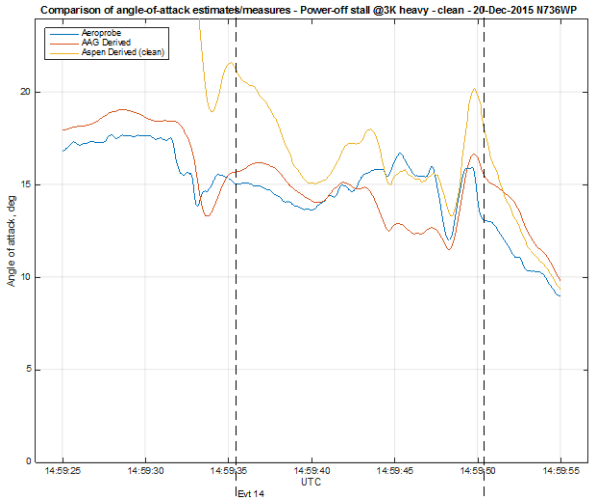

(a) 3000 ft

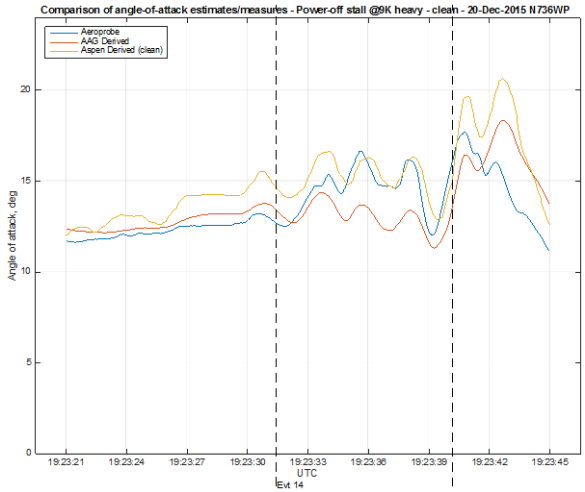

(b) 9000 ft

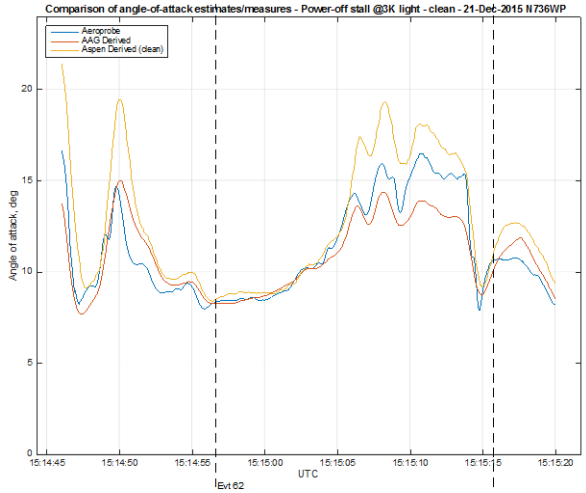

(c) 3000 ft (repeat)

Figure 26. Comparison of calibrated and two derived values of AoA during power-off stalls (clean configuration)

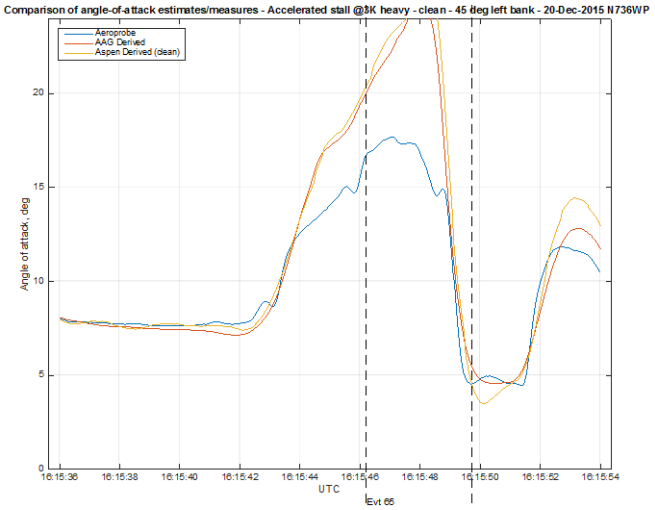

(a) Left 45° bank at 3000 ft

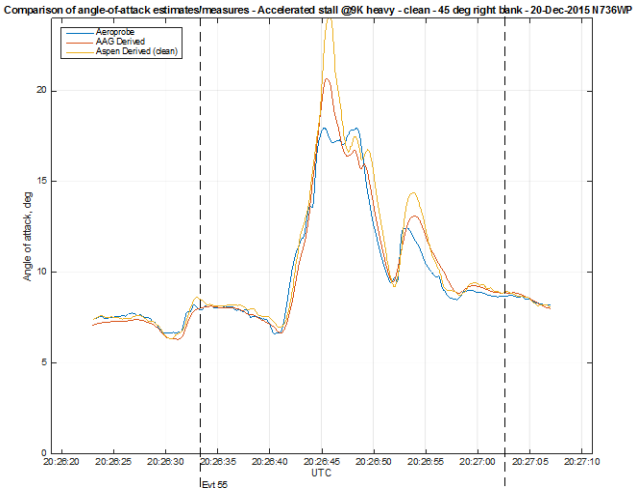

(b) Right 45° bank at 9000 ft

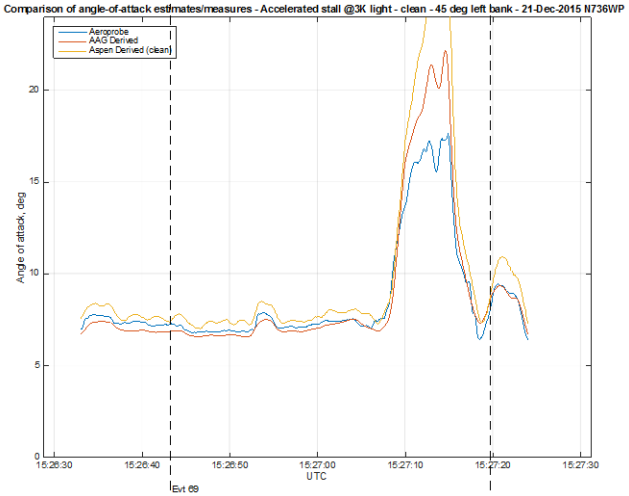

(c) Left 45° bank at 3000 ft (repeat)

Figure 27. Comparison of calibrated and two derived values of AoA during accelerated stalls (clean configuration)

5.4.2 AoA Estimation Comparisons (20° Flaps and Gear-Down Configuration)

In a similar fashion, the trimmed calibration values for each of the sensed and derived AoA sources with 20° flaps, gear down, is shown in figure 28 (this configuration was not tested during the third, 3000 ft "selected repeats," flight). Two items stand out in this set of plots: the derived Aspen AoA values were recorded for the clean configuration only, and the associated derived values used by the display for "flaps down" were not available for logging. As a result, the derived Aspen AoA values are consistently higher at all points. In addition, the ADAGE algorithm overestimates AoA by more than 10° (clipped by the plot) at the final low-speed,
high-AoA trim point shown in figure 28. The source of this disparity, which repeats in the 40° flaps, gear-down configuration as well, was not determined and remains unexplained.

Figure 29 compares two stalls performed with partial power with 20° flaps, gear down. With the engine generating some thrust, a good stall break was experienced. The large disparity between Aeroprobe calibrated AoA and ADAGE derived AoA is due partly to the same unmodeled phenomena noted previously (the numerical Aspen derived AoA value was available only for the clean configuration and is not shown). Because the calibrated C_N vs. AoA relationship (shown in figure 13) is based on AoAs in the 0°–12° range, AoA estimation near stall required extrapolation. In addition, the Aeroprobe was not able to record AoA correctly for most stalls with flaps extended because of the large AoA value; the Aeroprobe data processing limited the measurement in most cases to a pre-calibrated value of 21° AoA (14.5° calibrated AoA for 20° flaps, gear down).

Figure 30 shows derived and somewhat limited calibrated AoA for power-off stalls performed at 3000 and 9000 ft. As with the clean configuration, the lack of engine thrust yields a reduced elevator authority insufficient to achieve a good stall break, and a series of mushing, porpoising pitch excursions are apparent at 9000 ft, whereas the 3000 ft attempt appears to stall. Figure 30(a) shows a significant overestimate at 3000 ft, with the Aeroprobe saturating at calibrated 14.5° AoA, but does not saturate at 9000 ft. The amount of overestimate cannot be determined because of clipping of the calibrated sensor, but the ADAGE algorithm has an internal AoA limit of 25° (clipped by the plot).

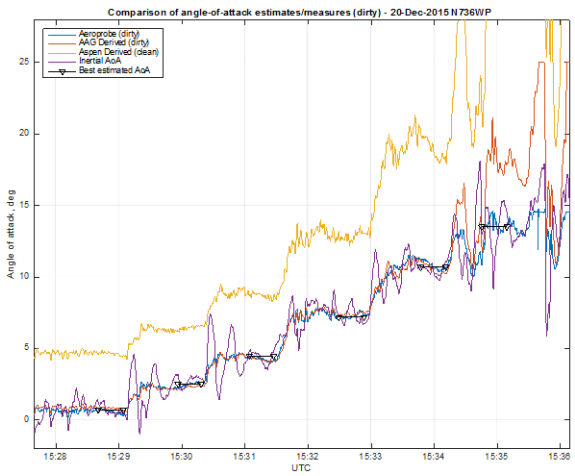

(a) 3000 ft

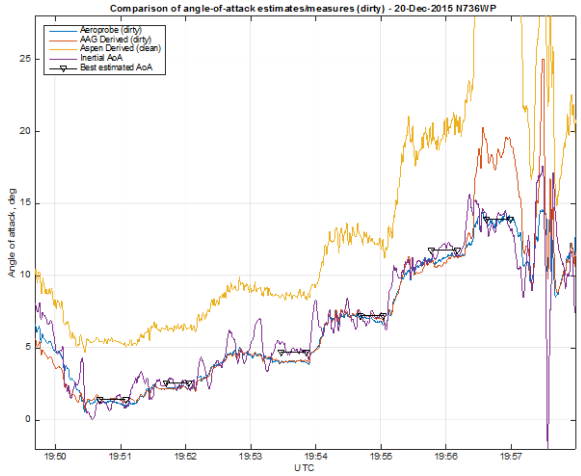

(b) 9000 ft

Figure 28. Comparison of various AoA measures and estimates during trimmed flight (20° flaps, gear down)

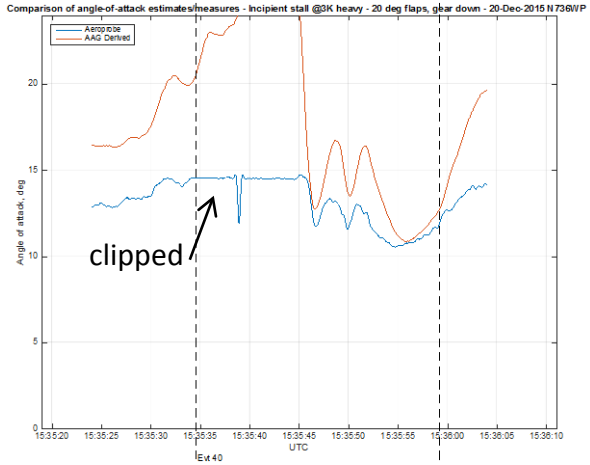

(a) 3000 ft

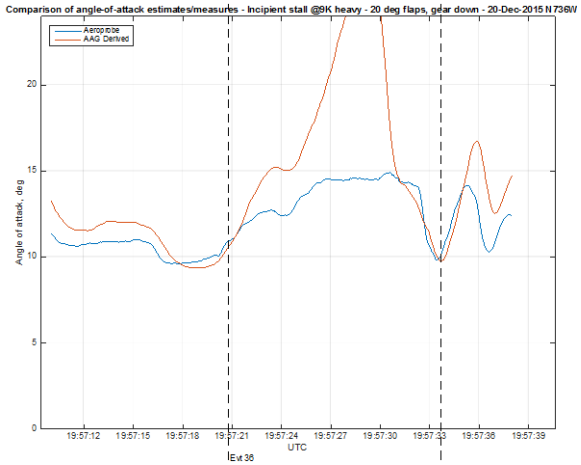

(b) 9000 ft

Figure 29. Comparison of calibrated and derived AoA during partial power stalls (20° flaps, gear down)

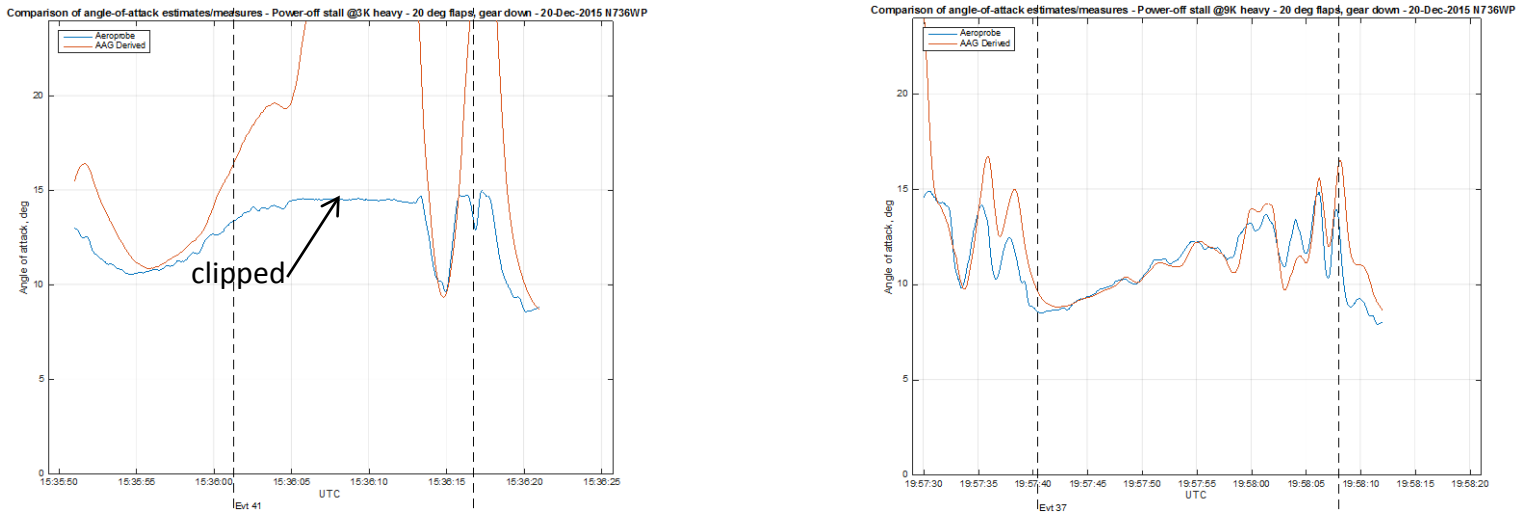

(a) 3000 ft

(b) 9000 ft

Figure 30. Comparison of calibrated and derived AoA during power-off stalls (20° flaps, gear down)

5.4.3 AoA Estimation Comparisons (40° Flaps and Gear-Down Configuration)

Figure 31 shows the trim shots for the 40° flaps, gear-down configuration performed in all three flights. Aside from a 2° discrepancy at the lowest speed trim point (approximately 42 knot indicated airspeed [KIAS]) in figure 31(a), a fairly good match is shown between best-estimated AoA and the ADAGE derived AoA. The numerical value of AoA was not available from the Aspen algorithm for this “dirty” aircraft configuration, so the “clean” derived AoA value is depicted.

Figure 32 compares calibrated Aeroprobe AoA with the ADAGE output in this 40° flap, gear-down configuration. The Aeroprobe pre-calibration saturation value of 21° AoA corresponds with a calibrated value of 13.5° AoA, so the calibrated AoA values saturated in each of these maneuvers. Though ADAGE seems to reach a reasonable stall AoA value between 18° and 20°, a good comparison with ADAGE was not possible.

Comparisons between calibrated and derived AoA during power-off stalls for each flight are shown in figure 33. Figure 33(a) shows that a stall break was achieved on the initial 3000 ft test, but the 9000 ft and 3000 ft repeats, shown in figures 33(b) and (c), depict the familiar lower AoA porpoising due to reduced elevator power. In the stall of figure 33(a), the Aeroprobe saturates at 13.5° AoA and the ADAGE indicates a maximum AoA above 20°.

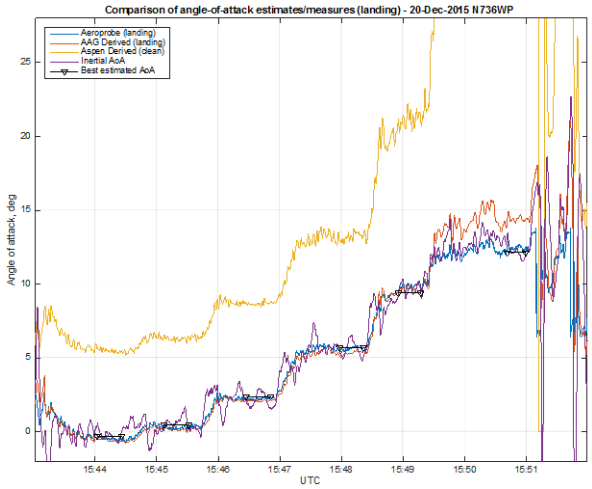

(a) 3000 ft

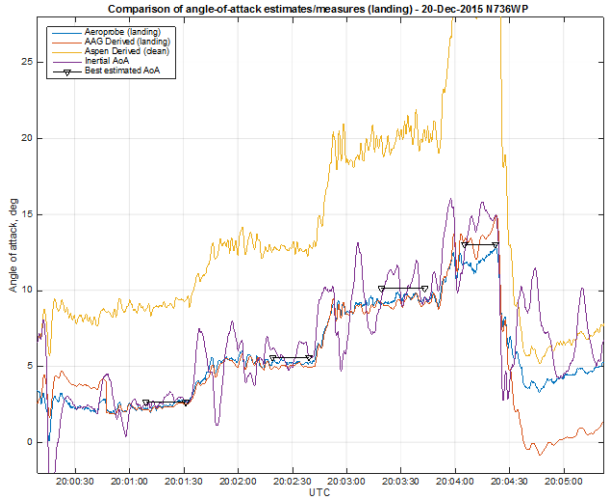

(b) 9000 ft

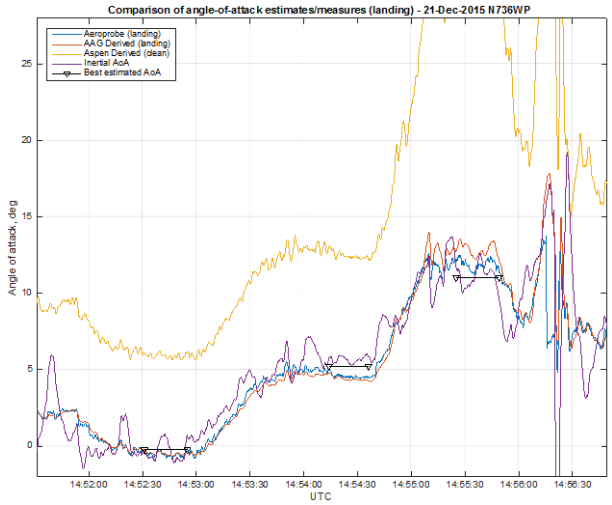

(c) 3000 ft (selected repeats)

Figure 31. Comparison of sensed and derived AoA during trimmed flight (40° flaps, gear down)

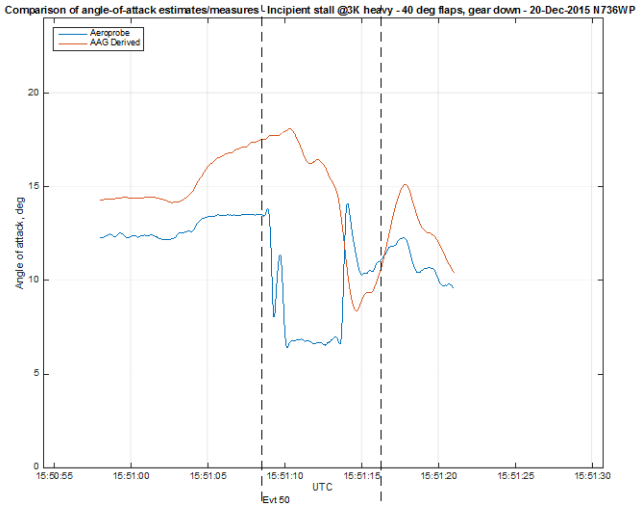

(a) 3000 ft

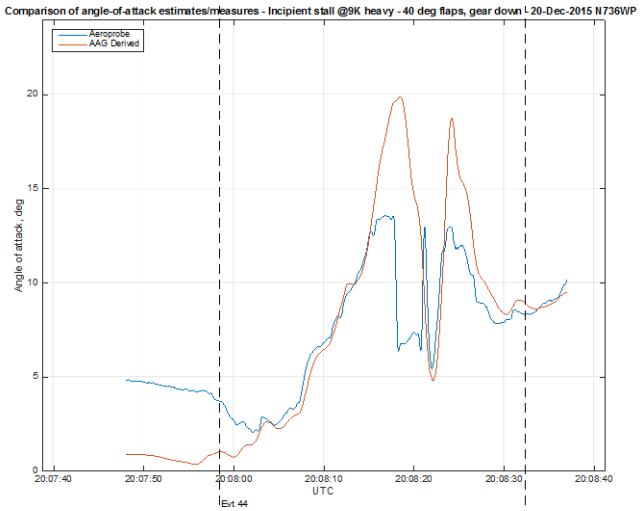

(b) 9000 ft

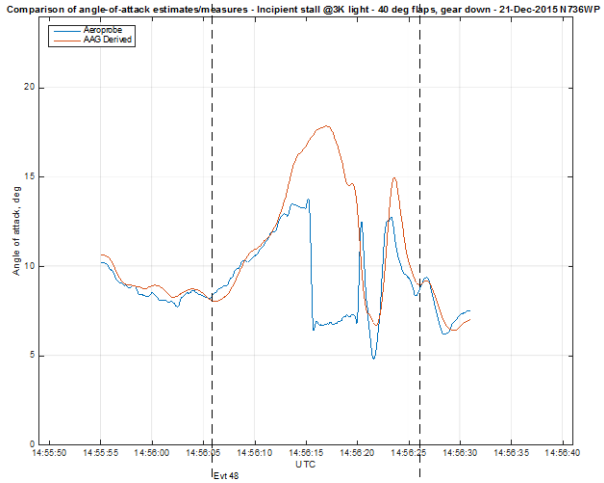

(c) 3000 ft (repeat)

Figure 32. Comparison of calibrated and derived AoA during partial power stalls (40° flaps, gear down)

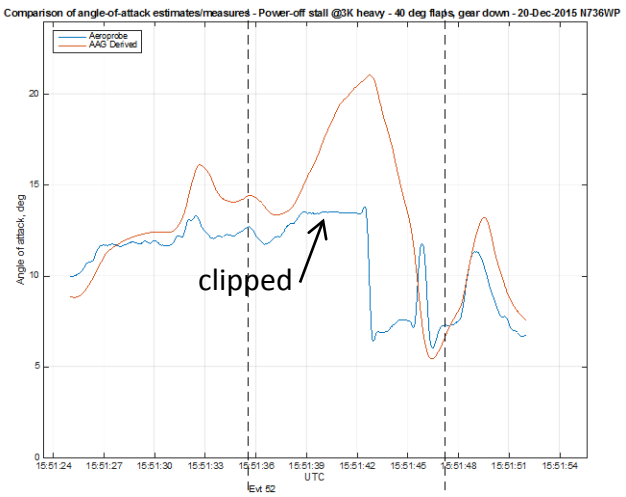

(a) 3000 ft

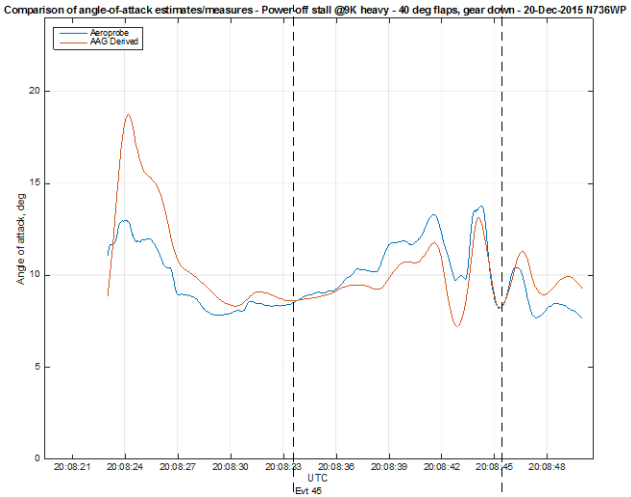

(b) 9000 ft

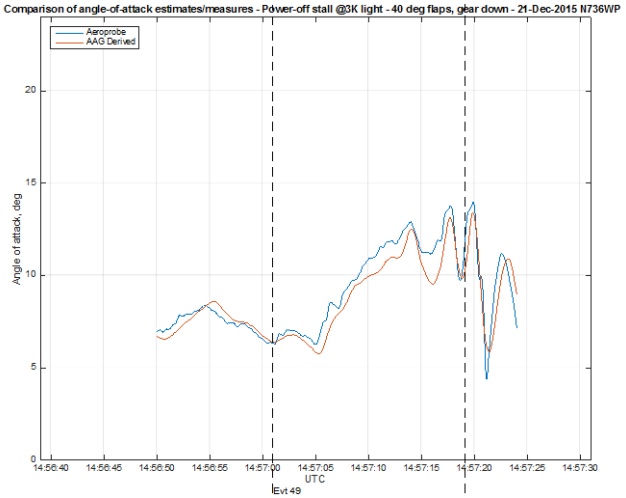

(c) 3000 ft (repeat)

Figure 33. Comparison of calibrated and derived AoA during power-off stalls (40° flaps, gear down)

5.4.4 AoA Estimation Comparisons (Uncoordinated Flight, Clean Configuration)

The effect of sideslip on AoA estimation was explored with a set of trim shots and stalls at 3000 and 9000 ft (two of the three flights), with some selected stall repeats at the lighter weight 3000 ft third flight. Neither the Aspen nor the ADAGE algorithms were calibrated for sideslip, but the Aeroprobe calibration included both left and right sideslips that were averaged from the first two data flights shown here.

The trim shots are shown in figure 34 for the first two data flights used to calibrate the Aeroprobe. A small 1° disparity is apparent between the ADAGE derived value and the calibrated Aeroprobe value of AoA, but on the 3000 ft left sideslip condition shown in figure 34(a), the amount of disparity decreases at lower speeds (higher AoA) and actually changes from an AoA underestimation to an overestimation of approximately 1°. This change of sign is not as apparent for the right sideslip, 9000 ft series, but the disparity is reduced at higher AoA.

Figure 35 shows the calibrated AoA from the Aeroprobe instrument plotted vs. two derived values of AoA from the Aspen algorithm (recorded during flight) and the ADAGE algorithm (calculated post-flight) for all three data flights during a partial-power stall. Because the vehicle was in a clean (flaps and gear up) configuration, the Aeroprobe saturated at 17.7°; this value was not exceeded for these maneuvers. With partial power, a stall break was achieved in each flight at approximately 18° calibrated AoA. The ADAGE gave a reasonable estimate within 3° throughout the maneuver for the first two data flights (figure 35(a) at 3000 ft and figure 35(b) at 9000 ft), whereas the Aspen continued to show a conservative estimate of AoA. However, during the 3000 ft repeat flight with the sideslip angle reversed, a large disparity is shown between calibrated and the derived value of AoA from the ADAGE algorithm. The cause for this disparity is unknown. A good comparison was indicated in the clean coordinated power-off stall immediately preceding this maneuver (shown in figure 26(c)) and in the clean accelerated stall immediately following the next maneuver (shown in figure 27(c)). Clearly this disparity was not caused by an inadvertent repositioning of the Aeroprobe sensor.

In similar fashion, figure 36 compares calibrated and two derived values of AoA for power-off stalls in the same three flight conditions. It does not appear that a stall break was achieved in power-off flight, and porpoising is again evident, especially in the 9000 ft case (figure 36(b)). The same large disparity in the ADAGE derived AoA is evident in figure 36(c) for the 3000 ft, right sideslip repeat stall, whereas the Aspen only slightly overestimated AoA in all three stalls.

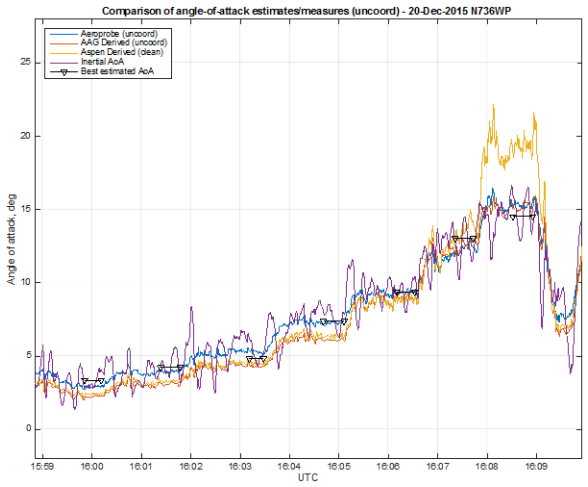

(a) One ball width to the left–3000 ft

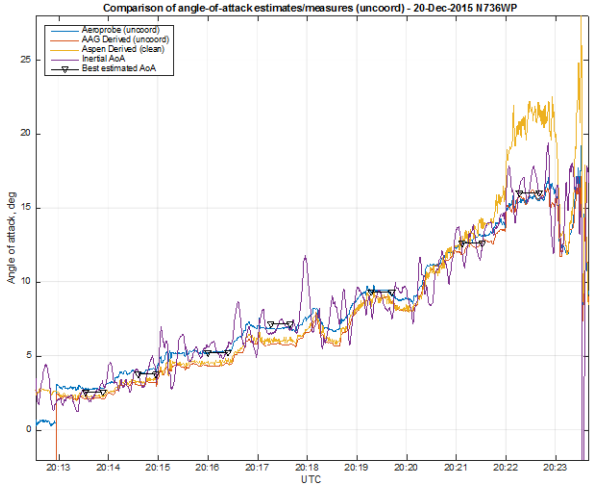

(b) One ball width to the right–9000 ft

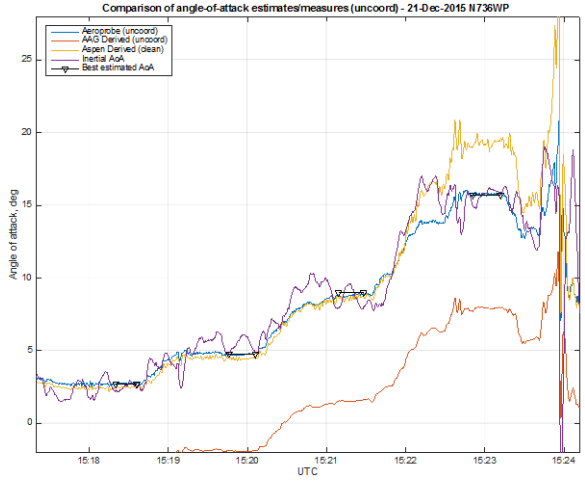

(c) One ball width to the right–3000 ft (repeat)

Figure 34. Comparison of calibrated and derived AoA during uncoordinated flight (clean configuration)

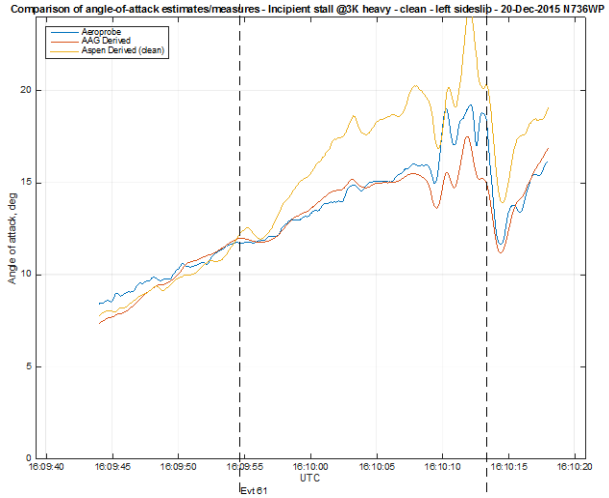

(a) One ball width to the left–3000 ft

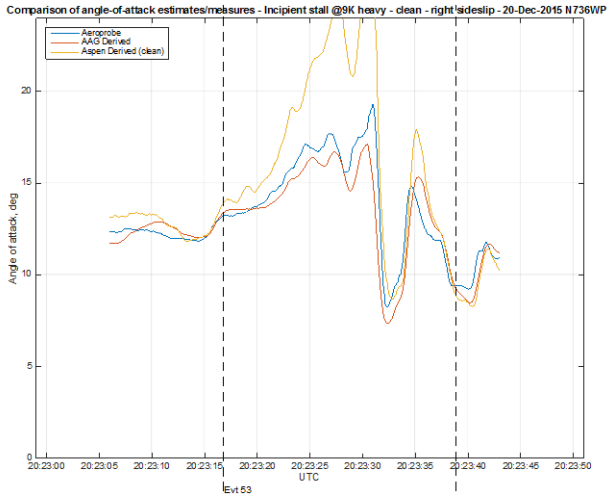

(b) One ball width to the right–9000 ft

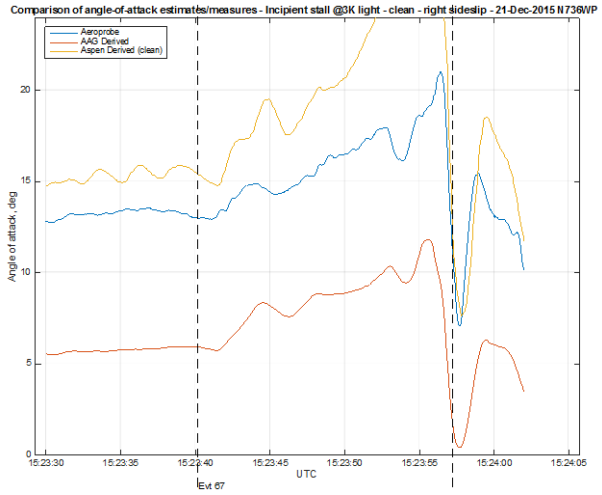

(c) One ball width to the right–3000 ft (repeat)

Figure 35. Comparison of calibrated and two derived values of AoA during partial power stalls (clean, uncoordinated)

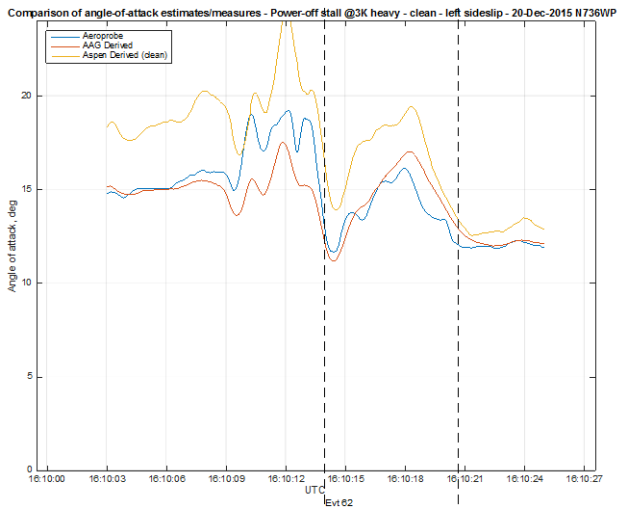

(a) One ball width to the left–3000 ft

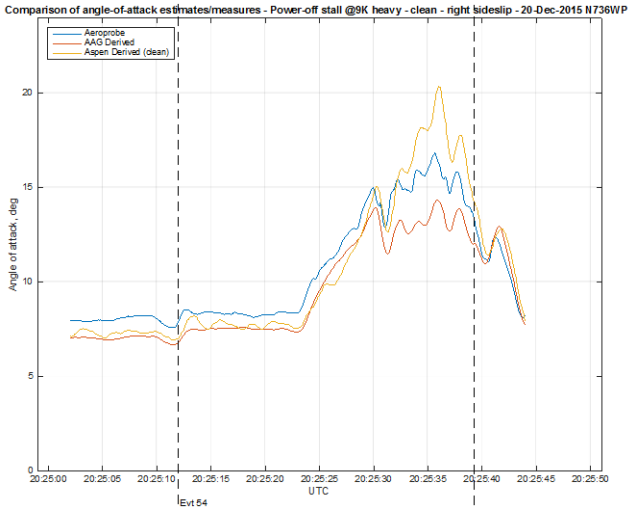

(b) One ball width to the right–9000 ft

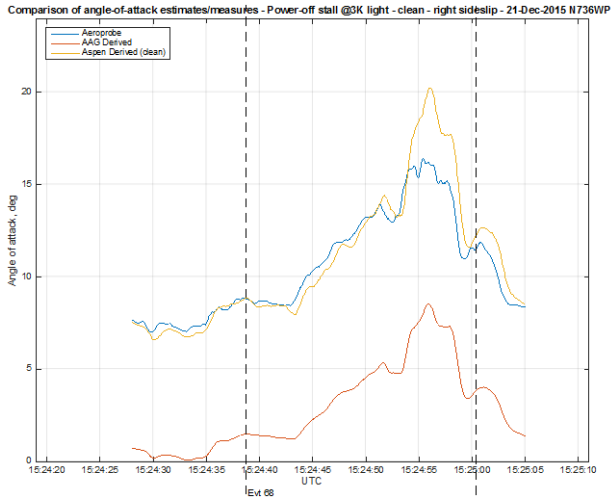

(c) 3000 ft (repeat)

Figure 36. Comparison of calibrated and two derived values of AoA during power-off stalls (clean, uncoordinated)

5.4.5 AoA Estimation Comparisons (10° Flaps and Gear-Down Configuration)

Trim shots and stalls were performed in a configuration with 10° flaps and gear down. This configuration was not included in the calibration points used by the ADAGE algorithm to see the effect of an unmodeled reconfiguration on the derived AoA values it provided. The Aeroprobe was recalibrated for this condition, however, to make the comparison as valid as possible. This configuration was not flown on the third, selected-repeats flight. Numerical derived values of AoA for this configuration were not available from the Aspen PFD.

Figure 37 shows the trim points performed at 3000 ft and 9000 ft in this configuration. Because the ADAGE was not calibrated for this configuration, but a clean configuration calibration was used, a 3°–4° overestimation of AoA is apparent when compared with both the Aeroprobe AoA and best estimated AoA.

Figure 38 compares calibrated Aeroprobe AoA with the ADAGE-generated AoA during partial-power stalls, which reflect the bias shown earlier in both altitudes. In this configuration, the Aeroprobe calibrated AoA was limited at 15.9°, so the disparity is even greater.

Similarly, figure 39 compares calibrated Aeroprobe AoA with the ADAGE-generated AoA during power-off stalls, which reflect the bias shown earlier in both altitudes. In this maneuver, the Aeroprobe did not reach saturation.

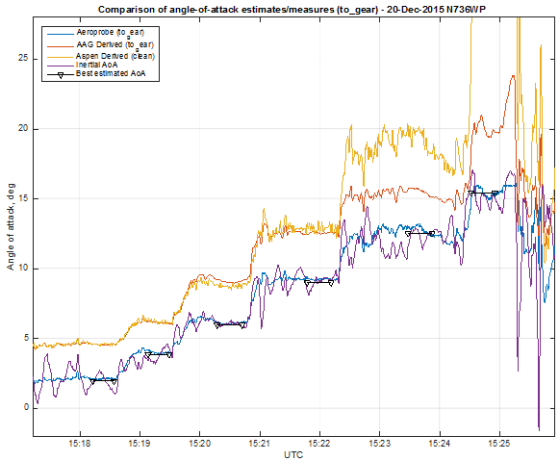

(a) 3000 ft

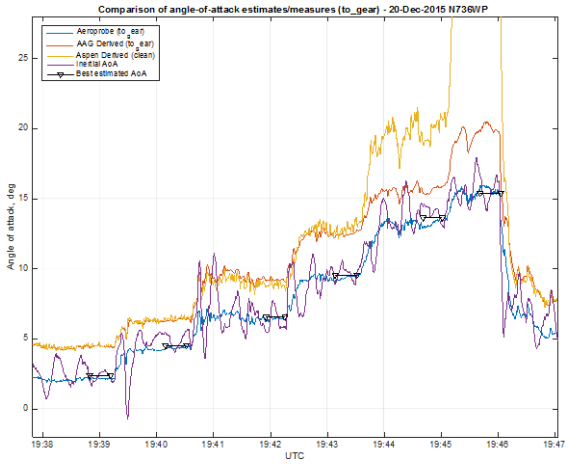

(b) 9000 ft

Figure 37. Comparison of various AoA measures and estimates during takeoff (10°) flaps + gear-down configuration

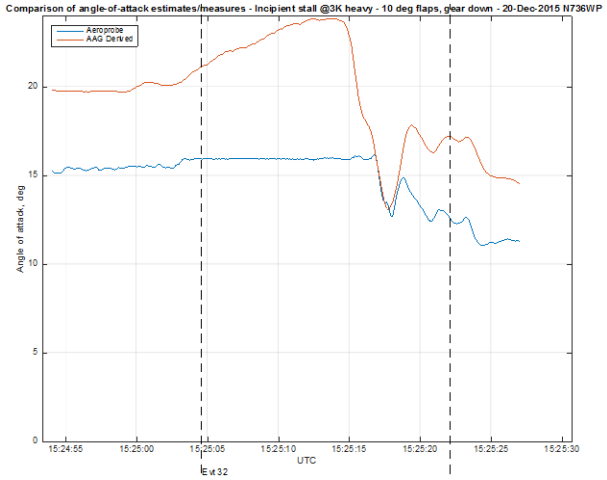

(a) 3000 ft

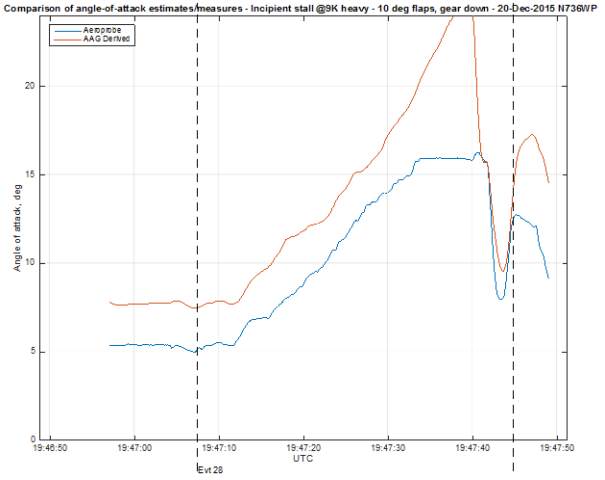

(b) 9000 ft

Figure 38. Comparison of calibrated and derived AoA during partial power stalls (10° flaps, gear down)

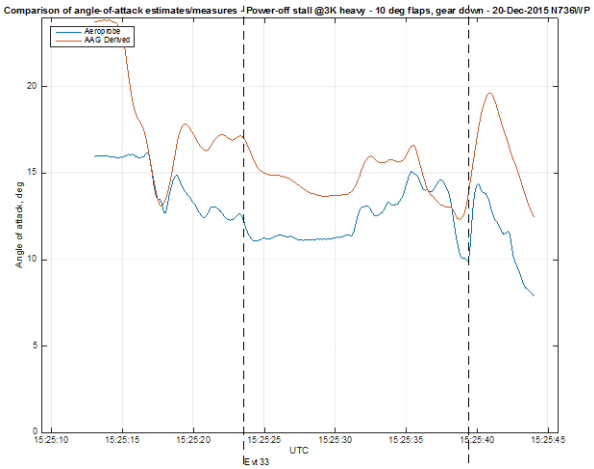

(a) 3000 ft

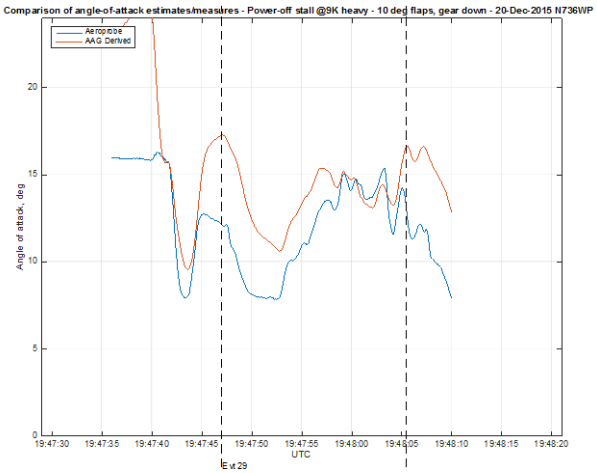

(b) 9000 ft

Figure 39. Comparison of calibrated and derived AoA during power-off stalls (20° flaps, gear down)

5.4.5.1 AoA Estimation Comparisons (10° Flaps and Gear-up Configuration)

Figures 40–42 show similar results to the previous section, except the gear was not extended. Results appear similar to the gear-down, 10° flap case.

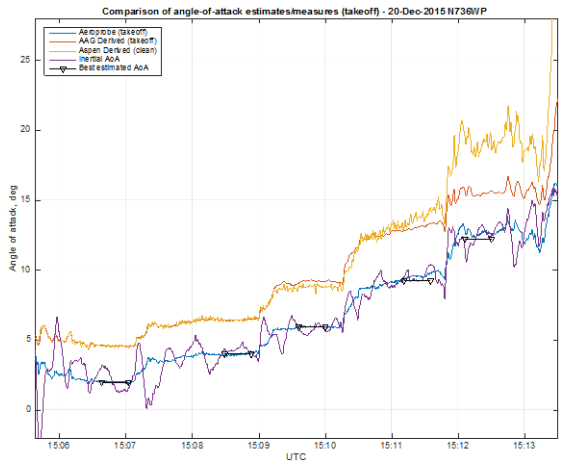

(a) 3000 ft

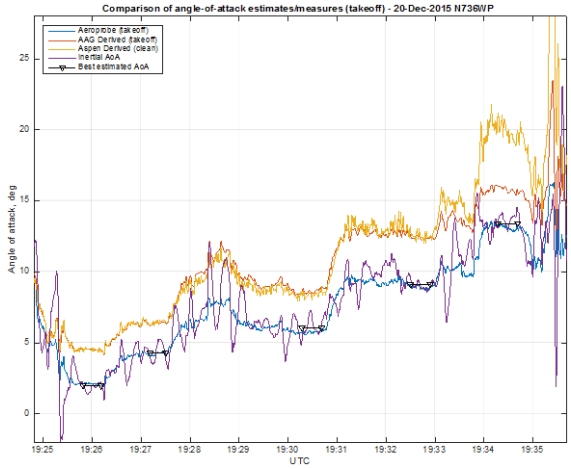

(b) 9000 ft

Figure 40. Comparison of various sensed and derived AoA values during takeoff (10°) flaps + gear-up configuration

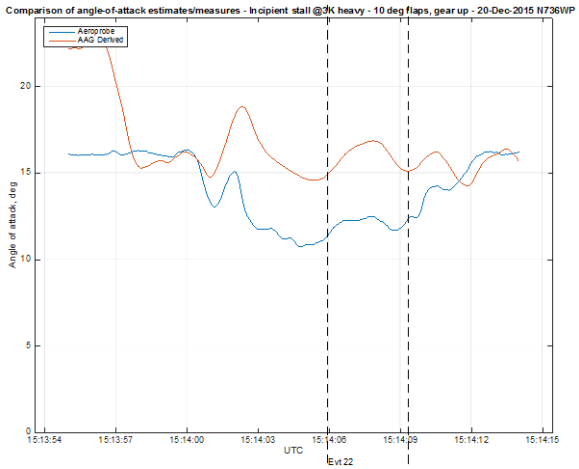

(a) 3000 ft

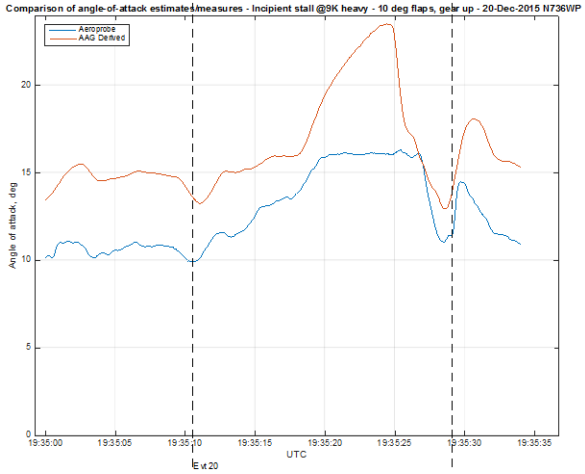

(b) 9000 ft

Figure 41. Comparison of calibrated and derived AoA during partial power stalls (10° flaps, gear up)

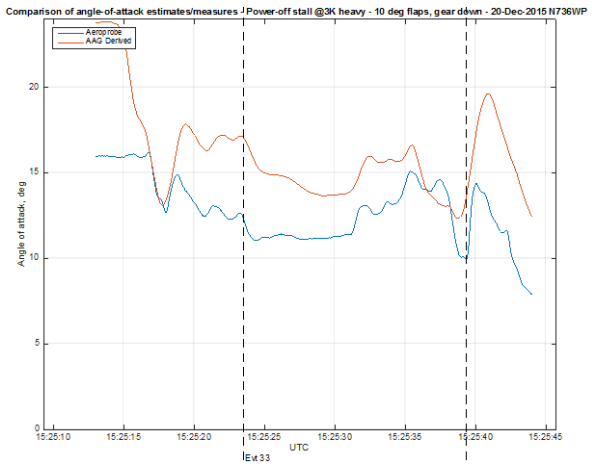

(a) 3000 ft

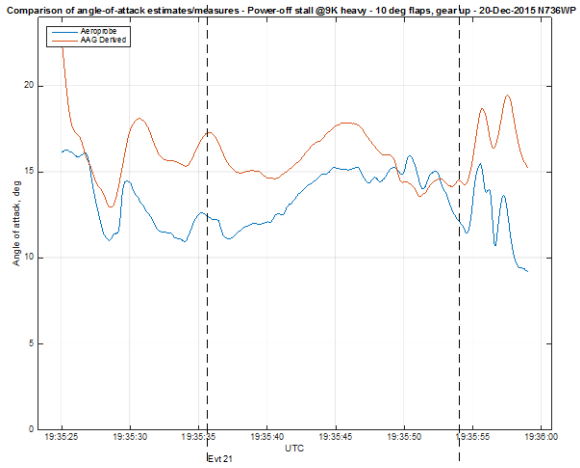

(b) 9000 ft

Figure 42. Comparison of calibrated and derived AoA during power-off stalls (10° flaps, gear up)

6. DISCUSSION OF RESULTS

During the course of this investigation, several observations were made and lessons learned about the different sensed or derived AoA systems. Some impacts to certification of such systems were also apparent and are addressed here.

6.1 DIRECT SENSED AOA MEASUREMENT SYSTEMS

The performance of both of the direct-measure Garmin and Aeroprobe AoA multi-hole probe systems were highly dependent on probe-mounting location. This is clearly a problem in the retrofit market, because each aircraft type has a different set of possible mounting locations and limitations. Given that the average avionics shop likely has no experience with and little understanding of the requirements and limitations of these new systems, installation and calibration procedures should, for now, be closely monitored.

The Garmin and Aeroprobe probes performed satisfactorily when properly located.

6.1.1 Aeroprobe Test Probe

Early in the use of the Aeroprobe as an independent measure of AoA, the probe was mounted with its tip just ahead of the leading edge of the right wing. This positioning resulted in a very nonlinear response due to the rapidly increasing local upwash at the leading edge as free-stream AoA increased. Mounting the probe lower and farther aft on the wing strut provided better results. However, the particular Aeroprobe model used in testing was limited to a range of ±20° AoA; as a result, the raw AoA measurement (uncalibrated for local flow angularity) hit the upper limit just before stall AoA with some flap configurations, even though the probe was mounted oriented somewhat tip down. A production AoA measurement system would have to avoid such an AoA range limitation.

6.1.2 Garmin Retrofit Probe

The Garmin probe was initially mounted at approximately 49% of the chord length in the longitudinal direction and well outboard of the trailing edge flap in the spanwise direction. It worked well at this position for the single-flap configuration used during its calibration. However, other flap deflections changed the local flow field at this location and yielded premature stall indications.

The manufacturer's installation manual called for location of the probe no farther aft than "60% chord length" with "best performance" obtained "within 20% of the chord length" from the leading edge of the wing.

The Garmin probe was subsequently relocated closer to the leading edge at approximately 17% chord length, with improved results; the variation in indication with different flap deflections was greatly reduced.

6.2 DERIVED AOA SYSTEMS

The Aspen- and AAG-developed derived AoA systems generally performed well. However, both showed some limitations.

6.2.1 Aspen Derived AoA

The Aspen derived AoA algorithm tended to indicate higher (conservative) AoA at slower speeds, especially near stall AoA. The divergence of indicated and calibrated airspeeds at lower speeds in the test aircraft may have been responsible for this conservative estimate of AoA. The Aspen PFD calculates and displays KIAS from pitot/static system inputs (correction to knots calibrated airspeed [KCAS] is apparently not performed, because no ability to provide calibration data is apparent). Given the divergence between indicated and calibrated airspeed that exists below 60 knots (KIAS starts to read lower) in the test aircraft, the Aspen AoA algorithm likely is using a lower dynamic pressure estimate. This would require a higher AoA to achieve the sensed normal acceleration (load factor). This overestimate of AoA near stall is actually conservative and likely adds safety in most cases, except if the AoA display is relied on for maximum performance. If the KIAS/KCAS calibration curve diverged from linearity in the other direction, the Aspen derived AoA value might be less conservative.

The calibration process for the Aspen involved flying three test points: two in the "clean" configuration and one in the "dirty" configuration. This implied a single lift-curve slope was identified for the clean case, and a bias was added to this line, with no change in slope, for the dirty case.

Note that AAG had no knowledge of the Aspen AoA estimation algorithm. The Aspen-specified calibration procedure was followed, from which some of the basic assumptions used therein could be inferred from the experience developing the AAG AoA estimation algorithm.

6.2.2 ADAGE

The ADAGE algorithm tended to overestimate AoA by 3°–8° with power settings higher than a 1-*g* level-flight thrust setting, such as during accelerated stalls. The Aspen derived AoA value was generally even higher by as much as 10°, originally shown in figure 27 and replotted with an expanded AoA scale in figure 43. This was likely due to a stronger propeller slipstream generating more downforce on the elevator, changing the lift distribution between wing to horizontal tail, and no longer matching the identified C_N vs. AoA relationship (obtained from calibrations in trimmed level flight). The AAG algorithm derivation (appendix A) assumed thrust and elevator effects were directly correlated with AoA (i.e., 1-***g*** level flight). In similar fashion, AoA was underestimated by approximately 2° for power-off stalls, likely due to the same effect, as shown in figure 26. Performing calibrations at other than trim thrust might improve this result, but would require feedback of power setting to the algorithm. It is not known if these effects would be similar in other typical GA aircraft.

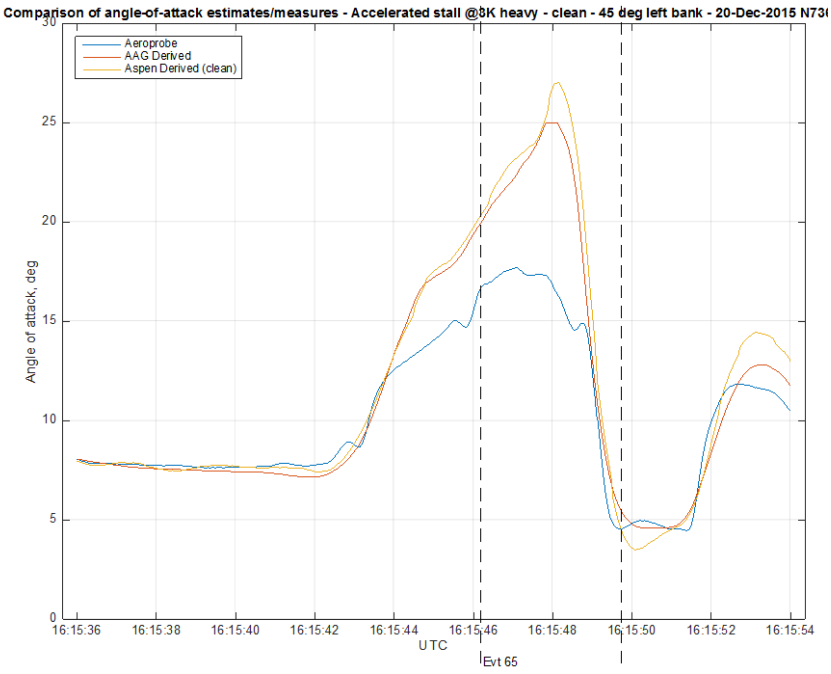

Figure 43. Comparison of calibrated and two derived values of AoA during accelerated stalls (clean configuration, left 45° bank, at 3000 ft; same data as plotted in figure 27(a) but with an expanded AoA scale)

The ADAGE algorithm utilized calibrated airspeed. This calibration was obtained through flight test in the specific test aircraft. Performing such an extensive calibration cannot be expected in retrofit systems. However, the resulting airspeed calibration closely matched the indications in the POH. Derived AoA systems like Aspen's might yield better results if the airspeed-calibration data from the POH were included so the airspeed used in the estimation algorithm would be closer to calibrated airspeed.

A strong dependence on configuration suggests the need for extensive calibrations, likely beyond the scope of a typical pilot owner, even if throttle and flap settings were inputs to the algorithm. One approach to reduce the number of calibration points would be flying the vehicle at only two different configurations (clean and landing) and at two speeds (approach and a higher speed —two points for each flap setting). A linear fit for C_N vs. AoA could be identified for these two configurations. Without flap-position information, the derived AoA could be displayed to the pilot with two indices, similar to the Aspen approach. However, accounting for power effects would not be included in the algorithm.

Other disparities in the ADAGE results remain unexplained, notably during 1-ball-width uncoordinated flight and at higher AoA with a 20° flap setting. For the 20° flap case, the discrepancy is conservative (overestimates AoA), as shown in figure 29; conservatism is not true for the uncoordinated flight case (see figure 35) in which the derived AoA is lower than actual. The reason for these disparities is as yet unidentified.

6.3 OBSERVATIONS OF DIFFERENCES BETWEEN DIRECT-MEASUREMENT AND DERIVED AOA METHODS

The direct-measurement and derived AoA systems share a common problem: lack of knowledge of flap position. This is an inherent limitation of retrofit GA aircraft. Proper position of the probe for a direct-measurement AoA system can reduce variation across flap deflections, but this location likely varies between aircraft types.

Current retrofit direct-measurement AoA systems operate independently of other avionics systems. This means they can provide backup information in the case of an airspeed indicator failure or a plugged or leaking pitot/static system. The derived AoA system is dependent on the same systems as the airspeed indicator, as well as other sensors and systems.

The direct-measurement and derived AoA systems tested in this investigation were both easy to calibrate. The derived system required three vs. two calibration points to be measured, but this yielded a benefit in providing an indication of lift reserve with two flap settings.

Aside from the redundancy observation, either approach seems quite suitable for displays to pilots and for use in haptic feedback systems or sophisticated autopilots.

6.4 LESSONS LEARNED

The AAG derived AoA algorithm might be calibrated in a fashion similar to Aspen's, using three trim points and assuming (1) linearity of C_N vs. AoA and (2) a constant offset in the C_N vs. AoA relationship for different flap deflections, and by using the airspeed calibration from the aircraft POH. However, as was shown in the calibration curve (see figure 13), three trim points would be insufficient to capture the change in slope and bias with different flap deflections. Two trim points per flap setting (at least four points) would provide a better characterization of C_N vs. AoA.

The results of the sensitivity study (discussed in section 4.3) indicated the algorithm could be simplified by removing the corrections to the algorithm for moment arm, local gravity, and vehicle weight, because variations in these parameters had little effect on the accuracy of derived AoA.

Better estimations could likely be obtained by including flap and throttle setting feedbacks during calibration and use.

6.4.1 Sensitivity to Vehicle Configuration

Appropriate location of a multi-hole probe in the airstream is important to reduce the effect of configuration changes (e.g., flap deflections) on the indicated AoA because of flow-field changes with wing geometry. Determining the best location appears to require somewhat of a trial-and-error approach and is likely to be aircraft-specific. However, once properly positioned, the average pilot could calibrate the probe relatively easily.

The derived AoA algorithms obviate the requirement for precision in mounting location, but the algorithms are also highly configuration specific, requiring calibration in each likely vehicle configuration and knowledge of the vehicle configuration for determining the AoA estimate.

Calibration is therefore more difficult and may require more piloting skill than for a measured AoA system.

The strong sensitivity of direct-measurement AoA systems to local flow conditions (and therefore highlighting the importance of finding an appropriate probe mounting location) for all likely aircraft/wing/flap configurations would seem to make it difficult to assure a generic direct-measurement AoA, indicating a solution for all aircraft. However, this sensitivity to mounting location might be ameliorated if a more stringent calibration technique is performed and flap position is fed back to the system.

The Garmin two-point calibration at one flap setting provided adequate results (minimal sensitivity to different flap settings), only with the probe installed at a proper location. However, a calibration technique that acquired at least two points at all flap settings, coupled with providing feedback of current flap position, would likely reduce sensitivity to mounting location.

At a minimum, calibration and checks of the system at all flap configurations should be recommended in the installation manual of these systems. Pilots should note the indication for on-speed for each flap deflection.

The technique of calibrating the Aeroprobe for all flap settings worked well for all configurations, with the exception of limiting near stall with some flap settings. A production system would not need to be calibrated at as many points and should not reach a limit.

Like the direct AoA measurement systems, knowing the position of the flaps and performing calibrations for all flap settings would yield a better overall result. Aspen's patent-pending display that indicates lift reserve for zero and full flaps is a good way to address the lack of availability of flap position information.

6.4.2 Elevator Power Limitation During Flight Test

The calibration and test method used was to establish straight-and-level trimmed flight for a given aircraft configuration at various indicated airspeeds, followed by incipient and full stalls with partial engine power and with engine power off. This method was used in an attempt to cover the widest possible range of AoA. The trim series began near cruise speed, proceeding to slower airspeeds in 10- to 15-knot decrements. The trim conditions were maintained for at least 5 and usually more than 10 seconds. The original intent was for the last two points to be power-off incipient and full stalls. The test aircraft, however, could not be fully stalled with power off because of a lack of elevator authority. Full stalls were therefore accomplished with some small amount of engine power because the thrust over the horizontal tail/elevator provided sufficient pitch authority to perform the stall.

6.5 CERTIFICATION CONSIDERATIONS

Given the dependence on vehicle configuration of both the sensed and derived AoA methods studied, certification requirements for both should consider at least groupings of aircraft by flap type and possibly thrust effects. Both sensor types are sensitive to flap deflection in different ways. Having flap deflection as an input and using it in calibration should address these effects when precise AoA is needed. The sensed systems can mitigate thrust effects by being sure the probe is

not in the propeller wash. However, the derived systems may need to know thrust to precisely determine AoA for broad flight conditions, based on these results.

Thrust effects on sensed AoA systems are worthy of additional study to assert certification requirements. The study would need to determine how extensive the effects can be because these flight tests only revealed significant differences near stall, but that is the only condition in the flight cards that had other than trim thrust for the test point. Power-on and power-off stalls yielded different results. The certification-related questions are:

1. Can a calibration technique be developed to mitigate this without needing power setting as an input?
2. How well can the thrust effects be mitigated if the data are available?
3. Do the thrust effects show up in significant ways (departure vs. approach stalls, for example)?
4. How configuration-dependent are the thrust effects?

Sensed AoA systems are sensitive to installation and to verification that the installation is yielding reasonable results with all aircraft configurations. This is a retrofit problem, because original equipment manufacturers would clearly work out the best approach to installing the probes and overall system for each make and model. Specifying installation requirements that work for different types of aircraft is an obvious key element that needs to be understood broadly. Stopping short of a Supplemental Type Certificate requirement, certification should require inclusion in the installation manual of clearly defined calibration and verification test procedures for all configurations of the aircraft to assure the system is operating properly and that the pilot understands the indications. The problems with this are that many avionics shops do not have the expertise to do the verification without some training, and the percentage of pilots who could reliably do the calibration and verification is unknown. Training of the shops could be affected through the Aircraft Electronics Association (AEA) done generically by the FAA or specifically by the manufacturers. Video training could also be established through the AEA. Similarly, pilots could be trained through FAA information, Aircraft Owners and Pilots Association Air Safety Foundation, Experimental Aircraft Association, and others. This recommendation comes from the initial installation for this study revealing problems and resulting in information used to modify the COTS system's installation manual. It is also observational in that the "on speed" indications are different in a sensible way on the test aircraft with different flap deflections.

In the aircraft used for flight test of the derived AoA algorithms in this study, indicated airspeed tended to be lower than true or calibrated airspeed at slower speeds, leading to a conservative overestimate of AoA when indicated was used without correction. If used on an aircraft when this was not the case (such that indicated airspeed was higher than actual), the derived AoA prediction would tend to be non-conservative (lower than actual) (e.g., indicating available lift margin where none existed).

Based on the simulation-based sensitivity studies of the algorithm developed for this study (ADAGE), errors in sensed pitch rate, true airspeed, and Z-axis acceleration can lead to poor estimates of AoA. Some maximum bounds on errors from these sensors would likely need to be specified, as would a maximum delay in attitude estimation, to ensure adequate derived AoA performance.

Though the simulation model showed only a small amount of sensitivity to vehicle weight, application of the derived AoA algorithm to an aircraft with a larger fuel fraction is likely to need some estimation of vehicle weight to avoid a larger variation in derived AoA.

The sensitivity study revealed which inputs were most likely to cause significant errors in derived AoA. Configuration changes were also shown to affect derived AoA accuracy when not managed properly. However, there is currently no guidance on how much AoA error is acceptable. Without this information, it will be difficult to definitively determine certification requirements or verification and validation techniques.

Finally, the sensed systems and the ADAHRS-based derived systems use a different set of sensors and probes. Having both types of AoA systems would assure that a pilot would have redundancy in the case that either system failed. This has potential benefits for AoA systems used to provide displays to pilots or AoA systems used in envelope protection and fly-by-wire systems. The redundancy offers a clear benefit, but confusion about which system to rely on short of a complete or very obvious error introduces additional complication. Developing a deep understanding of failure modes and detection techniques would be required for the two types of systems to be successfully used in envelope protection and fly-by-wire systems. Pilots can be trained to understand which system is correct similar to the way they are currently trained to cross-reference instruments to detect failures.

7. SUMMARY

Two COTS AoA systems were evaluated in flight against a calibrated AoA probe in an instrumented Cessna R182. One of the systems used a direct-measuring sensor that was mounted in the flow field. This is referred to as “sensed AoA.” The other system consisted of an algorithm to derive AoA from a commercial attitude and heading reference unit (hence the term “derived AoA”). In addition, an ADAGE was developed and tested in both ground simulation and in post-processing of actual flight test data for a variety of stalls.

Some effort was required to obtain satisfactory results from the sensed AoA commercial system, including relocation of the sensor. Following relocation, the sensed AoA system worked well, as did the derived AoA system using a commercially developed algorithm and AHRS unit.

The ADAGE algorithm used parameters available from a certified electronic flight information system; it also relied on estimates of key aerodynamic parameters, such as the lift slope coefficient, obtained through in-flight calibrations at different flap and landing-gear configurations. It also required readily available aircraft information (e.g., weight, surface area, and sensor location). This approach shows promise, but additional work is required to make it commercially feasible, including reducing the number of input signals required and simplification of the calibration procedure. A study of the sensitivity of the algorithm indicated which inputs are important for good AoA estimation and suggests other inputs that could be approximated.

Testing of the ADAGE algorithm showed good comparisons with calibrated AoA to near-stall conditions, where output signal limiting of the calibrated AoA probe led to poor comparisons with flaps extended, but tests with flaps retracted showed excellent estimation up to a stalled flight condition.

Having knowledge of AoA is the foundation for safety and therefore the focus of recent FAA research initiatives. AoA displays and sensor hardware have increased awareness for both pilots and the public. The integration into cockpits has led to stall awareness that is not available with speed-based systems alone. Stall speed values published in the flight manuals are not valid for all gross weights. They are also not valid for accelerated dynamic maneuvers, or in uncoordinated flight conditions. However, AoA can be used for stall margin awareness under all those conditions.

Having AoA displayed and coupled with descriptive audio annunciations provides two sensory channels to the pilot. Tactile cueing in the form of a stick shaker would add a third channel to the pilot. In startle situations, this can cue the pilot even when he/she is not looking at the display. This is critical in low-altitude situations when a simple stall horn may not be enough. Properly filtered AoA can be used as an input to envelope protection systems such as AoA limiters. Furthermore, AoA is a primary input signal for a stick pusher system. AoA can be used in fly-by-wire flight-control systems, enabling both flight-path control and envelope protection.

Accurate knowledge of AoA is a foundation for flight-safety enhancements, which could lower the fatal accident rate in both GA and commercial aviation operations. Each of the systems studied in this flight test provide the pilot with qualitative AoA awareness; modifications would be required to provide accurate measurements to an autoflight system for all vehicle configurations.

Based on the limited characterization of derived AOA algorithms in this study, it appears that the output of such algorithms could be used as a suitable input for real-time sensor consistency verification for detection of sensor failures driving flight-control and display systems.

8. RECOMMENDATIONS FOR FURTHER RESEARCH

Additional study is required to develop a sufficient understanding of some items to support definitive certification requirements. The following list contains high-level descriptions of each item.

- An understanding of how accurate AoA, sensed or derived, needs to be is needed to determine how to turn results from this and future studies into requirements. The AoA accuracy requirement could be developed from a study or be decreed by the FAA.
- Address the impact of flap deflection and lack of flap-deflection knowledge on derived AoA algorithms:
    - There may be a way to calibrate the AoA algorithm at the different flap deflections and definitively determine the flap position in situ after calibration. This seems very worthy of additional investigation, given the sensitivity of the result to flap position and the cost of requiring a flap position sensor.
    - The calibration approach used for the ADAGE algorithm was good for an experiment, but excessive for real-world application. Additional study is needed to determine the minimum set of calibration points needed to provide accurate AoA and to understand the tradeoff between number of points and overall accuracy.
    - Assessing thrust effects in more detail to understand how significant the effect can be, based on calibration technique, and to develop calibration procedures that may mitigate the effects, is worthy of additional study. Developing an algorithm and

calibration procedures that take power setting into account for aircraft that have the information digitally is worthy of additional investigation.

- The inertially navigated AoA algorithm showed promise, but is not fully matured. It also suffered from significant lags in vertical velocity values available from the sensors. An instantaneous vertical speed indicator can provide vertical rate with far less lag. An investigation into use of such a system seems worthy of additional study. With the navigated AoA working well, the benefits of merging it with the ADAHRS derived AoA are worthy of additional evaluation. This would provide a third AoA estimate based on a separate set of sensors, which could benefit envelope protection and fly-by-wire systems.
- The ADAGE algorithm should be tested on a different aircraft to improve confidence in the approach and to uncover additional configuration effects on the estimate.
- Operational experience with the ADAGE algorithm in a variety of aircraft is required to set minimum operational performance standards for sensor error bounds and latency, and to determine repeatability and accuracy.
- The ADAGE algorithm was executed after the fact, using data recorded during flight, in this study. Developing a real-time in situ capability and an associated display for the pilot is worthy of additional investigation.
- The source of the overestimation of AoA during stalls for the flight test with 20° of flap bears further attention. The ADAGE algorithm should be tested on a different aircraft to improve confidence in the approach and to uncover additional configuration effects on the estimate.
- A more thorough investigation of the effects of atmospheric motion on—and the feasibility of using published airspeed calibration (vs. performing an independent airspeed calibration maneuver) with—the ADAGE algorithm should be performed to improve confidence in the algorithm. (This was subsequently accomplished, prior to publication of this report and is documented in reference 6.)

9. REFERENCES

1. Hoadley, Arthur W. (1990). *Performance Instrumentation for Multiengine Safety*. AIAA/FAA Joint Symposium on General Aviation Systems, Ocean City, NJ.

2. National Transportation Safety Board. (2016). 2016 Most-Wanted List: Prevent Loss of Control In Flight in General Aviation. Retrieved from http://www.ntsb.gov/safety/mwl/Pages/mwl6-2016.aspx.

3. Peden, T. (1999). "c172_aero.c," part of the FlightGear open-source simulation code.

4. US Department of Defense. (2004). *Flying Qualities of Piloted Aircraft* (MIL-STD-1797A).

5. Cessna. (1978). *1979 Skylane RG Model R182 Pilot's Operating Handbook.* Wichita, KS: Cessna Aircraft Company.

6. Jackson, E. B, and Hoffler, K. H. (June, 2017). *Effects of Atmospheric Motion on a Derived Angle-of-Attack Estimator.* AIAA Paper 2017-4062. Presented at AIAA Atmospheric Flight Mechanics Conference, Denver, Colorado.

APPENDIX A—ADAPTIVE AEROSPACE GROUP, INC. DIGITAL ANGLE OF ATTACK G-BASED ESTIMATOR ALGORITHM

LIST OF SYMBOLS

$\vec{a}$	Measured accelerations at sensor location
C_N	Normal force coefficient
$\vec{\mathbf{F}}$	Aerodynamic reaction force (includes list, drag, side-force)
F	Scalar component of $\vec{\mathbf{F}}$ along one body axis
g	Scalar gravitational acceleration
$\vec{\mathrm{g}}$	Gravitational acceleration vector
g	Scalar component of $\vec{\mathrm{g}}$ along one body axis
m	Mass
N	Normal force
p	Angular rate around the body x axis
q	Angular rate around the body y axis
$\overline{q}$	Dynamic pressure
$\ddot{\vec{R}}$	Inertial acceleration of aircraft center of mass
r	Angular rate around the body Z axis
S	Reference area (wing area)
$\vec{s}$	Moment arm from sensor(s) to aircraft center of mass
s	Scalar distance from sensor to aircraft center of mass
$\vec{\mathbf{T}}$	Net thrust force vector
T	Scalar component of $\vec{\mathbf{T}}$ along one body axis
x	Body longitudinal axis
$\ddot{x}$	Acceleration along the body x axis
y	Body lateral axis
$\ddot{y}$	Acceleration along the body y axis
z	Body vertical axis
$\ddot{z}$	Acceleration along the body z axis
α	Angle of attack
$\overline{\alpha}$	Estimated angle of attack
δe	Elevator deflection
ϕ	Bank angle
θ	Pitch angle
ψ	Heading angle
$\vec{\omega}$	Aircraft angular rate vector
$\dot{\vec{\omega}}$	Aircraft angular acceleration

A.1. INTRODUCTION

This is a brief description of an approach to estimating angle of attack (α) for a general aviation aircraft using data derived from an onboard Air Data Attitude Heading Reference Systems (ADAHRS) package. A calibration of the aircraft's normal-force cs α curve is required, but an approximation of C_{N_α} as a constant value may make this calibration striaghtforward to perform.

A.2. ASSUMPTIONS

- Elevator deflection is correlated with α (true in steady-state)
- Thrust acts parallel to body *x* axis
- Quasi-static flight (angular accelerations zero)
- Roll rate is small of zero
- Pitch rate has no effect on normal force

A.3. DERIVATION

There are three forces or accelerations acting on a powered aircraft in flight: propulsive force ($\vec{\mathbf{T}}$); an aerodynamic reaction force ($\vec{\mathbf{F}}$) that uses lift, drag, and side-force; and gravity ($\vec{\mathrm{g}}$). The resulting inertial acceleration of the aircraft's center of mass is given by:

$$\ddot{\vec{R}} = \vec{\mathrm{g}} + \frac{\vec{\mathbf{T}} + \vec{\mathbf{F}}}{m} \tag{A-1}$$

Where *m* is the mass of the aircraft.

If the acceleration vector were to be measured by the onboard ADAHRS located some fixed distance, $\vec{s}$, from the center of mass, the measured accelerations, $\vec{a}$, would be those given by the so-called strap-down equation,

$$\vec{a} = \ddot{\vec{R}} + \dot{\vec{\omega}} \times \vec{s} + \vec{\omega} \times (\vec{\omega} \times \vec{s}) \tag{A-2}$$

If angular accelerations are ignored (assumed small, so $\dot{\vec{\omega}} = 0$), $\vec{\mathbf{F}}$ can be solved for:

$$\vec{\mathbf{F}} = m[\vec{a} - \vec{\mathrm{g}} - \vec{\omega} \times (\vec{\omega} \times \vec{s})] - \vec{\mathbf{T}} \tag{A-3}$$

If these vector equations are resolved in body axes,

$$\begin{bmatrix} F_x \\ F_y \\ F_z \end{bmatrix} = m\left\{ \begin{bmatrix} \ddot{x} \\ \ddot{y} \\ \ddot{z} \end{bmatrix} - \begin{bmatrix} g_x \\ g_y \\ g_z \end{bmatrix} + \begin{bmatrix} (q^2 + r^2)s_x - p(qs_y + rs_z) \\ (p^2 + r^2)s_y - q(ps_x + rs_z) \\ (p^2 + q^2)s_z - r(ps_x + qs_y) \end{bmatrix} \right\} - \begin{bmatrix} T_x \\ T_y \\ T_z \end{bmatrix} \tag{A-4}$$

One further simplification is to assume roll rate is zero ($p = 0$):

$$\begin{bmatrix} F_x \\ F_y \\ F_z \end{bmatrix} = m\left\{ \begin{bmatrix} \ddot{x} \\ \ddot{y} \\ \ddot{z} \end{bmatrix} - \begin{bmatrix} g_x \\ g_y \\ g_z \end{bmatrix} + \begin{bmatrix} (q^2 + r^2)s_x \\ r^2 s_y - qrs_z \\ q^2 s_z - qrs_y \end{bmatrix} \right\} - \begin{bmatrix} T_x \\ T_y \\ T_z \end{bmatrix} \tag{A-5}$$

Only one equation is needed to identify α. The principal effect of α is in the vertical axis, so attention can be focused there. In addition, the body *z* axis component of gravity, $g_z = \mathbf{g}\cos\phi\cos\theta$, can be substituted:

$$F_z = m(\ddot{z} - \mathbf{g}\cos\phi\cos\theta + q^2 s_z - rqs_y) - T_z \tag{A-6}$$

The α directly affects F_z, which has contributions from drag and lift. The familiar wind-tunnel measurement of "normal" force, or the aerodynamic reaction load in the vertical body-axis direction, can be used, signified by the *N* subscript. Note that normal force is simply negated body *z* axis force: $F_z = -N$.

One more assumption is made: that thrust has no vertical body-axis component ($T_z = 0$), to arrive at:

$$N = m(-\ddot{z} + \mathbf{g}\cos\phi\cos\theta - q^2 s_z + rqs_y) \tag{A-7}$$

Note that all the contributors on the right-hand side of the equation should be able to be measured. The task is now to determine α from *N*. Using standard aerodynamic nomenclature and a Taylor series expansion:

$$N(\alpha) = N_o + N_\alpha \alpha + N_q q + N_{\delta e}\delta e \tag{A-8}$$

or in normalized coefficient form:

$$N(\alpha) = \bar{q}S\{C_{N_o} + C_{N_\alpha} + C_{N_q} q + C_{N_{\delta e}}\delta e\} \tag{A-9}$$

A final simplification is to assume $C_{N_q} \approx 0$ and that elevator deflection δe and α are strongly correlated, in which case it is assumed that the $C_{N_{\delta e}}$ contribution is included in C_{N_α}; therefore:

$$N = \bar{q}S\{C_{N_o} + C_{N_\alpha}\alpha\} \tag{A-10}$$

Finally, this last equation can be arranged to obtain an estimate of α from the estimate of *N* obtained in equation A-7:

$$\bar{\alpha} = \left(\frac{N}{\bar{q}S} - C_{N_o} \right) / C_{N_\alpha} \tag{A-11}$$

Therefore, an estimate of α should be able to be obtained if the values to substitute for five constants can be found: C_{N_o}, C_{N_α} and *S* as well as ADAHRS moment arm s_y and s_z, and measurements of six time-changing values: $\bar{q}, q, r, \ddot{x}, \phi,$ and θ in equations A-7 and A-10.

A.4. IMPLEMENTATION CHALLENGES

The application of the foregoing derivation to an actual aircraft presents several challenges:

- Filtering of noisy measurements of acceleration, angular rates, and Euler angles
- Estimating dynamic pressure, $\bar{q}$
- Obtaining values for all five constants

Fortunately, the presence of an ADHARS box implies the availability of angular rates and positions and the ability to obtain true airspeed from calibrated airspeed and wind estimates (and therefor an estimate of dynamic pressure).

Obtaining the five constants C_{N_o}, C_{N_α}, *S*, s_y, and s_z is a bit more challenging.

The values of geometric measures of wing area (*S*) and ADAHRS sensor package moment arm s_y and s_z can be determined by the installer through inspection, but might be a challenge for the operator. However, it may be possible to identify these three parameters from flight maneuvers via system identification.

Identification of the aerodynamic parameters C_{N_o} and C_{N_α} turns out to be fairly simple if $N(\alpha)$ is approximated by a straight line (which should be adequate for stall warning) between some on-speed and stall, where precise values for α are not required. During installation, two flight conditions in calm air can be flown and two values for C_N can be calculated at these two conditions (on-speed and stall warning onset); a straight line can be fitted between these two points; C_{N_o} is the *y*-axis intersection and C_{N_α} the slope of a linear C_N vs. α line between the two calibration points.

APPENDIX B—ADAPTIVE AEROSPACE GROUP, INC. DIGITAL ANGLE OF ATTACK G-BASED ESTIMATOR IMPLEMENTATION IN SIMULINK/MATLAB

The Adaptive Aerospace Group, Inc. Digital Angle of Attack G-based Estimator (ADAGE) algorithm is implemented using The Mathworks Matlab®/Simulink® tool set, release version R2015b, as described in this appendix.

B.1. BLOCK LIBRARY

The estimator is realized from blocks defined in a Simulink library, shown in figure B-1.

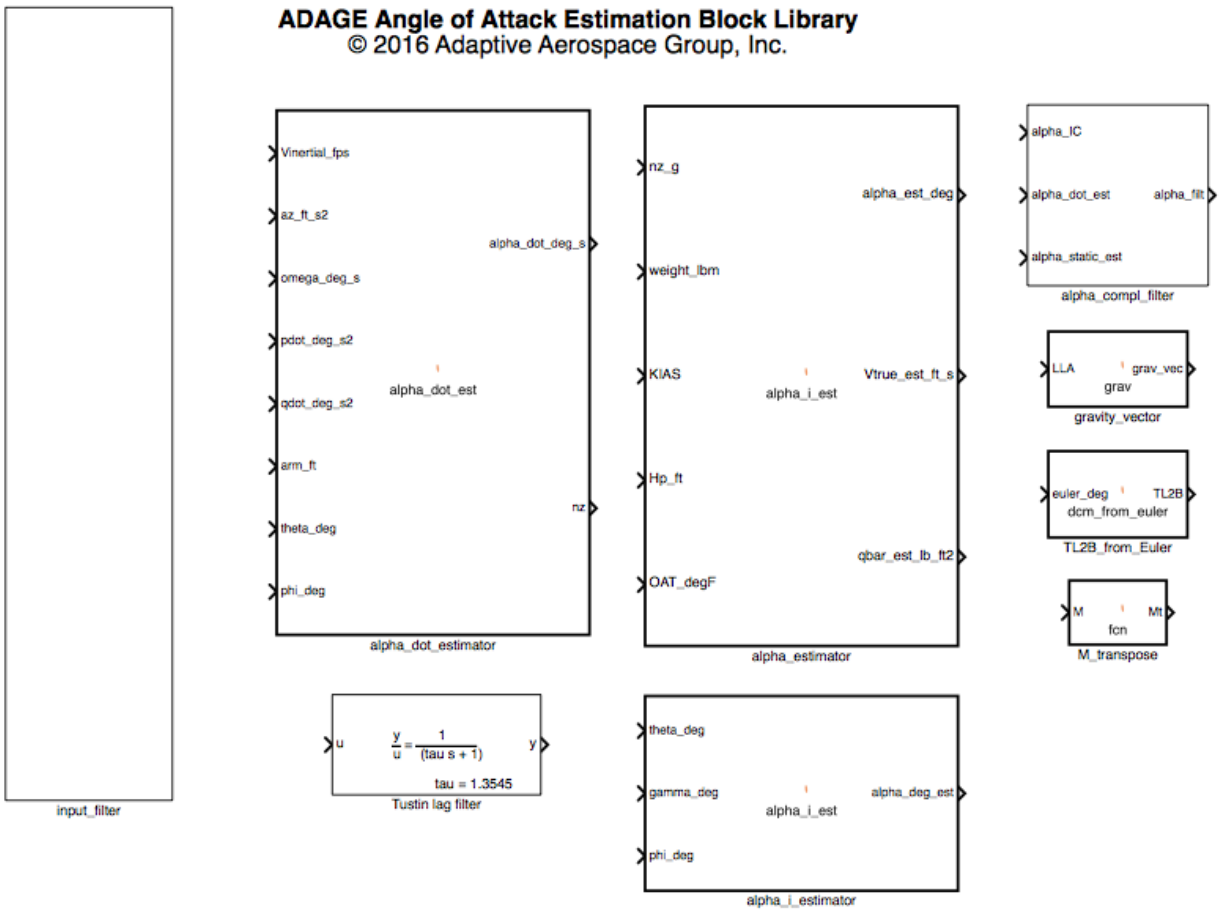

Figure B-1. ADAGE block library

B.2. TOP-LEVEL ESTIMATOR SYSTEM

Blocks from this library are used to define the angle of attack (AoA) estimator, shown in figure B-2. Here an input filter block (labeled as Configurable Subsystem) provides filtering for most signals used in the estimator. Selected inputs are fed into a single block (alpha_dot_estimator) to generate an estimate of AoA rate and vertical acceleration, and into three instances of a block to estimate AoA value and true airspeed for each calibrated vehicle configuration

(clean_alpha_estimator, dirty_alpha_estimator, landing_alpha_estimator) corresponding to 0°, 20°, and 40° flap deflections. Note these are mislabeled by Simulink as "alpha_dot_est" instances; internally, they are actually alpha_estimator blocks.

The single estimate of AoA rate and the three configuration-dependent estimates of AoA value are fed into three instances of a complementary filter (alpha_compl_filter, shown in figure B-1), where the inputs are combined into three estimates of AoA.

Another library block, alpha_i_estimator, is used to generate an estimate of inertial or navigated AoA based on pitch attitude, bank angle, inertial velocity, and vertical speed.

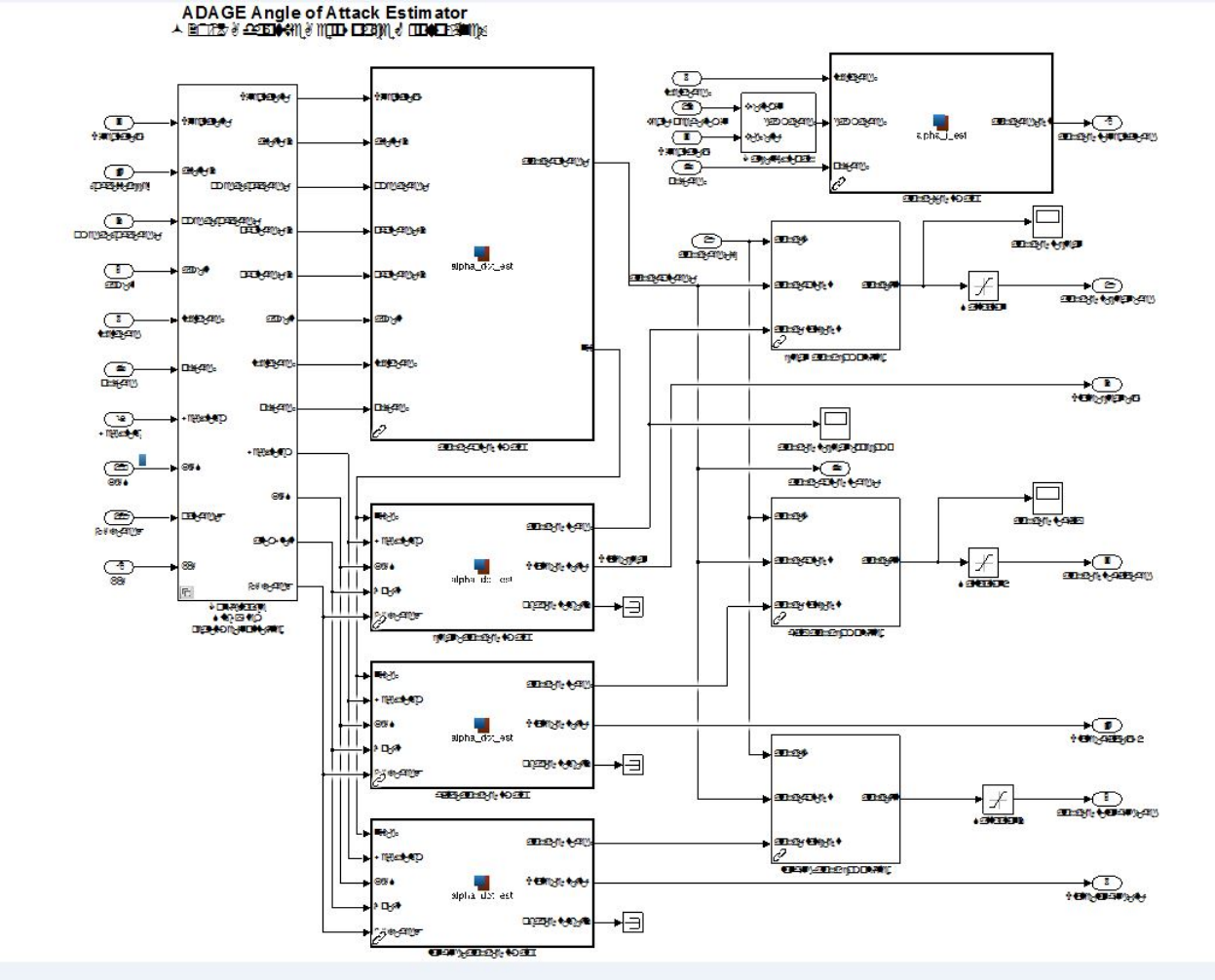

Figure B-2. Top-level AoA estimator schematic

B.3. INPUT FILTER

Inputs signals are filtered in the real_time_input_filter block found in the ADAGE block library, shown in figure B-3. Inside this block, inertial airspeed Vinertial_ft_s is limited to remain non-zero and reasonable; body-axis accelerometer measurement az_ft_s2 are filtered with a digital

implementation of a 0.5-s lag filter (implemented in az_lag_filter) and then calibrated to a previously identified linear fit; a vector of body-rate sensor inputs in each axis (omega_body_deg_s) have their biases removed and are filtered with a 0.5-s lag filter in the filters block. The roll- and pitch-rate filtered signals are then differentiated to form an estimate of roll and pitch acceleration (pdot_deg_s2 and qdot_deg_s2), and indicated airspeed input knot indicated airspeed is limited to reasonable non-zero values.

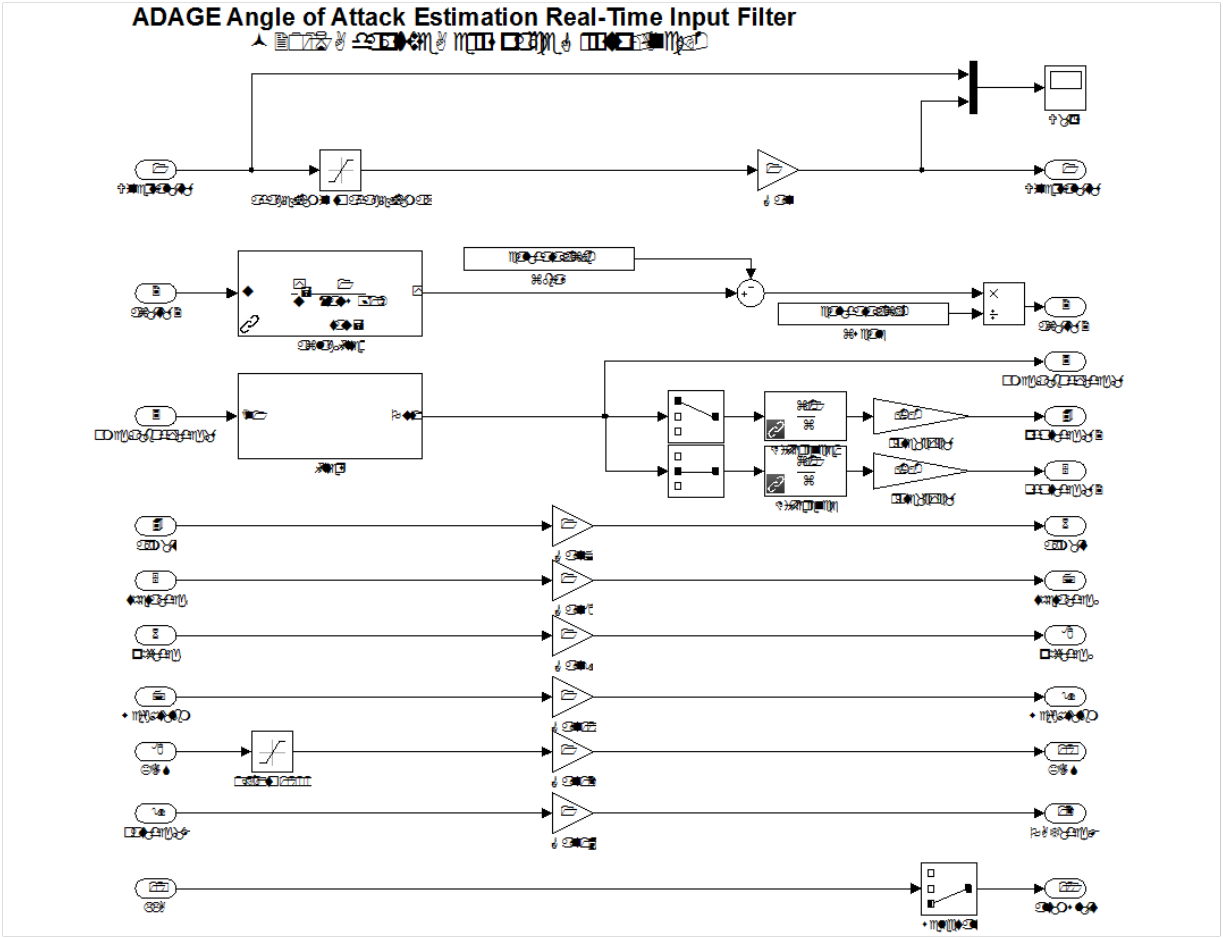

Figure B-3. Input signal filter block real_time_input_filter

B.4. AoA RATE ESTIMATOR

The AoA rate estimator block alpha_dot_estimator is realized as a Matlab script (not shown). Inputs are inertial airspeed, body Z-axis accelerometer measurement, body rates, roll and pitch axis angular accelerations, sensor package offset from center of mass, and pitch and roll angles. Outputs are estimates of AoA rate and normal axis G-load (N_Z).

B.5. AoA VALUE ESTIMATOR

The estimate of steady-state AoA is provided in the alpha estimator block. It is realized as a Matlab script (not shown). Inputs are vertical axis acceleration (a_Z), vehicle weight, indicated airspeed,

pressure altitude, outside air temperature, and the calibration values. Outputs are estimates of AoA rate and normal axis G-load (N_Z).

B.6. COMPLEMENTARY FILTER

The complementary filter that combines estimates of AoA value and AoA rate is shown in figure B-4. This block combines the two so that the higher-frequency component of the output is based on AoA rate, and the lower-to-DC component is based on the AoA value input; the knee in the curves is at 10 rad/s (filter time constant 0.1 s). Three instantiations of this filter are used for the clean, dirty, and landing configurations of the aircraft.

Figure B-4. Complementary filter

B.7. INERTIAL AOA ESTIMATOR

The inertial AoA estimator block labeled alpha_i_est in the library is realized as a Matlab script (not shown). Inputs are pitch and roll attitude and vertical flight-path angle; output is the estimate of AoA rate.

B.8. DISCRETE TUSTIN LAG FILTER

Figure B-5 shows the implementation of a discrete first-order lag, implemented in the "Tustin lag filter" masked block in the ADAGE library. Calculations for gains A and B are shown in the figure.

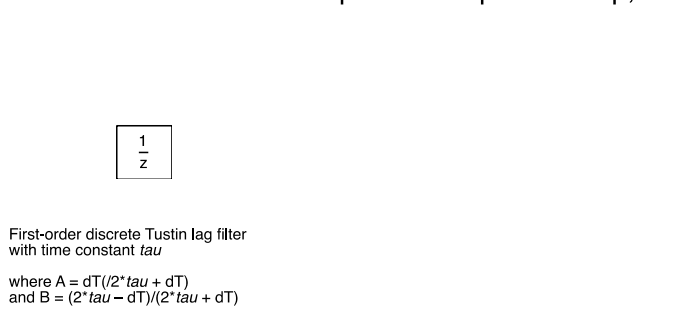

Figure B- 5. Discrete Tustin lag filter implementation

B.9. FLIGHT-PATH ANGLE CALCULATION

Vertical flight-path angle is calculated from ground speed and vertical speed in the Calc_flight_path block shown in the alpha estimator model. Figure B-6 shows the internal implementation of this calculation involving finding the arc tangent of the ratio of those inputs, with vertical speed scaled appropriately to ft/s units to match ground speed.

Figure B- 6. Flight path calculation block, Calc_flight_path

B.10. ADAGE PARAMETER VALUES

The parameter values used in the AoA estimation process covered in this report are shown in figure B-7.

```
rate__s: 64

dt_s: 0.0156

v_min: 0.0500

v_max: 300

filter_tau: 0.1000

pb_filt_tau: 0.5000

qb_filt_tau: 0.5000

rb_filt_tau: 0.5000

ax_filt_tau: 0.5000

ay_filt_tau: 0.5000

az_filt_tau: 0.5000

alpha_min: -5

alpha_max: 25
```

Figure B-7. Parameter value for AoA estimation

APPENDIX C—ADAPTIVE AEROSPACE GROUP, INC. DIGITAL ANGLE OF ATTACK G-BASED ESTIMATOR CALIBRATION METHOD

Flight test data were collected at various flight conditions and vehicle configurations on multiple flights. Normally, each flight was used to generate calibrations for accelerometer biases and scale errors, rate sensor biases, and estimates of normal force coefficient (C_N) versus angle of attack (AoA); as described in the text, the Adaptive Aerospace Group, Inc. Digital AoA G-based Estimator estimates of AoA for this report were based on a single-calibration flight flown prior to the data collection flights of this report. An additional calibration of the Aeroprobe AoA sensor was normally performed on each flight as well; for this report, the calibration of the Aeroprobe AoA sensor was based on data obtained in the calibration flight and all three data flights.

Nearly all flights included performing wind triangle maneuvers: the aircraft was flown at a constant speed and altitude (on autopilot) for approximately 60 seconds on three different headings approximately 120° apart while various parameters were recorded. A wind triangle was flown as the first and last maneuver of a calibration or data-collection flight. From this data, the motion of the atmosphere at the test altitude was determined at the beginning and end of data collection; any change to the wind was linearly interpolated through the data-collection portion of the flight.

The other calibration maneuver flown consisted of straight and level, constant-speed flight trim points of at least 5-seconds' duration; these were normally hand-flown. A series of trim points were obtained, starting at higher speed (130 knots for flaps up, slower with flaps down), and then the aircraft was decelerated 10 or 15 knots to perform another trim point, down to just above stall speed for the given configuration. These trim points were used to calculate true airspeed, true or best estimate AoA, calibrated airspeed, and estimates of C_N for each point, by configuration.

The data-reduction algorithm for each process is given in this appendix.

C.1. WIND TRIANGLE REDUCTION

The algorithm used to determine horizontal motion of the atmosphere at the test altitude was as follows:

1. Aircraft trimmed at constant airspeed, level flight (approximately 120 knot indicated airspeed [KIAS]) with autopilot set for altitude and heading hold.
2. Maintain conditions for approximately 60 seconds.
3. Turn 120° right; allow transient motion to damp out.
4. Repeat steps 1–3 for three legs.

Data recorded during each leg was processed into a wind direction and speed as follows:

1. Truncate the data from other two legs to match the duration of the shortest-duration leg.
2. Ending latitude and longitude from GPS was subtracted from starting latitude and longitude and converted to feet traveled north-south and east-west.
3. Average groundspeed for each leg was calculated by dividing distance traveled by leg elapsed time and converted to knots true airspeed (KTAS).
4. Place the starting point of each leg together at coordinates (0, 0) on the Cartesian plane.
5. Fit a circle through the three end points.

6. The center of the circle will be located downwind of the (0, 0) point; its displacement corresponds to the average horizontal motion of the atmosphere during the leg-duration interval.
7. Divide the drift of the circle center by the leg duration interval to obtain average wind speed; the direction of the drift identifies the wind direction.

C.2. AoA, C_N, AND AIRSPEED CALCULATIONS

The algorithm followed to determine actual AoA, CN, and airspeed (both true and calibrated) was as follows:

C.2.1 Data Conditioning

1. Calculate full fuel weight and balance.
2. Read data from CSV recorded files, one per data source (430W, Aeroprobe, etc).
3. Synchronize time using MILLISECOND time stamps in each file.
4. Determine start and stop time for common window recorded in each file; define t_0.
5. Load flight data into Matlab table structures (one per data source).
6. Convert each table channel into time series; resample to fixed 64 Hz clock.
7. Convert each table into time series collection.
8. Merge all time series into single collection with common time vector.
9. Calculate inertial velocity from GPS samples approximately 3 seconds apart; add as time series to the collection.
10. Calculate weight and center of gravity (CG) location vs. time based on fuel remaining.
11. Smooth most measurements using Fourier filter.
12. Solve starting and ending wind triangles for wind direction and velocity vs. time.

C.2.2 Calibration

For each vehicle configuration (trimmed point series):

1. For each trimmed "point" in trim series:

    a. Find start and stop indices into flight data collection; calculate ΔT.
    b. Calculate distance traveled from GPS positions at start and stop, ΔS.
    c. Calculate average inertial velocity, $V_{avg} = \Delta S/\Delta T$.
    d. Calculate average values over trim point for: θ, ψ, ΔH, a_z, KIAS, outside air temperature (OAT), Aeroprobe AoA.
    e. Calculate true a_z for given θ_{avg} and local gravity $=\boldsymbol{g}$ (latitude).
    f. Subtract atmospheric motion (integrated wind over trim point time) from ground path, ΔS, to get true air path distance, ΔA.
    g. Calculate average vertical flight path angle γ_{avg} from $\Delta H/\Delta S$.
    h. Find best-estimate of AoA from $\theta_{avg} - \gamma_{avg}$.
    i. Calculate true airspeed from $\Delta A/\Delta T$; convert to kt (KTAS).
    j. Calculate speed-of-sound from OAT_{avg}.
    k. Calculate Mach number from true airspeed/speed-of-sound.
    l. Calculate pressure ratio P_T/P_S from Mach.

m. Find static pressure P_S from pressure altitude H_P.
n. Find P_T from P_S, P_T/P_S.
o. Calculate density ρ from ideal gas, OAT, P_T.
p. Calculate dynamic pressure from Bernoulli equation.
q. Calculate impact pressure from $P_T - P_S$.
r. Calculate knots calibrated airspeed (KCAS).
s. Determine weight and CG position based on fuel remaining.
t. Calculate C_N from weight, true a_Z, dynamic pressure, wing area.

2. Fit line through C_N vs. best-estimate AoA.
3. Fit line through true aZ vs. measured aZ (identifies bias and gain error/alignment).
4. Fit parabola through Aeroprobe AoA vs. best-estimate AoA.
5. Plot KCAS vs. KIAS airspeed calibration points.

APPENDIX D—FLIGHT TEST PLAN AND FLIGHT CARDS

D.1. INTRODUCTION

This document outlines flight test procedures to capture data from one or more commercial off-the-shelf (COTS) and developmental direct-measuring angle of attack (AoA) sensors as well as devices that infer, or derive, AoA from other sensor data.

The plan assumes all tests will be flown in Second Century Aviation's Cessna R182, N736WP, from its home base of Hampton Roads Airport (KPVG) in Chesapeake, Virginia by staff members of Adaptive Aerospace Group, Inc. (AAG). It further assumes that the airspeed, air temperature, and inertial measurement units (ADAHRS) have been calibrated in previous test flights.

The tests are to be conducted in calm atmospheric conditions with a minimum of wind, when possible. The minimum crew required for conducting the flight is two: pilot and flight test engineer. Both shall be qualified and trained to conduct the flight and collect data. The flight test engineer will be familiar with the systems and procedures needed to collect the desired data.

In all cases the aircraft will be operated in accordance with the aircraft flight manual within limitations imposed for normal category operations, including aircraft loading/center of gravity (CG) limits, speeds, and maneuver limits. Flights will be conducted only in visual meteorological conditions weather. Clearing turns will be flown prior to any incipient and actual stall. No stall maneuvers will be performed lower than 2500 ft. AGL, and the test pilot will be appropriately rated and current.

D.2 PRIOR TO FLIGHT TESTING

D.2.1 CALIBRATE AIR TEMPERATURE GAUGE, ADAHRS, AND AIRSPEED

This calibration will be accomplished prior to initiation of data collection for the AoA and is the responsibility of AAG.

D.2.2 VERIFY OPERATION OF DATA COLLECTION

The calibration flight(s) will confirm proper operation of data-recording equipment, including audio, video, ADAHRS, GPS, and GPS-derived data (velocities, attitudes, and positions).

D.2.3 CALIBRATE COTS AOA SYSTEMS

Vendor-provided COTS AoA system calibration procedures will be followed prior to data collection and documented.

D.2.4 PRACTICE DATA COLLECTION SEQUENCE WITH TEST TEAM

To ensure maximum efficiency of test collection, the test team will practice data collection prior to taking data for the record, both during the calibration flights and in a desktop environment.

D.2.5 COORDINATE WITH AIR TRAFFICE CONTROL

The test team will coordinate with Norfolk Approach prior to test data-collection flights to define preferred airspace boundaries and radio procedures.

The test area will be negotiated with FAA's Norfolk Approach Control supervisor. The proposed test area is shown in figure D-1. It is located in the northeast quadrant of the Franklin VOR (FKN). The area is approximately 30 nm N-S by 10 nm E-W. The primary maneuvers to be performed, as listed in the appendix of flight cards, consist of straight-line, gradually decelerating trim points flown at constant altitudes (3000 ft, 6500 ft, and 9500 ft) and straight-ahead stalls, turning stalls, and wind-calibration triangles of approximately 2 minutes per leg.

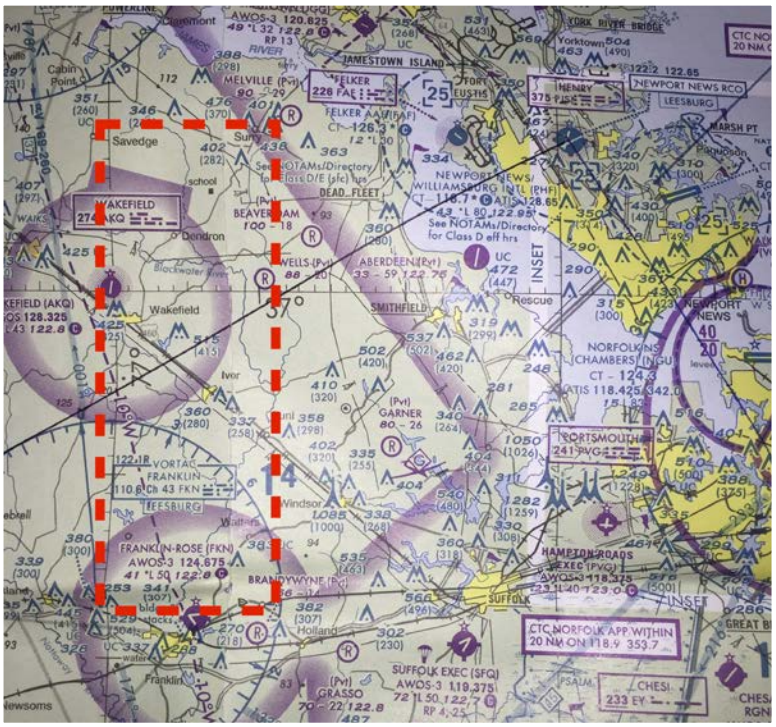

Figure D-1. Proposed flight test area

D.3. FLIGHT PROCEDURES

D.3.1 EQUIPMENT REQUIRED

The following equipment was required for the flight test:

- GoPro camera with empty data card and full battery, audio cable
- Tablet computer with full battery charge
- Garmin GLO™ with full battery charge
- Flight test card set

D.3.2 PREFLIGHT ACTIVITIES

D.3.2.1 Preflight Briefing

The test team will hold a preflight briefing, led by the test flight test engineer, covering weather, flight objectives, geographical test area, flight following procedures, changes to the test plan, and review safety procedures.

D.3.2.2 Record Takeoff Weights

The weight of the crew, any onboard equipment, and pre-start fuel will be recorded to determine aircraft weight and center of mass location.

D.3.2.3 Connect Data Equipment Into I/O box

Figure D-2 shows the configuration and connection of the data logging equipment to the ship's data systems.

D.3.2.4 Mount and Install GoPro Video Camera

The GoPro camera should be mounted, connected to power and audio, aligned, and verified through the iPad® app.

D.3.2.5 Start Video Recording (GoPro)

The GoPro camera should be activated prior to engine start to record video out-the-nose as well as primary flight displays and the Garmin AoA indicator.

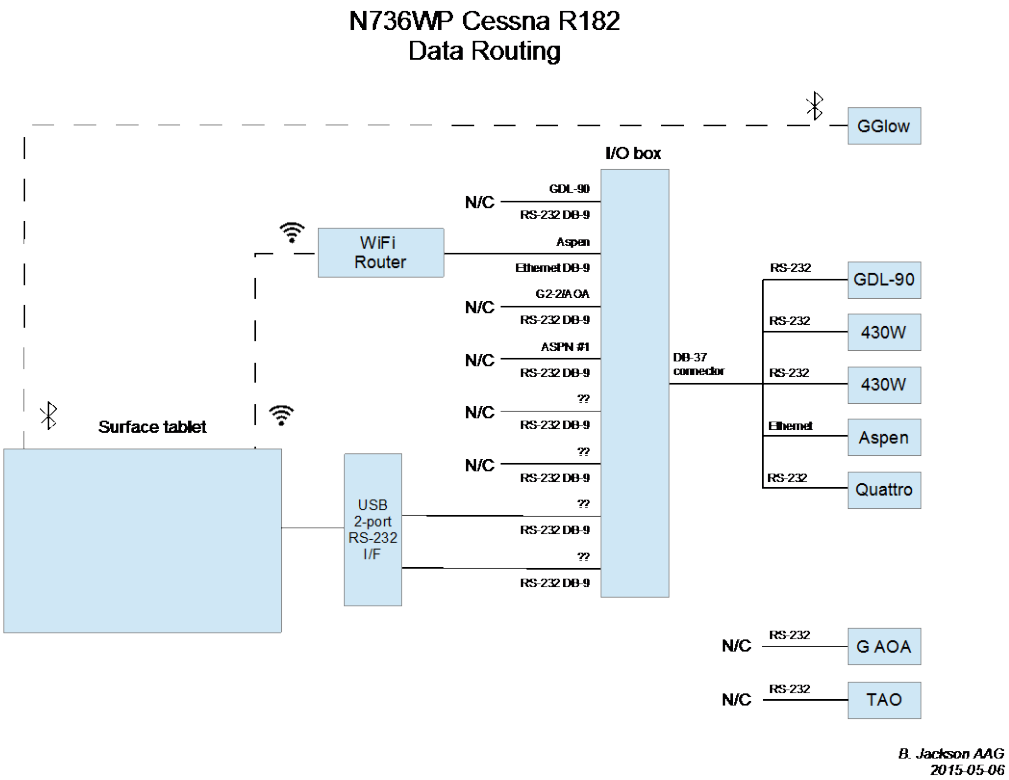

Figure D-2. Data-collection system schematic

D.3.3 POST-START CHECKLIST ITEMS

The following items should be added to the checklist following engine start:

- Record outside air temperature from KPVG automated weather-observing system (AWOS).
- Record barometric pressure setting from KPVG AWOS.
- Record surface winds from KPVG AWOS.
- Record fuel remaining from JPI totalizer.

D.3.3.1 Start Data Collection

Once onboard electrical power is provided, the recording computer will be connected to all data systems and proper operation will be verified. The data-logging computer will be adjusted for maximum screen brightness and to disable screen-saving operation.

D.3.3.1.1 Start Data Logging App

The data-logging application should be started and operation verified on the onboard data computer.

D.3.3.1.2 Sync Audio and Video

The test pilot should count down from 3, then say ”Mark” and clap in front of the video camera at same time to sync audio and video.

D.3.4 TAXI OUT

During taxi to the active runway, the data-logging system should be examined by the flight test engineer to confirm operation and ensure proper recording of all subsystem parameters.

D.3.5 AIRBORNE

Once the test aircraft is airborne and the cruise climb checklist is completed, the flight should proceed as described below:

- Change standby altimeter barometer reading to 29.92″ for pressure altitude reference (ASPEN altimeter to remain at current Norfolk International Airport or nearby barometer setting).
- Proceed to test area and climb to test altitude, noting temperature readings every 250 ft.
- Verify smooth air at altitude.
- Configure aircraft (flaps, gear).
- Note initial fuel, outside air temperature, pressure altitude.

D.3.5.1 Commence Single-Altitude Test Series

Upon reaching the target altitude band, the initial set of flight cards will be executed in the following sequence:

- Level steady airspeed sequence
- Clearing turns
- Incipient stalls
- Power-off stalls
- Higher-power stalls
- Accelerated stalls

D.3.5.2 Repeat at Other Altitudes

As dictated by test progress, the test series may be conducted at additional altitudes. If time and atmospheric conditions permit, the test series may be repeated at the original altitude with a lighter weight. Keep data system running until taxiing off the runway after the flight.

D.3.6 TAXI IN

During taxi from the active runway, the flight engineer should note the outside air temperature on the ground, the current altimeter setting, fuel remaining, and winds at the surface from the KPVG AWOS.

D.3.7 AFTER LANDING BEFORE SHUTDOWN

The data-logging application should be shut down prior to engine shutdown.

D.3.8 AFTER SHUTDOWN

After shutdown, the JPI digital engine monitor data should be downloaded to a data card for post-flight processing.

D.4. POST-FLIGHT PROCESSING

After each flight, the following actions should be taken:

1. Archival of flight data (video, audio, onboard measurement streams) prior to any post-processing.
2. Initial data-quality confirmation.
3. Flight audio and video synchronization and combination into single .mp4 video.
4. Reconstruction of flight data with filtering and conversion of raw measurements into engineering units using preflight calibration information.
5. Initial comparisons of measured vs. calibrated direct and derived AoA data.

D.4.1 REFINE CARDS

Following the initial flight, the flight cards should be reviewed for refinement of both procedures and content, with the goal of maximizing efficient use of flight time.

D.5. APPENDIX TO FLIGHT TEST PLAN–FLIGHT CARDS

D.5.1 LOW ALTITUDE

1 Coordinated steady state – 130 kt and below – clean

2 Low-power stall coordinated – 50 kt – clean

3 Power-off stall coordinated – 50 kt – clean

4 Coordinated steady state – 90 kt and below – 10° flap

5 Low-power stall coordinated – 50 kt – 10° flap

6 Power-off stall coordinated – 50 kt – 10° flap

7 Coordinated steady state – 90 kt and below – 10° flap w/gear

8 Low-power stall coordinated – 50 kt – 10° flap w/gear

9 Power-off stall coordinated – 50 kt – 10° flap w/gear

10 Coordinated steady state – 90 kt and below – 20° flap w/gear

11 Low-power stall coordinated – 40 kt – 20° flap w/gear

12 Power-off stall coordinated – 40 kt – 20° flap w/gear

13 Coordinated steady state – 90 kt and below – 40° flap w/gear

14 Low-power stall coordinated – 40 kt – 40° flap w/gear

15 Power-off stall coordinated – 40 kt – 40° flap w/gear

16 Uncoordinated steady state – 110 kt and below – clean (left skid)

17 Low-power stall uncoordinated – 50 kt – clean (left skid)

18 Power-off stall uncoordinated – 50 kt – clean (left skid)

19 Accel stall coordinated – 70 kt – clean (left turn)

D.5.2 HIGH ALTITUDE

20 Coordinated steady state – 130 kt and below – clean

21 Low-power stall coordinated – 50 kt – clean

22 Power-off stall coordinated – 50 kt – clean

23 Coordinated steady state – 90 kt and below – 10° flap

24 Low-power stall coordinated – 50 kt – 10° flap

25 Power-off stall coordinated – 50 kt – 10° flap

26 Coordinated steady state – 90 kt and below – 10° flap w/gear

27 Low-power stall coordinated – 50 kt – 10° flap w/gear

28 Power-off stall coordinated – 50 kt – 10° flap w/gear

29 Coordinated steady state – 90 kt and below – 20° flap w/gear

30 Low-power stall coordinated – 40 kt – 20° flap w/gear

31 Power-off stall coordinated – 40 kt – 20° flap w/gear

32 Coordinated steady state – 90 kt and below – 40° flap w/gear

33 Low-power stall coordinated – 40 kt – 40° flap w/gear

34 Power-off stall coordinated – 40 kt – 40° flap w/gear

35 Uncoordinated steady state – 110 kt and below – clean (right skid)

36 Low-power stall uncoordinated – 50 kt – clean (right skid)

37 Power-off stall uncoordinated – 50 kt – clean (right skid)

38 Accel stall coordinated – 70 kt – clean (left turn)

D.5.3 LOW ALTITUDE (REPEAT SELECTED CARDS *1-22* [R*XX*] AT LOWER WEIGHT AND DIFFERENT CG)

39 (R1) Coordinated steady state – 130 kt and below – clean

40 (R2) Low-power stall coordinated – 50 kt – clean

41 (R3) Power-off stall coordinated – 50 kt – clean

42 (R4) Coordinated steady state – 90 kt and below – 10° flap

43 (R5) Low-power stall coordinated – 50 kt – 10° flap

44 (R13) Coordinated steady state – 90 kt and below – 40° flap w/gear

45 (R14) Low-power stall coordinated – 40 kt – 40° flap w/gear

46 (R15) Power-off stall coordinated – 40 kt – 40° flap w/gear

47 (R16) Uncoordinated steady state – 110 kt and below – clean (left skid)

48 (R17) Low-power stall uncoordinated – 50 kt – clean (left skid)

49 (R18) Power-off stall uncoordinated – 50 kt – clean (left skid)

50 (R22) Accel stall coordinated – 70 kt – clean (left turn)

1007 Coord stdy state – 130 kt & below – clean – Low

Steady state coordinated flight, clean configuration, low altitude, approx 130 KIAS

Configuration	P Alt (ft)	MP (in)	RPM	KIAS
Clean	3000	23	2400	130

Pilot actions

1. Obtain steady state conditions at initial speed
2. Maintain conditions for 30 seconds
3. Accelerate and repeat at specified airspeeds ±10
4. Repeat at 15, 95, 85, 75, 65, and 55 KIAS

Flt Engineer actions

1. Announce card number
2. Record fuel, time, altitude, indicated airspeed, manifold pressure, engine RPM, OAT
3. Record OAT and heading(s)

Time: OAT:

Pt #	RPM	MP	KIAS	P ALT	HDG	FUEL R	AoA	Pt Note (turb, etc.)

Notes:

Card 1 **Coord stdy state – 130 kt & below – clean – Low (1007)**

7001 Power-off stall coord – 50 kt – clean – Low

Power off coordinated stall, clean configuration, low altitude, approx 50 KIAS

Configuration	P Alt (ft)	MP (in)	RPM	KIAS
Clean	3000	as req'd	Pwr	50

Pilot actions

1. Ensure clearing turns have been performed
2. Trim for minimum speed, full flaps, RPM
3. Slowly close throttle while raising nose and maintain altitude until full throttle entered, hold
4. Recover from stall immediately when nose drops and altitude increases

Flt Engineer actions

1. Announce card number
2. Record fuel, time, altitude, indicated airspeed, manifold pressure, engine RPM, OAT and stall
3. Record OAT and heading(s)

Time: OAT:

Pt #	RPM	MP	KIAS	P ALT	HDG	FUEL R	AoA	Pt Note (turb, etc.)

Notes:

Card 3 **Power-off stall coord – 50 kt – clean – Low (7001)**

4001 Incipient stall coord – 50 kt – clean – Low

In stall buffet, coordinated level flight, clean configuration, low altitude, approx 60 KIAS

Configuration	P Alt (ft)	MP (in)	RPM	KIAS
Clean	3000	as req'd	Pwr	50

Pilot actions

1. Perform clearing turns
2. Trim for minimum speed, full flaps, RPM
3. Close throttle until buffet while maintaining altitude, hold entered, hold
4. Maintain conditions for 30 seconds

Flt Engineer actions

1. Announce card number
2. Record fuel, time, altitude, indicated airspeed, manifold pressure, engine RPM, OAT
3. Record OAT and heading(s)

Time: OAT:

Pt #	RPM	MP	KIAS	P ALT	HDG	FUEL R	AoA	Pt Note (turb, etc.)

Notes:

Card 2 **Incipient stall coord – 50 kt – clean – Low (4001)**

1103 Coord stdy state – 90 kt & below – 10° flap – Low

Steady state coordinated flight, 10° flaps, gear up, low altitude, approx 90 KIAS

Configuration	P Alt (ft)	MP (in)	RPM	KIAS
Flaps 10°, Gear up	3000	18	2400	90

Pilot actions

1. Obtain steady state conditions at initial speed
2. Maintain conditions for 30 seconds
3. Accelerate and repeat at specified airspeeds ±10
4. Repeat at 80, 70, 60, and 50 KIAS

Flt Engineer actions

1. Announce card number
2. Record fuel, time, altitude, indicated airspeed, manifold pressure, engine RPM, OAT
3. Record OAT and heading(s)

Time: OAT:

Pt #	RPM	MP	KIAS	P ALT	HDG	FUEL R	AoA	Pt Note (turb, etc.)

Notes:

Card 4 **Coord stdy state – 90 kt & below – 10° flap – Low (1103)**

4101 Incipient stall coord – 50 kt – 10° flap – Low

Incipient stall coordinated level flight, 0° flaps, gear up, low altitude, approx. 0% KIAS

Configuration	P.ALT (ft)	MP (in)	RPM	KIAS
Flaps 0°, gear up	3000	as req'd	Pwd	50

Pilot actions

1. Perform clearing turns
2. Trim for minimum speed, full pwd RPM
3. Close throttle, until inflection while maintaining altitude and entered hdg
4. Maintain conditions for 5 seconds

Flt Engineer actions

1. Announce card number
2. Record fuel, time, altitude, indicated airspeed, manifold pressure, engine RPM, OAT
3. Record OAT reading(s)

Pt id	RPM	MP	KIAS	P ALT	HDG	FUEL R	AnA	Pt Note (turb, etc.)

Notes

Card 5 **Incipient stall coord – 50 kt – 10° flap – Low (4101)**

7101 Power-off stall coord – 50 kt – 10° flap – Low

Power off coordinated stall, 0° flaps, gear up, low altitude, approx. 0% KIAS

Configuration	P.ALT (ft)	MP (in)	RPM	KIAS
Flaps 0°, gear up	3000	as req'd	Pwd	50

Pilot actions

1. Ensure clearing turns have been performed
2. Trim for minimum speed, full pwd RPM
3. Slowly close throttle while raising nose to maintain altitude until full with entered hdg
4. Recover from stall immediately when nose drops or altitude increases

Flt Engineer actions

1. Announce card number
2. Record fuel, time, altitude, indicated airspeed, manifold pressure, engine RPM, OAT, hdg
3. Record OAT reading(s)

Time OAT

Pt id	RPM	MP	KIAS	P ALT	HDG	FUEL R	AnA	Pt Note (turb, etc.)

Notes

Card 6 **Power-off stall coord – 50 kt – 10° flap – Low (7101)**

1203 Coord stdy state – 90 kt & below – 10° flap w/gear – Low

Steady state coordinated flight, 0° flaps, gear down, low altitude, approx. 90 KIAS

Configuration	P.ALT (ft)	MP (in)	RPM	KIAS
Flaps 0°, gear down	3000	18	2400	90

Pilot actions

1. Obtain steady state conditions at initial speed
2. Maintain conditions for 5 seconds
3. Accelerate and repeat at specified airspeeds ±3
4. Repeat at 80, 70, 60 and 50 KIAS

Flt Engineer actions

1. Announce card number
2. Record fuel, time, altitude, indicated airspeed, manifold pressure, engine RPM, OAT
3. Record OAT reading(s)

Time OAT

Pt id	RPM	MP	KIAS	P ALT	HDG	FUEL R	AnA	Pt Note (turb, etc.)

Notes

Card 7 **Coord stdy state – 90 kt & below – 10° flap w/gear – Low (1203)**

4201 Incipient stall coord – 50 kt – 10° flap w/gear – Low

In stall buffet, coordinated level flight, 0° flaps, gear down, low altitude, approx. 50 KIAS.

Configuration	P.Alt (ft)	MP (in)	RPM	KIAS
Flaps 0°, gear down	3000	as req'd	Fwd	50

Pilot actions

1. Perform clearing turns.
2. Trim for minimum speed, full fwd RPM.
3. Close throttle, initiate buffet while maintaining altitude and centered ball.
4. Maintain conditions for 2 seconds.

Flt Engineer actions

1. Announce aircraft number.
2. Record fuel, time, altitude, indicated airspeed, manifold pressure, engine RPM, OAT.
3. Record OAT reading(s).

Pt #	RPM	MP	KIAS	P ALT	HDG	FUEL #	AnA	Pt Note (turb, etc.)

Time: OAT:

Notes:

Card 8 Incipient stall coord – 50 kt – 10° flap w/gear – Low (4201)

1403 Coord stdy state – 90 kt & below – 20° flap w/gear – Low

Steady state coordinated flight, 0° flaps, gear down, low altitude, approx. 90 KIAS.

Configuration	P.Alt (ft)	MP (in)	RPM	KIAS
Flaps 0°, gear down	3000	19	2400	90

Pilot actions

1. Obtain steady state conditions at initial speed.
2. Maintain conditions for 30 seconds.
3. Accelerate to next specified airspeeds ±3 kts.
4. Repeat 2 & 3 for each specified airspeed.

Flt Engineer actions

1. Announce aircraft number.
2. Record fuel, time, altitude, indicated airspeed, manifold pressure, engine RPM, OAT.
3. Record OAT reading(s).

Pt #	RPM	MP	KIAS	P ALT	HDG	FUEL #	AnA	Pt Note (turb, etc.)

Time: OAT:

Notes:

Card 10 Coord stdy state – 90 kt & below – 20° flap w/gear – Low (1403)

7201 Power-off stall coord – 50 kt – 10° flap w/gear – Low

Power off coordinated stall, 0° flaps, gear down, low altitude, approx. 50 KIAS.

Configuration	P.Alt (ft)	MP (in)	RPM	KIAS
Flaps 0°, gear down	3000	as req'd	Fwd	50

Pilot actions

1. Ensure clearing turns were performed.
2. Trim for minimum speed, full fwd RPM.
3. Slowly close throttle while raising nose maintaining altitude until ball centered.
4. Recover from ball immediately when nose drops or altitude increases.

Flt Engineer actions

1. Announce aircraft number.
2. Record fuel, time, altitude, indicated airspeed, manifold pressure, engine RPM, OAT, all ball.
3. Record OAT reading(s).

Pt #	RPM	MP	KIAS	P ALT	HDG	FUEL #	AnA	Pt Note (turb, etc.)

Time: OAT:

Notes:

Card 9 Power-off stall coord – 50 kt – 10° flap w/gear – Low (7201)

4400 Incipient stall coord – 40 kt – 20° flap w/gear – Low

In stall buffet, coordinated level flight, 0° flaps, gear down, low altitude, approx. 40 KIAS.

Configuration	P.Alt (ft)	MP (in)	RPM	KIAS
Flaps 0°, gear down	3000	as req'd	Fwd	40

Pilot actions

1. Perform clearing turns.
2. Trim for minimum speed, full fwd RPM.
3. Close throttle until buffet while maintaining altitude and centered ball.
4. Maintain conditions for 2 seconds.

Flt Engineer actions

1. Announce aircraft number.
2. Record fuel, time, altitude, indicated airspeed, manifold pressure, engine RPM, OAT.
3. Record OAT reading(s).

Pt #	RPM	MP	KIAS	P ALT	HDG	FUEL #	AnA	Pt Note (turb, etc.)

Time: OAT:

Notes:

Card 11 Incipient stall coord – 40 kt – 20° flap w/gear – Low (4400)

7400 Power-off stall coord – 40 kt – 20° flap w/gear – Low

Power-off coordinated stall, 20° flaps, gear down, low altitude, approx. 40 KIAS

Configuration	P. Alt (ft)	MP (in)	RPM	KIAS
Flaps 20°, Gear down	3000	as req'd	Fwd	40

Pilot actions	Flt Engineer actions
1. Ensure clearing turns have been performed 2. Trim for minimum speed, full fwd RPM 3. Slowly close throttle while raising nose to maintain altitude until stall with centered ball 4. Recover from stall immediately when nose drops or altitude decreases	1. Announce card number 2. Record fuel, time, altitude, indicated airspeed, manifold pressure, engine RPM, OAT at stall 3. Record AOA reading(s)

Time: OAT:

Pt #	RPM	MP	KIAS	P-ALT	HDG	FUEL-R	AoA	Pt Note (turb, etc.)

Notes

Card 12 Power-off stall coord – 40 kt – 20° flap w/gear – Low (7400)

4600 Incipient stall coord – 40 kt – 40° flap w/gear – Low

Incipient stall buffet in coordinated level flight, 40° flaps, gear down, low altitude, approx. 40 KIAS

Configuration	P. Alt (ft)	MP (in)	RPM	KIAS
Flaps 40°, Gear down	3000	as req'd	Fwd	40

Pilot actions	Flt Engineer actions
1. Perform clearing turns 2. Trim for minimum speed, full fwd RPM 3. Close throttle until buffet while maintaining altitude and centered ball 4. Maintain conditions for 5 seconds	1. Announce card number 2. Record fuel, time, altitude, indicated airspeed, manifold pressure, engine RPM, OAT 3. Record AOA reading(s)

Time: OAT:

Pt #	RPM	MP	KIAS	P-ALT	HDG	FUEL-R	AoA	Pt Note (turb, etc.)

Notes

Card 14 Incipient stall coord – 40 kt – 40° flap w/gear – Low (4600)

1603 Coord stdy state – 90 kt & below – 40° flap w/gear – Low

Steady-state coordinated flight, 40° flaps, gear down, low altitude, approx. 90 KIAS

Configuration	P. Alt (ft)	MP (in)	RPM	KIAS
Flaps 40°, Gear down	3000	20	2400	90

Pilot actions	Flt Engineer actions
1. Obtain steady-state conditions at initial speed 2. Maintain conditions for 5 seconds 3. Decelerate and repeat at specified airspeeds ±3 kt 4. Repeat at 80, 70, 60, 50 and 40 KIAS	1. Announce card number 2. Record fuel, time, altitude, indicated airspeed, manifold pressure, engine RPM, OAT 3. Record AOA reading(s)

Time: OAT:

Pt #	RPM	MP	KIAS	P-ALT	HDG	FUEL-R	AoA	Pt Note (turb, etc.)

Notes

Card 13 Coord stdy state – 90 kt & below – 40° flap w/gear – Low (1603)

7600 Power-off stall coord – 40 kt – 40° flap w/gear – Low

Power-off coordinated stall, 40° flaps, gear down, low altitude, approx. 40 KIAS

Configuration	P. Alt (ft)	MP (in)	RPM	KIAS
Flaps 40°, Gear down	3000	as req'd	Fwd	40

Pilot actions	Flt Engineer actions
1. Ensure clearing turns have been performed 2. Trim for minimum speed, full fwd RPM 3. Slowly close throttle while raising nose to maintain altitude until stall with centered ball 4. Recover from stall immediately when nose drops or altitude decreases	1. Announce card number 2. Record fuel, time, altitude, indicated airspeed, manifold pressure, engine RPM, OAT at stall 3. Record AOA reading(s)

Time: OAT:

Pt #	RPM	MP	KIAS	P-ALT	HDG	FUEL-R	AoA	Pt Note (turb, etc.)

Notes

Card 15 Power-off stall coord – 40 kt – 40° flap w/gear – Low (7600)

2005 Uncoord stdy state – 110 kt & below – clean – Low

Steady state flight with one ball deslip, clean configuration, low altitude, approx. 110 KIAS.

Configuration	P. Alt (ft)	MP (in)	RPM	KIAS
Clean	3000	23	2400	110

Pilot actions

1. Obtain steady heading, deslip conditions (initial speed while maintaining one ball sideslip to the LEFT)
2. Maintain conditions for 30 seconds
3. Accelerate to and repeat at specified airspeeds ±5 kt
4. Repeat at 100, 90, 80, 70, 60, 50 KIAS

Flt Engineer actions

1. Announce card number
2. Record fuel, time, altitude, indicated airspeed, manifold pressure, engine RPM, OAT
3. Record OAT, heading(s)

Time: ____ OAT: ____

Pt #	RPM	MP	KIAS	P ALT	HDG	FUEL R	AnA	Pt # Note (turb, etc.)

Notes:

Card 16 Uncoord stdy state – 110 kt & below – clean – Low (2005)

8001 Power-off stall uncoord – 50 kt – clean – Low

Power off stall with one ball deslip, clean configuration, low altitude, approx. 90 KIAS.

Configuration	P. Alt (ft)	MP (in)	RPM	KIAS
Clean	3000	as req'd	Fwd	50

Pilot actions

1. Ensure clearing turns have been performed
2. Obtain steady heading, deslip conditions while maintaining one ball LEFT
3. Maintain conditions for 5 seconds

Flt Engineer actions

1. Announce card number
2. Record fuel, time, altitude, indicated airspeed, manifold pressure, engine RPM, OAT, all
3. Record OAT, heading(s)

Time: ____ OAT: ____

Pt #	RPM	MP	KIAS	P ALT	HDG	FUEL R	AnA	Pt # Note (turb, etc.)

Notes:

Card 18 Power-off stall uncoord – 50 kt – clean – Low (8001)

5001 Incipient stall uncoord – 50 kt – clean – Low

In stall buffer with one ball deslip, level flight, clean configuration, low altitude, approx. 90 KIAS.

Configuration	P. Alt (ft)	MP (in)	RPM	KIAS
Clean	3000	as req'd	Fwd	50

Pilot actions

1. Obtain steady heading, deslip conditions while maintaining one ball deslip to the LEFT
2. Maintain conditions for 5 seconds

Flt Engineer actions

1. Announce card number
2. Record fuel, time, altitude, indicated airspeed, manifold pressure, engine RPM, OAT
3. Record OAT, heading(s)

Time: ____ OAT: ____

Pt #	RPM	MP	KIAS	P ALT	HDG	FUEL R	AnA	Pt # Note (turb, etc.)

Notes:

Card 17 Incipient stall uncoord – 50 kt – clean – Low (5001)

13002 Accel stall coord – 70 kt – clean – Low

Accelerated stall turn coordinated flight, clean configuration, low altitude, approx. 70 KIAS.

Configuration	P. Alt (ft)	MP (in)	RPM	KIAS
Clean	3000	as req'd	Fwd	70

Pilot actions

1. Perform clearing turns
2. Trim for target speed
3. Roll to LEFT, establish increase RPM, maintain airspeed, increase back pressure with constant throttle until AI
4. Recover from stall immediately

Flt Engineer actions

1. Announce card number
2. Record fuel, time, altitude, indicated airspeed, manifold pressure, engine RPM, OAT, all
3. Record OAT, heading(s)

Time: ____ OAT: ____

Pt #	RPM	MP	KIAS	P ALT	HDG	FUEL R	AnA	Pt # Note (turb, etc.)

Notes:

Card 19 Accel stall coord – 70 kt – clean – Low (13002)

1027 Coord stdy state – 130 kt & below – clean – High

Steady-state coordinated flight, clean configuration, high altitude, approx 30% IAS

Configuration	P Alt (ft)	MP (in)	RPM	KIAS
Clean	9000	20	2400	130

Pilot actions

1. Obtain steady-state conditions at initial speed
2. Maintain conditions for 20 seconds
3. Accelerate 3 kts per second to specified airspeeds +3 -0 KIAS
4. Repeat 4, 5, 6, 5, 4, 5, 6, 5, and 4 KIAS

Flt Engineer actions

1. Announce card number
2. Record fuel, time, altitude, indicated airspeed, manifold pressure, engine RPM, OAT
3. Record OAT reading(s)

Pt #	RPM	MP	KIAS	P ALT	HDG	FUEL R	AnA	Pt Note (turb, etc.)

Notes

Card 20 **Coord stdy state – 130 kt & below – clean – High (1027)**

4021 Incipient stall coord – 50 kt – clean – High

Incipient stall buffet coordinated level flight, clean configuration, high altitude, approx 50% IAS

Configuration	P Alt (ft)	MP (in)	RPM	KIAS
Clean	9000	as req'd	Fwd	50

Pilot actions

1. Perform clearing turns
2. Trim for minimum speed, full RPM
3. Close throttle until buffet while maintaining altitude and entered hdg
4. Maintain conditions for 20 seconds

Flt Engineer actions

1. Announce card number
2. Record fuel, time, altitude, indicated airspeed, manifold pressure, engine RPM, OAT
3. Record OAT reading(s)

Time OAT

Pt #	RPM	MP	KIAS	P ALT	HDG	FUEL R	AnA	Pt Note (turb, etc.)

Notes

Card 21 **Incipient stall coord – 50 kt – clean – High (4021)**

7021 Power-off stall coord – 50 kt – clean – High

Power-off coordinated stall, clean configuration, high altitude, approx 0% IAS

Configuration	P Alt (ft)	MP (in)	RPM	KIAS
Clean	9000	as req'd	Fwd	50

Pilot actions

1. Ensure clearing turns have been performed
2. Trim for minimum speed, full RPM
3. Slowly close throttle while raising nose to maintain altitude until full with entered hdg
4. Recover from stall immediately when nose drops to altitude decreases

Flt Engineer actions

1. Announce card number
2. Record fuel, time, altitude, indicated airspeed, manifold pressure, engine RPM, OAT at stall
3. Record OAT reading(s)

Time OAT

Pt #	RPM	MP	KIAS	P ALT	HDG	FUEL R	AnA	Pt Note (turb, etc.)

Notes

Card 22 **Power-off stall coord – 50 kt – clean – High (7021)**

1123 Coord stdy state – 90 kt & below – 10° flap – High

Steady-state coordinated flight, 10° flaps, gear up, high altitude, approx. 90 KIAS

Configuration	P. Alt (ft)	MP (in)	RPM	KIAS
Flaps 10°, gear up	9000	18	2400	90

Pilot actions	Flt Engineer actions
1. Obtain steady-state conditions, initial speed 2. Maintain conditions for 30 seconds 3. Decelerate and repeat at specified airspeeds ±3 kt 4. Repeat at 80, 70, 60, 50 and 40 KIAS	1. Announce card number 2. Record fuel, time, altitude, indicated airspeed, manifold pressure, engine RPM, OAT 3. Record OAT reading(s)

Time: OAT:

Pt #	RPM	MP	KIAS	P ALT	HDG	FUEL flt	AoA	Pt Note (turb, etc.)

Notes:

Card 23 **Coord stdy state – 90 kt & below – 10° flap – High (1123)**

7121 Power-off stall coord – 50 kt – 10° flap – High

Power-off coordinated stall, 10° flaps, gear up, high altitude, approx. 90 KIAS

Configuration	P. Alt (ft)	MP (in)	RPM	KIAS
Flaps 10°, gear up	9000	as req'd	Pwr idle	50

Pilot actions	Flt Engineer actions
1. Ensure all clearing turns have been performed 2. Trim for minimum speed, 90 RPM 3. Slowly close throttle while raising nose and maintain altitude until full stall with entered roll 4. Recover from stall immediately when nose drops or altitude increases	1. Announce card number 2. Record fuel, time, altitude, indicated airspeed, manifold pressure, engine RPM, OAT at stall 3. Record OAT reading(s)

Time: OAT:

Pt #	RPM	MP	KIAS	P ALT	HDG	FUEL flt	AoA	Pt Note (turb, etc.)

Notes:

Card 25 **Power-off stall coord – 50 kt – 10° flap – High (7121)**

4121 Incipient stall coord – 50 kt – 10° flap – High

In stall buffet, coordinated level flight, 10° flaps, gear up, high altitude, approx. 90 KIAS

Configuration	P. Alt (ft)	MP (in)	RPM	KIAS
Flaps 10°, gear up	9000	as req'd	Pwr idle	50

Pilot actions	Flt Engineer actions
1. Perform clearing turns 2. Trim for minimum speed, full aft CP 3. Close throttle until full aft stick while maintaining altitude and entered roll 4. Maintain conditions for 30 seconds	1. Announce card number 2. Record fuel, time, altitude, indicated airspeed, manifold pressure, engine RPM, OAT 3. Record OAT reading(s)

Time: OAT:

Pt #	RPM	MP	KIAS	P ALT	HDG	FUEL flt	AoA	Pt Note (turb, etc.)

Notes:

Card 24 **Incipient stall coord – 50 kt – 10° flap – High (4121)**

1223 Coord stdy state – 90 kt & below – 10° flap w/gear – High

Steady-state coordinated flight, 10° flaps, gear down, high altitude, approx. 90 KIAS

Configuration	P. Alt (ft)	MP (in)	RPM	KIAS
Flaps 10°, gear down	9000	18	2400	90

Pilot actions	Flt Engineer actions
1. Obtain steady-state conditions, initial speed 2. Maintain conditions for 30 seconds 3. Decelerate and repeat at specified airspeeds ±3 kt 4. Repeat at 80, 70, 60, 50 and 40 KIAS	1. Announce card number 2. Record fuel, time, altitude, indicated airspeed, manifold pressure, engine RPM, OAT 3. Record OAT reading(s)

Time: OAT:

Pt #	RPM	MP	KIAS	P ALT	HDG	FUEL flt	AoA	Pt Note (turb, etc.)

Notes:

Card 26 **Coord stdy state – 90 kt & below – 10° flap w/gear – High (1223)**

4221 Incipient stall coord – 50 kt – 10° flap w/gear – High

Incipient stall coordinated level flight, 0° flaps, gear down, high altitude, approx 50 KIAS

Configuration	P.Alt (ft)	MP (in)	RPM	KIAS
Flaps 0° Gear down	9000	as req'd	Fwd	50

Pilot actions

1. Perform clearing turns
2. Trim for minimum speed, all R/C RPM
3. Close throttle and pull nose to maintain altitude and entered hdg
4. Maintain conditions for 5 sec

Flt Engineer actions

1. Announce card number
2. Record fuel, time, altitude, indicated airspeed, manifold pressure, engine RPM, OAT
3. Record OAT reading(s)

Pt #	RPM	MP	KIAS	P ALT	HDG	FUEL R	AoA	Pt Note (turb, etc.)

Notes:

Card 27 Incipient stall coord – 50 kt – 10° flap w/gear – High (4221)

7221 Power-off stall coord – 50 kt – 10° flap w/gear – High

Power-off coordinated stall, 0° flaps, gear down, high altitude, approx 90 KIAS

Configuration	P.Alt (ft)	MP (in)	RPM	KIAS
Flaps 0° Gear down	9000	as req'd	Fwd	50

Pilot actions

1. Ensure clearing turns have been performed
2. Trim for minimum speed, all R/C RPM
3. Slowly close throttle while raising nose to maintain altitude until full aft stick is entered, hold
4. Recover from stall immediately when nose drops or altitude increases

Flt Engineer actions

1. Announce card number
2. Record fuel, time, altitude, indicated airspeed, manifold pressure, engine RPM, OAT
3. Record OAT reading(s)

Time: OAT:

Pt #	RPM	MP	KIAS	P ALT	HDG	FUEL R	AoA	Pt Note (turb, etc.)

Notes:

Card 28 Power-off stall coord – 50 kt – 10° flap w/gear – High (7221)

1423 Coord stdy state – 90 kt & below – 20° flap w/gear – High

Steady state coordinated flight, 0° flaps, gear down, high altitude, approx 90 KIAS

Configuration	P.Alt (ft)	MP (in)	RPM	KIAS
Flaps 0° Gear down	9000	19	2400	90

Pilot actions

1. Obtain steady state conditions at initial speed
2. Maintain conditions for 5 sec
3. Accelerate to repeat specified airspeed ±3 kts
4. Repeat 2 & 3 for each specified airspeed

Flt Engineer actions

1. Announce card number
2. Record fuel, time, altitude, indicated airspeed, manifold pressure, engine RPM, OAT
3. Record OAT reading(s)

Time: OAT:

Pt #	RPM	MP	KIAS	P ALT	HDG	FUEL R	AoA	Pt Note (turb, etc.)

Notes:

Card 29 Coord stdy state – 90 kt & below – 20° flap w/gear – High (1423)

%

4420 Incipient stall coord – 40 kt – 20° flap w/gear – High

In%tall%buffet%to%coordinated%level%flight,%0°%flaps,%gear%down,%high%altitude,%approx.%40%KIAS%

Configuration+	P.Alt (ft)+	MP (in)+	RPM+	KIAS+
Flaps%0°%Gear%Down%	9000%	as%req'd%	Pwr%	40%

Pilot actions+

1.%Perform%clearing%turns%
2.%Trim%for%minimum%speed,%MP%or%RPM%
3.%Close%throttle%to%reflect%full%climb%training%altitude%and%entered%stall%
4.%Maintain%conditions%for%%seconds%

Flt Engineer actions+

1.%Announce%card%number%
2.%Record%fuel,%time,%altitude,%indicated%airspeed,%manifold%pressure,%engine%RPM,%OAT%
3.%Record%OA%reading(s)%
%

%

Pt #+	RPM+	MP+	KIAS+	P-ALT+	HDG+	FUEL#+	AnA+	Pt Note (turb, etc.)+
%	%	%	%	%	%	%	%	%
%	%	%	%	%	%	%	%	%
%	%	%	%	%	%	%	%	%
%	%	%	%	%	%	%	%	%
%	%	%	%	%	%	%	%	%
%	%	%	%	%	%	%	%	%
%	%	%	%	%	%	%	%	%
%	%	%	%	%	%	%	%	%
%	%	%	%	%	%	%	%	%
%	%	%	%	%	%	%	%	%

Notes:%

%

%

Card 30 **Incipient stall coord – 40 kt – 20° flap w/gear – High (4420)**

%

7420 Power-off stall coord – 40 kt – 20° flap w/gear – High

Power-off%coordinated%stall,%0°%flaps,%gear%down,%high%altitude,%approx.%0%KIAS%

Configuration+	P.Alt (ft)+	MP (in)+	RPM+	KIAS+
Flaps%0°%Gear%Down%	9000%	as%req'd%	Pwr%	40%

Pilot actions+

1.%Ensure%clearing%turns%have%been%performed%
2.%Trim%for%minimum%speed,%MP%or%RPM%
3.%Slowly%close%throttle%while%rising%nose%%maintaining%altitude%until%stall%with%entered%ball%
4.%Recover%from%stall%immediately%when%nose%drops%%altitude%decreases%

Flt Engineer actions+

1.%Announce%card%number%
2.%Record%fuel,%time,%altitude,%indicated%airspeed,%manifold%pressure,%engine%RPM,%AT%%all%
3.%Record%OA%reading(s)%
%

%

%%%%%%Time+ OAT+ %

Pt #+	RPM+	MP+	KIAS+	P-ALT+	HDG+	FUEL#+	AnA+	Pt Note (turb, etc.)+
%	%	%	%	%	%	%	%	%
%	%	%	%	%	%	%	%	%
%	%	%	%	%	%	%	%	%
%	%	%	%	%	%	%	%	%
%	%	%	%	%	%	%	%	%
%	%	%	%	%	%	%	%	%
%	%	%	%	%	%	%	%	%
%	%	%	%	%	%	%	%	%
%	%	%	%	%	%	%	%	%
%	%	%	%	%	%	%	%	%

Notes:%

%

%

Card 31 **Power-off stall coord – 40 kt – 20° flap w/gear – High (7420)**

%

1623 Coord stdy state – 90 kt & below – 40° flap w/gear – High

Steady-state%coordinated%flight,%0°%flaps,%gear%down,%high%altitude,%approx.%90%KIAS%

Configuration+	P.Alt (ft)+	MP (in)+	RPM+	KIAS+
Flaps%0°%Gear%Down%	9000%	20%	2400%	90%

Pilot actions+

1.%Obtain%steady-state%conditions%at%initial%speed%
2.%Maintain%conditions%for%%seconds%
3.%Decelerate%at%the%rate%of%%specified%airspeed,%±5%%
4.%Repeat%%at%0,%0,%0%at%%IAS%

Flt Engineer actions+

1.%Announce%card%number%
2.%Record%fuel,%time,%altitude,%indicated%airspeed%manifold%pressure,%engine%RPM,%AT%
3.%Record%OA%reading(s)%
%

%

%%%%%%Time+ OAT+ %

Pt #+	RPM+	MP+	KIAS+	P-ALT+	HDG+	FUEL#+	AnA+	Pt Note (turb, etc.)+
%	%	%	%	%	%	%	%	%
%	%	%	%	%	%	%	%	%
%	%	%	%	%	%	%	%	%
%	%	%	%	%	%	%	%	%
%	%	%	%	%	%	%	%	%
%	%	%	%	%	%	%	%	%
%	%	%	%	%	%	%	%	%
%	%	%	%	%	%	%	%	%
%	%	%	%	%	%	%	%	%
%	%	%	%	%	%	%	%	%

Notes:%

%

%

Card 32 **Coord stdy state – 90 kt & below – 40° flap w/gear – High (1623)**

4620 Incipient stall coord – 40 kt – 40° flap w/gear – High

In all inflt coordinated vel flight, flaps, gear down, high altitude, approx 40 KIAS

Configuration	P ALT (ft)	MP (in)	RPM	KIAS
Flaps 40°, gear down	9000	as req'd	Fwd	40

Pilot actions

1. Perform clearing turns
2. Trim for minimum speed, full flaps, 2400 RPM
3. Close throttle until inflt while maintaining altitude, hdg entered, ball
4. Maintain conditions for 5 seconds

Flt Engineer actions

1. Announce card number
2. Record fuel, time, altitude, indicated airspeed, manifold pressure, engine RPM, OAT
3. Record OAT reading(s)

Pt id	RPM	MP	KIAS	P ALT	HDG	FUEL QR	AnA	Pt Note (turb, etc.)

Notes

Card 33 **Incipient stall coord – 40 kt – 40° flap w/gear – High (4620)**

3025 Uncoord stdy state – 110 kt & below – clean – High

Steady state flight with ball deslip, clean configuration, high altitude, approx 110 KIAS

Configuration	P ALT (ft)	MP (in)	RPM	KIAS
Clean	9000	20	2400	110

Pilot actions

1. Obtain steady heading, deslip conditions while maintaining one ball deslip, lean RIGHT
2. Maintain conditions for 5 seconds
3. Accelerate and repeat at specified airspeed ±3

Flt Engineer actions

1. Announce card number
2. Record fuel, time, altitude, indicated airspeed, manifold pressure, engine RPM, OAT
3. Record OAT reading(s)

Pt id	RPM	MP	KIAS	P ALT	HDG	FUEL QR	AnA	Pt Note (turb, etc.)

Notes

Card 35 **Uncoord stdy state – 110 kt & below – clean – High (3025)**

7620 Power-off stall coord – 40 kt – 40° flap w/gear – High

Power off coordinated all, 40° flaps, gear down, high altitude, approx 40 KIAS

Configuration	P ALT (ft)	MP (in)	RPM	KIAS
Flaps 40°, gear down	9000	as req'd	Fwd	40

Pilot actions

1. Assure clearing turns have been performed
2. Trim for minimum speed, full flaps, 2400 RPM
3. Slowly close throttle while easing nose up to maintain altitude until 40 KIAS with entered ball
4. Recover from stall immediately when nose drops or altitude increases

Flt Engineer actions

1. Announce card number
2. Record fuel, time, altitude, indicated airspeed, manifold pressure, engine RPM, OAT at stall
3. Record OAT reading(s)

Pt id	RPM	MP	KIAS	P ALT	HDG	FUEL QR	AnA	Pt Note (turb, etc.)

Notes

Card 34 **Power-off stall coord – 40 kt – 40° flap w/gear – High (7620)**

%

6021 | **Incipient stall uncoord – 50 kt – clean – High**

In%tall%uffer%with%ne"ball%deslip,%level%light,%lean%nfiguration,%igh%ltitude,%approx.%0%KIAS%

Configuration+	P.Alt (ft)+	MP (in)+	RPM+	KIAS+
Clean%	9000%	as%eq'd%	Fwd%	50%

Pilot uctions+

1.%btain%teady"heading%de"slip%nditions%while%aintaining%ne%ll%de-slip%ball%RIGHT%
2.%aintain%nditions%r%0%econds%

Flt Engineer uctions+

1.%nnounce%ord%umber%
2.%econd%uel,%me,%ltitude,%dicated%irspeed,%manifold%ressure,%ngine%PM,%AT%
3.%econd%OA%eading(s)%
%

%

9%% % % + Time+ * OAT+ %

Pt-#+	RPM+	MP+	KIAS+	P ALT+	HDG+	FUEL-R+	AoA+	Pt-Note (turb, etc.)+
%	%	%	%	%	%	%	%	%
%	%	%	%	%	%	%	%	%
%	%	%	%	%	%	%	%	%
%	%	%	%	%	%	%	%	%
%	%	%	%	%	%	%	%	%
%	%	%	%	%	%	%	%	%
%	%	%	%	%	%	%	%	%
%	%	%	%	%	%	%	%	%
%	%	%	%	%	%	%	%	%
%	%	%	%	%	%	%	%	%

Notes:%

%

%

Card 36 **Incipient stall uncoord – 50 kt – clean – High (6021)**

%

13022 | **Accel stall coord – 70 kt – clean – High**

Accelerated%tall%rom%oordinated%light,%lean%onfiguration,%igh%ltitude,%approx.%70%KIAS%

Configuration+	P.Alt (ft)+	MP (in)+	RPM+	KIAS+
Clean%	9000%	as%eq'd%	Fwd%	70%

Pilot uctions+

1.%erform%learing%urns%
2.%tart%he%arget%peed%
3.%-P%%EET%/%"ank,%crease%PM%% maintain%irspeed,%crease%back%ressure%with%onstant%hrottle%ntil%tall%
4.%ecover%rom%tall%mediately%

Flt Engineer uctions+

1.%nnounce%ord%umber%
2.%econd%uel,%me,%ltitude,%dicated%irspeed,%manifold%ressure,%ngine%PM,%AT%%tall%
3.%econd%OA%eading(s)%
%

%

9%% % % + Time+ * OAT+ %

Pt-#+	RPM+	MP+	KIAS+	P ALT+	HDG+	FUEL-R+	AoA+	Pt-Note (turb, etc.)+
%	%	%	%	%	%	%	%	%
%	%	%	%	%	%	%	%	%
%	%	%	%	%	%	%	%	%
%	%	%	%	%	%	%	%	%
%	%	%	%	%	%	%	%	%
%	%	%	%	%	%	%	%	%
%	%	%	%	%	%	%	%	%
%	%	%	%	%	%	%	%	%
%	%	%	%	%	%	%	%	%
%	%	%	%	%	%	%	%	%

Notes:%

%

%

Card 38 **Accel stall coord – 70 kt – clean – High (13022)**

!

%

9021 | **Power-off stall uncoord – 50 kt – clean – High**

Power"off%tall%with%ne"ball%deslip,%lean%nfiguration,%igh%ltitude,%approx.%0%KIAS%

Configuration+	P.Alt (ft)+	MP (in)+	RPM+	KIAS+
Clean%	9000%	as%eq'd%	Fwd%	50%

Pilot uctions+

1.%ssure%learing%urns%ave%een%erformed%
2.%btain%teady"heading%de"slip%nditions%while%aintaining%ne%ll%RIGHT%
3.%aintain%nditions%r%0%econds%

Flt Engineer uctions+

1.%nnounce%ord%umber%
2.%econd%uel,%me,%ltitude,%dicated%irspeed,%manifold%ressure,%ngine%PM,%AT%%tall%
3.%econd%OA%eading(s)%
%

%

9%% % % + Time+ * OAT+ %

Pt-#+	RPM+	MP+	KIAS+	P ALT+	HDG+	FUEL-R+	AoA+	Pt-Note (turb, etc.)+
%	%	%	%	%	%	%	%	%
%	%	%	%	%	%	%	%	%
%	%	%	%	%	%	%	%	%
%	%	%	%	%	%	%	%	%
%	%	%	%	%	%	%	%	%
%	%	%	%	%	%	%	%	%
%	%	%	%	%	%	%	%	%
%	%	%	%	%	%	%	%	%
%	%	%	%	%	%	%	%	%
%	%	%	%	%	%	%	%	%

Notes:%

%

%

Card 37 **Power-off stall uncoord – 50 kt – clean – High (9021)**

1007 Coord stdy state – 130 kt & below – clean – Low

Steady-state coordinated flight, clean configuration, low altitude, approx. 130 KIAS

Configuration	P. Alt (ft)	MP (in)	RPM	KIAS
Clean	3000	23	2400	130

Pilot actions

1. Obtain steady-state conditions at initial speed
2. Maintain conditions for [illegible] seconds
3. Decelerate and repeat at specified airspeeds ±3 [illegible]
4. Repeat at …15, …05, …5, …5, …5, …5, and …5 KIAS

Flt Engineer actions

1. Announce card number
2. Record fuel, time, altitude, indicated airspeed, manifold pressure, engine RPM, OAT
3. Record AOA reading(s)

Time: OAT:

Pt #	RPM	MP	KIAS	P-ALT	HDG	FUEL-R	AoA	Pt Note (turb, etc.)

Notes

Card 39 Coord stdy state – 130 kt & below – clean – Low (1007)

4001 Incipient stall coord – 50 kt – clean – Low

In stall buffet in coordinated level flight, clean configuration, low altitude, approx. 50 KIAS

Configuration	P. Alt (ft)	MP (in)	RPM	KIAS
Clean	3000	as req'd	Fwd	50

Pilot actions

1. Perform clearing turns
2. Trim for minimum speed, full fwd RPM
3. Close throttle until buffet while maintaining altitude and centered ball
4. Maintain conditions for [illegible] seconds

Flt Engineer actions

1. Announce card number
2. Record fuel, time, altitude, indicated airspeed, manifold pressure, engine RPM, OAT
3. Record AOA reading(s)

Time: OAT:

Pt #	RPM	MP	KIAS	P-ALT	HDG	FUEL-R	AoA	Pt Note (turb, etc.)

Notes

Card 40 Incipient stall coord – 50 kt – clean – Low (4001)

7001 Power-off stall coord – 50 kt – clean – Low

Power-off coordinated stall, clean configuration, low altitude, approx. 50 KIAS

Configuration	P. Alt (ft)	MP (in)	RPM	KIAS
Clean	3000	as req'd	Fwd	50

Pilot actions

1. Ensure clearing turns have been performed
2. Trim for minimum speed, full fwd RPM
3. Slowly close throttle while raising nose to maintain altitude until stall with centered ball
4. Recover from stall immediately when nose drops or altitude decreases

Flt Engineer actions

1. Announce card number
2. Record fuel, time, altitude, indicated airspeed, manifold pressure, engine RPM, OAT at stall
3. Record AOA reading(s)

Time: OAT:

Pt #	RPM	MP	KIAS	P-ALT	HDG	FUEL-R	AoA	Pt Note (turb, etc.)

Notes

Card 41 Power-off stall coord – 50 kt – clean – Low (7001)

1103 | Coord stdy state – 90 kt & below – 10° flap – Low

Steady-state coordinated flight, 10° flaps, gear up, low altitude, approx. 90 KIAS

Configuration	P. Alt (ft)	MP (in)	RPM	KIAS
Flaps 10°, Gear up	3000	18	2400	90

Pilot actions	Flt Engineer actions
1. Obtain steady-state conditions at initial speed 2. Maintain conditions for [illegible] seconds 3. Decelerate and repeat at specified airspeeds ±3 [illegible] 4. Repeat at [illegible] KIAS	1. Announce card number 2. Record fuel, time, altitude, indicated airspeed, manifold pressure, engine RPM, OAT 3. Record AOA reading(s)

Time: | OAT:

Pt #	RPM	MP	KIAS	P-ALT	HDG	FUEL-R	AoA	Pt Note (turb, etc.)

Notes:

Card 42 Coord stdy state – 90 kt & below – 10° flap – Low (1103)

1603 | Coord stdy state – 90 kt & below – 40° flap w/gear – Low

Steady-state coordinated flight, 40° flaps, gear down, low altitude, approx. 90 KIAS

Configuration	P. Alt (ft)	MP (in)	RPM	KIAS
Flaps 40°, Gear down	3000	20	2400	90

Pilot actions	Flt Engineer actions
1. Obtain steady-state conditions at initial speed 2. Maintain conditions for [illegible] seconds 3. Decelerate and repeat at specified airspeeds ±3 [illegible] 4. Repeat at [illegible] KIAS	1. Announce card number 2. Record fuel, time, altitude, indicated airspeed, manifold pressure, engine RPM, OAT 3. Record AOA reading(s)

Time: | OAT:

Pt #	RPM	MP	KIAS	P-ALT	HDG	FUEL-R	AoA	Pt Note (turb, etc.)

Notes:

Card 44 Coord stdy state – 90 kt & below – 40° flap w/gear – Low (1603)

4101 | Incipient stall coord – 50 kt – 10° flap – Low

In stall buffet in coordinated level flight, 10° flaps, gear up, low altitude, approx. 50 KIAS

Configuration	P. Alt (ft)	MP (in)	RPM	KIAS
Flaps 10°, Gear up	3000	as req'd	Fwd	50

Pilot actions	Flt Engineer actions
1. Perform clearing turns 2. Trim for minimum speed, full fwd RPM 3. Close throttle until buffet while maintaining altitude and entered stall 4. Maintain conditions for [illegible] seconds	1. Announce card number 2. Record fuel, time, altitude, indicated airspeed, manifold pressure, engine RPM, OAT 3. Record AOA reading(s)

Time: | OAT:

Pt #	RPM	MP	KIAS	P-ALT	HDG	FUEL-R	AoA	Pt Note (turb, etc.)

Notes:

Card 43 Incipient stall coord – 50 kt – 10° flap – Low (4101)

4600 | Incipient stall coord – 40 kt – 40° flap w/gear – Low

In stall buffet in coordinated level flight, 40° flaps, gear down, low altitude, approx. 40 KIAS

Configuration	P. Alt (ft)	MP (in)	RPM	KIAS
Flaps 40°, Gear down	3000	as req'd	Fwd	40

Pilot actions	Flt Engineer actions
1. Perform clearing turns 2. Trim for minimum speed, full fwd RPM 3. Close throttle until buffet while maintaining altitude and entered stall 4. Maintain conditions for [illegible] seconds	1. Announce card number 2. Record fuel, time, altitude, indicated airspeed, manifold pressure, engine RPM, OAT 3. Record AOA reading(s)

Time: | OAT:

Pt #	RPM	MP	KIAS	P-ALT	HDG	FUEL-R	AoA	Pt Note (turb, etc.)

Notes:

Card 45 Incipient stall coord – 40 kt – 40° flap w/gear – Low (4600)

7600 Power-off stall coord – 40 kt – 40° flap w/gear – Low

Power-off coordinated stall, 40° flaps, gear down, low altitude, approx. 40 KIAS.

Configuration	P.Alt (ft)	MP (in)	RPM	KIAS
Flaps 40°, Gear down	3000	as req'd	Fwd	40

Pilot actions	Flt Engineer actions
1. Ensure clearing turns have been performed	1. Announce card number
2. Trim for minimum speed, full flaps, 1500 RPM	2. Record fuel, time, altitude, indicated airspeed, manifold pressure, engine RPM, OAT
3. Slowly close throttle while raising nose to maintain altitude until full aft control ball	3. Record OAT reading(s)
4. Recover from stall immediately when nose drops or altitude decreases	

Pt #	RPM	MP	KIAS	P ALT	HDG	FUEL R	AmA	Pt Note (turb, etc.)

Notes:

Card 46 **Power-off stall coord – 40 kt – 40° flap w/gear – Low (7600)**

2005 Uncoord stdy state – 110 kt & below – clean – Low

Steady state flight with one ball deslip, clean configuration, low altitude, approx. 110 KIAS.

Configuration	P.Alt (ft)	MP (in)	RPM	KIAS
Clean	3000	23	2400	110

Pilot actions	Flt Engineer actions
1. Obtain steady heading, decelerate, slip conditions, initial speed while maintaining one ball sideslip, use LEFT	1. Announce card number
2. Maintain conditions for 20 seconds	2. Record fuel, time, altitude, indicated airspeed, manifold pressure, engine RPM, OAT
3. Accelerate and repeat at specified airspeeds, ±10	3. Record OAT reading(s)
4. Repeat at 100, 90, 80, 70, 60 KIAS	

Time: OAT:

Pt #	RPM	MP	KIAS	P ALT	HDG	FUEL R	AmA	Pt Note (turb, etc.)

Notes:

Card 47 **Uncoord stdy state – 110 kt & below – clean – Low (2005)**

5001 Incipient stall uncoord – 50 kt – clean – Low

In stall buffer with one ball deslip, level flight, clean configuration, low altitude, approx. 50 KIAS.

Configuration	P.Alt (ft)	MP (in)	RPM	KIAS
Clean	3000	as req'd	Fwd	50

Pilot actions	Flt Engineer actions
1. Obtain steady heading, decelerate, slip conditions, while maintaining one ball, deslip, level flight, clean configuration, low altitude, approx. 50 KIAS	1. Announce card number
	2. Record fuel, time, altitude, indicated airspeed, manifold pressure, engine RPM, OAT
2. Maintain conditions for 20 seconds	3. Record OAT reading(s)

Time: OAT:

Pt #	RPM	MP	KIAS	P ALT	HDG	FUEL R	AmA	Pt Note (turb, etc.)

Notes:

Card 48 **Incipient stall uncoord – 50 kt – clean – Low (5001)**

8001 Power-off stall uncoord – 50 kt – clean – Low

Power-off stall with one ball sideslip, clean configuration, low altitude, approx. 50 KIAS

Configuration	P. Alt (ft)	MP (in)	RPM	KIAS
Clean	3000	as req'd	Fwd	50

Pilot actions

1. Ensure clearing turns have been performed
2. Obtain steady heading side slip conditions while maintaining one ball LEFT
3. Maintain conditions for 3 seconds

Flt Engineer actions

1. Announce card number
2. Record fuel, time, altitude, indicated airspeed, manifold pressure, engine RPM, OAT at stall
3. Record AOA reading(s)

Time: OAT:

Pt #	RPM	MP	KIAS	P ALT	HDG	FUEL R	AoA	Pt Note (turb, etc.)

Notes

13002 Accel stall coord – 70 kt – clean – Low

Accelerated stall from coordinated flight, clean configuration, low altitude, approx. 70 KIAS

Configuration	P. Alt (ft)	MP (in)	RPM	KIAS
Clean	3000	as req'd	Fwd	70

Pilot actions

1. Perform clearing turns
2. Trim for target speed
3. Roll to LEFT 45° bank, increase RPM to maintain airspeed, increase back pressure with constant throttle until stall
4. Recover from stall immediately

Flt Engineer actions

1. Announce card number
2. Record fuel, time, altitude, indicated airspeed, manifold pressure, engine RPM, OAT at stall
3. Record AOA reading(s)

Time: OAT:

Pt #	RPM	MP	KIAS	P ALT	HDG	FUEL R	AoA	Pt Note (turb, etc.)

Notes